2009-09-09

Hypoxia Inducible Factors in Alcoholic Liver Disease: A Dissertation

Bharath D. Nath
University of Massachusetts Medical School


Hypoxia Inducible Factors
in Alcoholic Liver Disease.
A dissertation presented by
Bharath Dwaraka Nath
9.9.2009

Hypoxia Inducible Factors in Alcoholic Liver Disease

A Dissertation Presented

By

Bharath Dwaraka Nath

The Signatures of the Dissertation Defense Committee signifies completion and approval as to style and content of the Dissertation

Gyongyi Szabo MD PhD, Thesis Advisor

Jason Kim PhD, Member of Committee

Evelyn-Kurt-Jones PhD, Member of Committee

Brian Lewis PhD, Member of Committee

Alex Lentsch PhD, External Member of Committee

The signature of the Chair of the Committee signifies that the written dissertation meets the requirements of the Dissertation Committee

Steven Grossman MD PhD, Chair of the Committee

The signature of the Dean of the Graduate School of Biomedical Sciences signifies that the student has met all graduation requirements of the school.

Anthony Carruthers PhD
Dean of the Graduate School of Biomedical Sciences

MD/PhD Program in Biomedical Sciences
University of Massachusetts Medical School
9 September 2009

Acknowledgements

I am deeply thankful to Gyongyi Szabo for her mentorship and guidance. Dr. Szabo has created in the lab an environment that gave me freedom to pursue my ideas. The existence of that environment owes entirely to her example of tireless dedication and commitment. Over the past three years I have benefitted not solely from her time, judgement, keen editorial eye, and scientific acumen, but also from her friendship. Her achievements are inspirational, and I have learned much about what this career path takes by working in her presence. For all of these things, and for her personal attention and support to my developing career, I will always be grateful.

I wish to thank the members of the Szabo lab. Karen Kodys and Donna Catalano deserve special thanks for their friendship. Their hard work is the backbone of the lab, and I will always be appreciative of the efforts they always made to keep the lab running and the science moving forward. I wish to thank the post-doctoral associates in the lab, Ivan Levin, Timi Csak, Jan Petrasek, Arumugam Velayudham, Shashi Bala, and others who have moved on to other roles, for their friendship, camaraderie and intellectual contributions. Finally, I wish to thank Angela Dolganiuc and Pranoti Mandrekar for many useful discussions along the way.

Gail Bird and Janice Lagace have been incredibly helpful throughout my time in the lab. Both have been a pleasure to work with and I will miss interacting them.

I owe a great deal to the guidance of my TRAC committee. Particular thanks is due to Steven Grossman, under whose tutelage I began my journey in graduate school and in whose lab I qualified. I am grateful for his friendship and his support. Brian Lewis and Evelyn Kurt Jones have been invaluable in the development of this project; and I am grateful for their guidance. I also thank Dr. Jason Kim and Dr. Alex Lentsch for giving their time to my defense.

I am grateful to Dr William Kim, UNC, for the provision of HIF1dPA mice and HIF plasmids, as well as for several helpful conversations and advice along the way.

I owe Christian Mueller thanks for his assistanc with the acquisition of data in multiplex cytokine assays, and the Flotte lab for making equipment available to us.

I wish to thank members of the Grossman lab, in particular Seema Paliwal and Ramesh Kovi, for their friendship and assistance with designing protocols for in vitro work.

I will always be grateful to Dr. Elliot Androphy, the past director of the MD-PhD program. and the second person I met on this campus on my interview day (Ellen Goguen was the first!). He gave me perhaps the toughest interview experience I had ever had and followed it in the years since with unfailingly thoughtful guidance and insight.

I wish to thank one past member of my TRAC committee, whose retirement precluded his participation: Dr Aldo Rossini. I am thankful that I had the chance to benefit from his vision of clarity in scientific presentation. I also wish to thank the members of my qualifying committee, Michelle Kelliher, Michael Czech, and Dario Altieri.

The work performed in this dissertation was generously funded in part by an F30 fellowship from the National Institutes of Alcohol Abuse and Alcoholism. (NIAAA F30 AA017030). I am grateful for the helpful assistance of several individuals at the NIAAA, including Jose Velazquez and Svetlana Radaeva.

I wish to acknowledge the mentorship from which I have benefited on the other side of the campus, in particular the friendship and guidance of Dr. Michele Pugnaire, Dr. Mai-Lan Rogoff, Dr. David Hatem, and Dr. Michael Ennis. All have enabled me to pursue my interest in medical education even as I have worked in the lab. I am grateful for the opportunities.

Many fellow MD-PhD students have been sources of support and, occasionally, worthwhile distraction. Two stand out in my mind in particular for both of those reasons, Michael Straza and Kate Cullion. I thank them for their friendship and willingness to take time to reflect on our mutual progress.

Thanks for the friendship of my medical school classmate Arun Panigrahi and the other members of the UMMS class of 2007, many of whom will have ample opportunity to order me around over the next few years of my training. Seriously folks, that's why I am including all of you in the acknowledgements.

My family will always be the very center of my life; I wish to thank all the members of the Chengaiah clan for making family reunions the best part of the year. And the best part of the best part is always the time spent with my sister Maya and my brother-in-law Ben Curtis

My parents-in-law, Thomas Braciale and Vivian Lam Braciale have been wonderful sources of guidance throughout this process. I am thankful for their wisdom and their love.

As I write these words, my father is awaiting a potentially life-saving procedure for a condition that presented itself this morning. He is incredibly lucky, and I am incredibly grateful for all that my parents have taught me about the preciousness of life and the blessing of the life lived as a physician. I am humbled by the selfless love and the example of my parents, and I wish to dedicate this effort to them: Dr. Gopala and Dr. Shashikala Dwarakanath

Most important, I wish to thank my darling wife Kara for her her love, support, friendship, and everything else. I know that I would not be where I am today without you, and I am overjoyed at the journey ahead, alongside you.

And...thanks and love to my most precious and boisterous daughter, Pia Sharada Isabel Nath

ABSTRACT

Chronic intake of alcohol can result in a range of pathology in the liver. Whilst the earliest changes observed with chronic ethanol, including the accumulation of lipid, or steatosis, are readily reversible upon cessation of alcohol consumption, longer exposure to ethanol may achieve more complex disease states including steatohepatitis, fibrosis, and cirrhosis that can cause irreversible damage and progress to fulminant hepatic failure. A key concept in the pathogenesis of alcoholic liver disease is that chronic ethanol primes the liver to increased injury through an interplay between hepatocytes and non-parenchymal cells, chiefly immune cells, of the liver. These relationships between hepatocytes and non-parenchymal cell types in alcoholic liver disease are reviewed in Chapter 1A.

The Hypoxia Inducible Factors are a set of transcription factors that classically have been described as affecting a homeostatic response to conditions of low oxygen tension. Alcoholic liver disease is marked by increased hepatic metabolic demands, and some evidence exists for increased hepatic tissue hypoxia and upregulation of hypoxia-inducible factor mRNA with chronic alcohol. However, the biological significance of these findings is unknown. In Chapter 1B, we review the literature on recent investigations on the role of hypoxia inducible factors in a broad array of liver diseases, seeking to find common themes of biological function

In subsequent chapters, we investigate the hypothesis that a member of the hypoxia-inducible-factor family, HIF1α , has a role in the pathogenesis of alcoholic liver disease. In Chapter 2, we establish a mouse model of alcoholic liver disease and report data confirming HIF1α activation with chronic ethanol. We demonstrate that HIF1α protein, mRNA, and DNA binding activity is upregulated in ethanol-fed mice versus pair-fed mice, and that some

upregulation of HIF2α protein is observable as well. In Chapter 3, we utilize a mouse model of hepatocyte-specific HIF1α activation and demonstrate that such mice have exacerbated liver injury, including greater triglyceride accumulation than control mice. Using cre-lox technology, we introduce a degradation resistant mutant of HIF1α in hepatocytes, and after four weeks of ethanol feeding, we demonstrate that mice with the HIF1α transgene have increased liver-weight to body weight ratio and higher hepatic triglyceride levels. Additionally, several HIF1α target genes are upregulated. In Chapter 4, we examine the relationship between HIF1α activation and hepatic lipid accumulation using a recently published *in vitro* system, in which lipid accumulation was observed after treating Huh7 cells with the chemokine Monocyte Chemoattractant Protein-1 (MCP-1). We report that MCP-1 treatment induces HIF1α nuclear protein accumulation, that HIF1α overexpression in Huh7 cells induces lipid accumulation, and finally, that HIF1α siRNA prevents MCP-1 induced lipid accumulation. In Chapter 5, we use mouse models to investigate the hypothesis that suppression of HIF1α in hepatocytes or cells of the myeloid lineage may have differing effects on the pathogenesis of alcoholic liver disease. We find that ethanol-fed mice expressing a hepatocyte-specific HIF1α deletion mutant exhibit less elevation in liver-weight body ratio and diminished hepatic triglycerides versus wild-type mice; furthermore, we find that challenging these mice with lipopolysaccharide (LPS) results in less liver enzyme elevation and inflammatory cytokine secretion than in wild-type mice. In Chapter 6, we offer a final summary of our findings and some directions for future work.

TABLE OF CONTENTS

LIST OF FIGURES

LIST OF TABLES

Abbreviations used in this text:

ADRP, adipocyte-differentiation-related protein;AE, Acute ethanol; ALD, Alcoholic liver disease; ALT, alanine aminotransferase; AMPK, Adenosine monophosphate-activated protein kinase; aPl, Anti-phospholipid antibodies; CE, Chronic Ethanol; CIH, Chronic intermittment hypoxia; CYP2E1, cytochrome P450 2E1; DC, dendritic cells; EGR1, Early growth response-1; ERK, extracellular signal regulated kinase; HepHIF(-), Mouse mutant with hepatocyte-specific trasncriptionally inactive allele of HIF1α; HIF1dPA, mouse mutant with constitutive HIF1α activation; HIF1α, Hypoxia Inducible Factor-1-alpha; HIF2α, Hypoxia Inducible Factor-2-alpha IFN, interferon; IL, interleukin; iNOS, Inducible Nitric Oxide Synthase; IRF, interferon regulatory factor; KC, Kupffer Cells; KpfC, murine homolog of IL-8; LBP, lipopolysaccharide binding protein; LPS, lipopolysaccharide; MAPK, mitogen activated protein kinase; MCMV, murine cytomegalovirus; MCP-1, Monocyte Chemoattractant Protein; MYD88, myeloid differentiation primary response gene 88; MyeHIF(-), Mouse mutant with myeloid lineage-specific transcriptionally inactive HIF1α allele; NFκB, Nuclear factor kappa B; NRF2, nuclear factor/Erythroid related factor-2; NK, natural killer; NKT, natural killer T; PAI-1, plasminogen activator inhibitor-1; PGC1-α, peroxisome-proliferator coactivator 1-α; poly I:C, polyinosinic/ polycytidylic double-stranded RNA; PPAR, peroxisome proliferator-activated receptor; ROS, reactive oxygen species; RXR, retinoic acid receptor; SREBP, Sterol-regulatory element binding protein; SIRT1, sirtuin 1; STAT3, signal transducer and activator of transcription 3; TLR, Toll-like receptor; TNFα, tumor necrosis factor-α; TRIF, TIR domain containing adaptor inducing IFNB; WT, Wild-type

PREFACE

Much of the introductory material is adapted from Bharath Nath and Gyongyi Szabo, ‘Alcohol-induced modulation of signaling pathways in liver parenchymal and nonparenchymal cells: implications for immunity.‘ *Seminars in Liver Diseases*. 2009 May;29(2):166-77

Data for some figures in subsequent chapters were gathered in collaboration with other members of the Szabo laboratory. Figures generated from such data are identified in prefatory material in the relevant chapters of the dissertation.

CHAPTER 1

INTRODUCTION

Summary

Alcoholic liver injury involves a complex array of derangements in cellular signaling of hepatic parenchymal and non-parenchymal cells as well as cells of the immune system. In the first part of the introduction, we review the literature on the role of parenchymal and non-parenchymal cells of the liver in the pathogenesis of alcoholic liver disease. In the hepatocyte, chronic ethanol abuse leads to lipid accumulation and liver steatosis. Multiple pathways are affected to promote lipid accumulation in the ethanol-exposed hepatocyte. Chronic ethanol renders Kupffer cells hyper-responsive to endotoxin, which results in production of inflammatory cytokines and the tumor necrosis factor-α via a Toll-like receptor 4 dependent pathway, leading to inflammation and hepatic necrosis. Dysfunction of the innate and adaptive immune responses caused by ethanol contributes to impaired anti-viral response, inflammatory injury, and autoimmune activation. Recent developments in the literature are reviewed, and we suggest lipid accumulation, dysregulation of immunity, and impaired anti-viral and autoimmune responses as three distinct though interwoven pathophysiological mechanisms of alcoholic liver injury.

Hypoxia has been shown to have a role in the pathogenesis of several forms of liver disease. In the second part of the introduction, we review the evidence for a role of hypoxia and the Hypoxia -Inducible Factors, a family of transcription factors that affect a homeostatic response to low oxygen tension, in liver diseases. We describe regulation of the hypoxia

inducible factors, and review earlier investigations that demonstrate a role for HIFs in the development of liver fibrosis, activation of innate immune pathways, hepatocellular carcinoma, as well as other liver diseases in both human disease and murine models.

CHAPTER 1A

Alcohol and cellular signaling pathways in hepatic parenchymal and non-parenchymal cells

Alcoholic liver disease [ALD] can be broadly described as varying degrees of impairment of hepatic function following chronic and excessive ethanol consumption. The pathophysiological changes in ALD are provoked by complex effects of ethanol on all cell types within the liver, affecting metabolic, immunologic, and inflammatory processes. Within the effects of alcohol, a few broad trends emerge. First, chronic ethanol (CE) consumption diverts metabolic pathways in the hepatocyte towards the accumulation of intracellular lipid in the form of triglycerides.[1] Recent investigation reveals that this accumulation of lipid is unlikely to be an effect of ethanol alone on the hepatocyte, but rather a complex interplay of ethanol-induced alterations in cellular redox state, the transcription of lipogenic and anti-lipolytic factors, and cellular signaling from other cell types and distant tissues. Second, ALD involves activation of the signaling axis of the innate immune pathway, which is characterized by a hepatic inflammatory response to gut derived endotoxin, chiefly orchestrated by the Kupffer cell (KpfC), the resident macrophage of the liver. The main output of this inflammatory response is the production of tumor necrosis factor-alpha and other pro-inflammatory cytokines, which in turn are major determinants and causative agents of subsequent liver damage. Third, prolonged inflammation and hepatocyte damage appear to give rise to several other cellular and immune events that provoke further deterioration of hepatic function, including effects that span a range from impaired anti-viral response, fibrotic change, and autoimmune attack. Thus, (for purposes of this introductory review), we will adopt a three-part description of signaling pathways in alcoholic liver disease, one that summarizes pathways leading to lipid accumulation, the

endotoxin/innate immune signaling axis, and other cellular and immune events as three distinct, though overlapping, themes in the biological narrative of liver injury as a consequence of prolonged ethanol exposure.

Ethanol and Pathways of Lipid Accumulation in the Hepatocyte

Ethanol exerts effects on the hepatocyte that divert metabolic pathways to favor the accumulation of intracellular lipid (Figure 1). This correlates with the earliest histopathological alterations detectable in murine models of acute ethanol or CE consumption, and the clinical observation that virtually all individuals who chronically consume ethanol develop steatosis.[2] In vitro work using precision-cut thin slices of liver tissue have demonstrated lipid accumulation within 48 hours of ethanol exposure.[3] Ethanol directly affects the activity of several nuclear receptors that exert transcriptional control on lipid metabolism, including the peroxisome proliferator-activated receptors alpha and gamma (PPARα and PPARγ), the sterol regulatory element binding protein-1 (SREBP1), the liver retinoic acid/X receptors (RXR and LXR), and other associated regulators and cofactors.

Peroxisome Proliferator Activated Receptors (PPAR) and Steatosis. The peroxisome-proliferator-activated-receptors are a family of proteins that act as nuclear receptors and exert transcriptional effects on pathways of lipid metabolism. Natural PPAR ligands include various lipid derived biomolecules, including eicosanoids, leukotrienes, prostaglandins, and free fatty acids.[4] PPARα may be pharmacologically activated by drugs of the fibrate class, whereas PPARγ may be activated by thiazolidinediones. Upon ligand activation, all PPARs bind with the retinoid-X

Figure 1. Chronic Ethanol and Pathways to Lipid Accumulation in the Hepatocyte. PPARα suppresses lipid accumulation which may be mimicked by (A) PPARα agonists that induce PPAR-DNA binding. (B) PPARα is downregulated by chronic ethanol, and knockout of PPARα or its binding partner RXR exacerbated liver injury. (C) PPARγ agonists activate PPARγ and inhibit lipid accumulation, possibly by a PPARγ independent mechanism. (D)Inhibition of PGC-1α or its interacting partner SIRT by ethanol relieves the suppressive effect of these factors on SREBP1c. (E) Induction of SREBP1c by ethanol upregulated lipid accumulation, and knockout of SREBP1 partially reduced ethanol-induced hepatic triglyceride (F) Stat3 signaling appears to limit SREBP1 activation. (G) Ethanol stimulated osteopontin, and knockout of osteopontin resulted in higher PPARα. (H) Ethanol upregulated CYP2E1, which in turn blocked PPARα though conflicting results have been reported. (I) AMPK signaling induces PPARα and ethanol suppressed AMPK. (J) Adiponectin maintains PPARα levels, and is decreased by chronic ethanol.

Figure 1

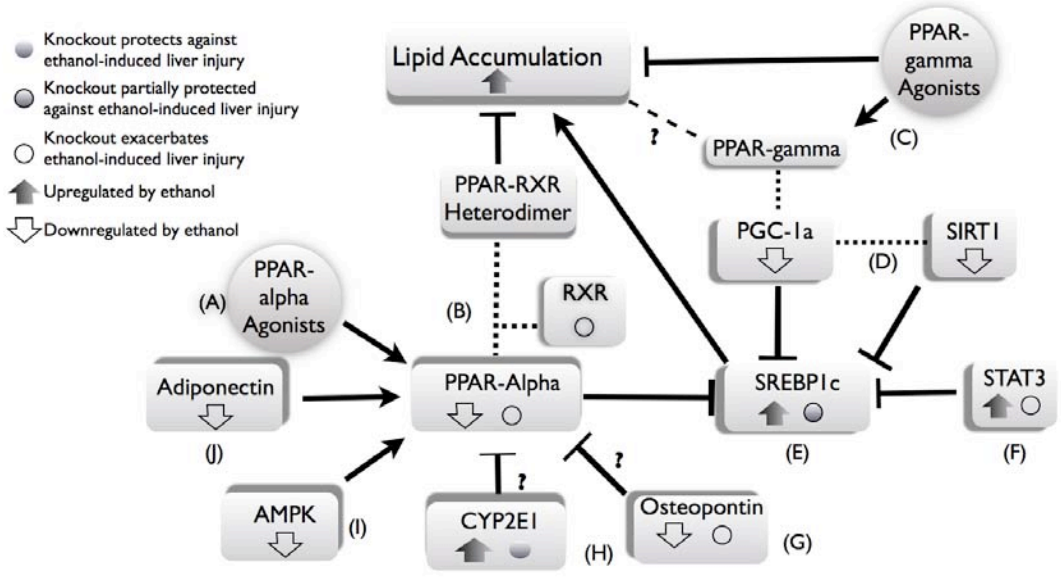
Knockout protects against ethanol-induced liver injury
Knockout partially protected against ethanol-induced liver injury
Knockout exacerbates ethanol-induced liver injury
Upregulated by ethanol
Downregulated by ethanol
Lipid Accumulation
PPAR-gamma Agonists
(C)
?
PPAR-gamma
PPAR-RXR Heterodimer
PGC-1a
(D)
SIRT1
(A)
PPAR-alpha Agonists
(B)
RXR
Adiponectin
PPAR-Alpha
SREBP1c
STAT3
(J)
(E)
(F)
AMPK
(I)
?
?
CYP2E1
(H)
Osteopontin
(G)

receptor (RXR), and the heterodimer formed thereby binds to peroxisome-proliferator response elements (PPREs) in the genome.[4] Suppression of PPAR gene expression by ethanol was described over a decade ago.[5] CE feeding diminishes PPARα/RXR DNA binding in the liver, and ethanol-induced hepatic lipid accumulation can be reversed by treatment with PPARα agonists in mouse and rat models of ethanol feeding.[6, 7] Conversely, CE feeding resulted in worsened liver injury in PPARα-knockout mice versus wild-type mice, indicating that PPARα activation may be protective in ALD.[8] Similarly, hepatocyte RXR deficient mice displayed worsened liver injury with CE.[9]

Osteopontin and PPARα. To date, the mechanism of ethanol-induced decrease in PPARα activation remains controversial. Some evidence suggests that the glycoprotein osteopontin may have a role.[10] Treatment of macrophages with PPARα agonists suppressed osteopontin production and circulating osteopontin was diminished in patients treated with PPARα agonists. Conversely, CE feeding in osteopontin-null mice resulted in greater lipid accumulation and liver injury than in wild-type mice, with higher PPARα mRNA levels.[11]

Adiponectin and PPARα. Another potential mechanism involves adiponectin, an adipocyte-derived hormone that is dysregulated in rats with CE exposure.[12] In vitro studies suggest that adiponectin is a potent stimulator of PPARα DNA binding.[13] Treatment of mice with a pharmacological inhibitor of the Inhibitory Kappa Kinase-2 in a mouse model of diet-induced non-alcoholic steatohepatitis (NASH) maintained adiponectin levels and PPARα activation, strengthening the link between adiponectin and PPARα and suggesting that the dysregulation of

NFκB signaling in CE exposure, discussed below, may interface hepatic lipid accumulation along an adiponectin-PPARα axis.[14]

While compelling, the data linking adiponectin to hepatic lipid accumulation is not without controversy. Adiponectin is known to exert some of its effects via activation of the AMP-activated protein kinase (AMPK) which in turn acts to downregulate lipid accumulation by a variety of mechanisms.[15] Briefly, stimulation of AMPK is thought to inactivate acetyl-coA carboxylase, which in turn prevents the formation of malonyl-CoA, itself an inhibitor of the fatty acid transporter carnitine palmitoyl transferase. Treatment of ethanol-fed animals with an AMPK inhibitor (AICAR) prevented lipid accumulation and normalized serum alanine aminotransferase (ALT) levels, suggesting that the beneficial effect of adiponectin may be modulated through adiponectin effects on AMPK.[16] While these studies were conducted in models of CE, a recent study investigated the effects of metformin, a biguanide pharmaceutical agent known to act in part through AMPK pathway activation, in both AE and CE fed mice.[17] Despite robust prevention of hepatic lipid accumulation in mice treated with metformin and AE, AMPK activation was not observed. In metformin/CE fed mice, hepatic lipid accumulation remained lower than mice fed ethanol alone, and AMPK activation again appeared unchanged.[17]

Plasminogen Activator Inhibitor-1. Metformin treatment in alcohol-fed mice also correlated with diminished Plasminogen-activator-inhibitor-1 (PAI-1), expression and PAI-1 knockout mice were protected from ethanol-induced liver injury.[17] In support of the notion that inhibition of PAI-1 may be an important mechanism of the protective effects of adiponectin on hepatic lipid

accumulation in CE feeding, investigators found that treatment of HepG2 cells with the PPARα agonist fenofibrate suppressed PAI-1 levels.[18]

Oxidant Stress and Lipid Accumulation. Evidence also suggests that hepatic lipid accumulation and PPARα activation are profoundly affected by oxidant stress. An inhibiting effect of antioxidant administration on hepatic lipid accumulation in CE was described almost 40 years ago. Knockout of the p47 NADPH oxidase subunit was able to prevent ethanol induced liver injury in a model of continuous enteral CE feeding.[19] Cytochrome P4502E1 (CYP2E1), a member of the p450 mixed-oxidase system of xenobiotic metabolizing enzymes, has been proposed as a potential source of oxidant stress in response to ethanol feeding.[20] CYP2E1 mRNA is upregulated by ethanol.[21] However, conflicting experimental results suggest that the role of CYP2E1 is as yet unresolved. Most recently, in an oral CE feeding model, neither CYP2E1 null mice nor wild-type mice fed ethanol and a chemical inhibitor of CYP2E1 developed steatosis.[22] Intriguingly, ethanol caused an upregulation in hepatic PPARα in CYP2E1-null mice, suggesting a role for endogenous CYP2E1 in the negative regulation of PPARα.[22] In distinction, earlier studies found that AE or CE in CYP2E1-knockout mice had no effect or increased lipid accumulation and liver injury.[23, 24]

Other Pathways and Hepatic Lipid Accumulation.

The developing picture of decreased PPARα activation and subsequent hepatic lipid accumulation is complicated by observations that PPARγ activation may have a protective effect on ALD. The PPARγ agonist pioglitazone repeatedly prevented injury in rat models of

ALD[25-27] However, though several studies report a reduction of PPARγ mRNA with ethanol treatment in vivo and in vitro, others report no effect of ethanol on PPARγ protein expression.[28, 29] Indeed, in the studies cited previously, no effect of pioglitazone on PPARγ gene expression was observed in one study, whereas PPARγ mRNA levels were restored by pioglitazone in ethanol treated animals in a second study.[26, 27] Although studies on a third member of the PPAR family, PPARδ, are limited in ALD, a recent report demonstrated that PPARδ activation ameliorates hepatic steatosis in a mouse-model of non-alcoholic fatty liver disease.[30]

An alternative mechanism may involve activation of the peroxisome proliferator activated receptor-gamma coactivator 1 alpha (PGC-1α). PGC1α interacts both with PPARγ as well as with the histone deacetylase Sirtuin 1 (SIRT1). Both PGC1α and SIRT1 protein are suppressed by ethanol, and reversal of these effects (with resveratrol treatment, which upregulates both SIRT1 and PGC1α) prevented ALD in a mouse model.[31, 32] This effect of resveratrol was coupled with AMPK activation and increased expression of adiponectin and adiponectin receptors. However, in a rat model of continuous enteral CE feeding, conjunct resveratrol treatment exacerbated liver injury.[33] Sirt1 was recently identified as a regulator of sterol-regulatory element binding protein1c (SREBP1c)[31] CE upregulated SREBP1c and its downstream targets, and overexpression of SREBP1c caused steatosis in a mouse model.[34] However, ethanol feeding in an SREBP-null mouse resulted in only a partial reduction of hepatic triglyceride.[35] STAT3 activation may limit SREBP1c activation in ethanol-fed animals, as a hepatocyte-specific STAT3 knockout model accumulated greater lipid and showed increased SREBP1 induction versus wild-type controls.[36] As SREBP1c protein levels and activity may

be regulated by PPARα,[37, 38] it is possible that the failure of the SREBP1c knockout to completely protect against ethanol-induced effects on lipid accumulation is due to coordinate regulation of multiple pathways of lipid accumulation by PPARα.

Ethanol and the TLR4-Innate Immune Signaling Axis in Kupffer cells

Toll-like Receptor Signaling Pathways.

A second broad area of liver physiology that is impacted by CE exposure involves signaling pathways of innate immunity (Figure 2.) Kupffer cells (KpfCs) play a major role in hepatic innate immunity and the development of ALD [39]. KpfCs, along with other cell types in the liver, express the Toll-like Receptor 4 (TLR4) which responds to endotoxin and results in production of pro-inflammatory cytokines such as Tumor Necrosis Factor Alpha (TNFα.)[40] TNFα alpha plays an important role in the pathobiology of alcoholic liver disease, as administration of anti-TNFα antibodies or utilization of a TNF-Receptor 1 knockout mouse resulted in diminished liver injury in an enteral CE feeding model.[41, 42]

A major concept in the pathogenesis of liver injury in the setting of CE exposure postulates that endotoxin from commensal gram-negative gut flora enters the hepatic portal vein as a consequence of CE-induced heightened gut permeability, with subsequent stimulation of KpfCs. ALD has been correlated with increased portal vein endotoxin levels.[43, 44] Gut permeability may be increased by ethanol-induced increases in levels of mir212, a microRNA that downregulates proteins of the zona occludens in intestinal cell culture, and whose levels are higher in human colonic biopsy samples in patients with ALD.[45] Alternatively, studies in other

Figure 2. The Endotoxin-Innate Immune Signaling Axis in Ethanol mediated liver injury. Ethanol causes increased gut permeability and results in exposure of the liver to LPS. Components of the LPS receptor complex, including TLR4, MD2, and CD14 are upregulated by ethanol. TLR4 and CD14 are essential for the development of ALD. Alcohol causes hyper-responsiveness in downstream signaling from the TLR4 receptor leading to increased inflammatory cytokine production, which is potentiated by alcohol induction of P47 and PDE4B, and suppressed by alcohol induction of STAT3. The TRIF-dependent limb of the TLR4 pathway is essential for alcohol-induced liver injury, and leads to TNFα induction via NFκB activation. TNFR knockout or anti-TNFαantibody prevents TNFα -induced apoptosis. ERK1 signaling is upregulated by ethanol, prevented by adiponectin, and leads to increased EGR1, which contributes to enhanced NFκB activation. Ethanol upregulates hepcidin expression in the hepatocyte, which leads to increased gut iron uptake, one mechanism for the ethanol-induced increase in KpfC iron. Increased KpfC iron contributes to LPS hyper-responsiveness.

Figure 2

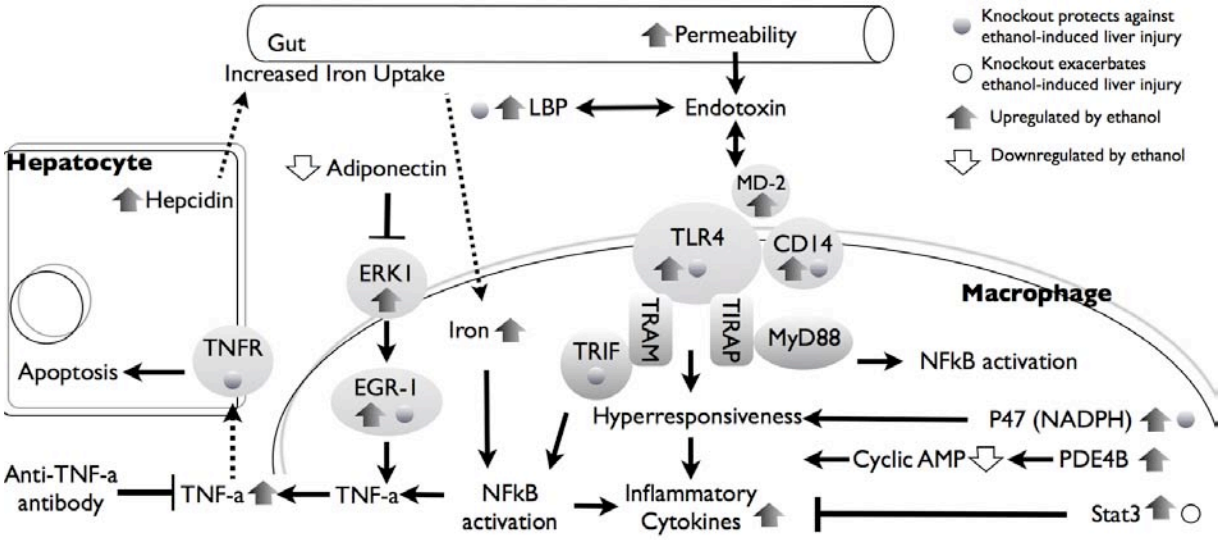
Gut
Permeability
Increased Iron Uptake
LBP
Endotoxin
Knockout protects against ethanol-induced liver injury
Knockout exacerbates ethanol-induced liver injury
Upregulated by ethanol
Downregulated by ethanol
Hepatocyte
Hepcidin
Adiponectin
MD-2
TLR4
CD14
ERK1
Macrophage
Iron
TRAM
TIRAP
TRIF
MyD88
NFkB activation
TNFR
Apoptosis
EGR-1
Hyperresponsiveness
P47 (NADPH)
Cyclic AMP
PDE4B
Anti-TNF-a antibody
TNF-a
TNF-a
NFkB activation
Inflammatory Cytokines
Stat3

models suggest a role for TNFα, IL-6, and other inflammatory cytokines in altered gut permeability.[46, 47]

In the circulation, free endotoxin is in equilibrium with endotoxin bound to LPS Binding Protein (LBP). LBP facilitates the dissociation of LPS into a monomeric form that enhances LPS transfer to TLR4 and its associated co-receptors, CD14 and MD-2.[48] Both KpfC CD14 expression and hepatic LBP binding protein were demonstrated to be upregulated by CE, offering some insight into the manner by which CE confers hypersensitivity to LPS stimulation (LPS hyper-responsiveness.)[49] The effect of CE on TLR4 or TLR2 mRNA is more controversial, as CE feeding for several weeks did not result in any change in TLR4 or TLR2 expression.[50] However, another model demonstrated an increase in the mRNA expression of almost all TLRs in response to a shorter term (10 day) ethanol feeding protocol.[51] Demonstrating the dependence of ALD on TLR4 signaling, CD14 knockout mice in an intragastric CE model had less ALT elevation but had similar increase in liver-weight to body-weight ratios as wild-type mice, [52] while LBP knockout mice fed on an intragastric CE model had diminished ALT, inflammation, and necrosis and diminished liver weight/body weight ratios in comparison to wild-type mice. No changes were observed in CYP2E1, TGFB1, or portal vein endotoxin levels, but IL-6 and TNFα were reduced in LBP KO mice versus controls.[53]

Signaling through the TLR4 receptor complex results in activation of at least two distinct intracellular signaling cascades.[54] The first of these, the MyD88 (Myeloid Differentiation Primary Response Gene 88) -dependent pathway utilizes the common adaptor protein MyD88 that is used by all TLRs with the exception of TLR3.[55] The MyD88 dependent pathway leads to activation of the Nuclear Factor Kappa B (NFκB) and subsequent stimulation of TNFα. A

second pathway of TLR4 dependent signaling, the MyD88-independent pathway, converges with a TLR3 signaling pathway utilizing the adaptor molecule Tir-domain-containing-adaptor-inducing-IFNB (TRIF). TRIF activation results in production of type I interferons through the Interferon Regulatory Factor-3 (IRF3), and delayed NFκB activation.[56, 57] A recent finding reported from our laboratory is that the hepatoprotective effect of TLR4 knockout is independent of the MyD88 pathway.[58] MyD88-knockout mice developed steatosis and elevated ALTs after CE similar to wild-type mice, though TLR4-knockout mice were protected from this effect. The involvement of the MyD88-independent TLR4 signaling pathway was indicated by upregulation of Interferon-Regulatory-Factor 7 (IRF7), an IRF3-inducible gene, in KpfCs. [55] A recent study corroborates this finding using TRIF pathway knock-out animals, as TRIF knockout mice were protected against alcoholic liver injury, showing diminished lipid accumulation by microscopy and normalized ALT after CE plus endotoxin injection.[59] In that model, the authors argued for an IRF3-dependent mechanism of LPS hyper-responsiveness and TNFα secretion, using strategies including mutation of the IRF3 response element in a TNFα promoter fragment.

The Nuclear Factor Kappa B

The Nuclear Factor Kappa B (NFκB) serves as a master regulator in the inflammatory response. NFκB subunits are normally sequestered in an inactive form but pro-inflammatory stimuli, such as TLR4 ligand stimulation, cause NFκB activation and TNFα production. Some NFκB activity is essential to prevent massive hepatocyte apoptosis in response to TNFα.[60, 61] NFκB activation in response to ethanol has been widely investigated in many hepatic and non-hepatic cell types. In isolated human monocytes, AE suppresses NFκB activation and the inflammatory

response to LPS by inhibiting p65 phosphorylation and IκK activity, but CE causes LPS hypersensitivity and NFκB activation.[62] Changes in LPS sensitivity have been linked to chromatin remodeling in other experimental systems.[63]

Several other mechanisms of regulation of NFκB signaling have been investigated in KpfCs. Among these, recent work utilizing a myeloid-lineage specific cre-recombinase enzyme to achieve specific deletion of Stat3 in KpfCs revealed that STAT3 signaling is essential to suppress inflammatory cytokine production from KpfCs from CE-fed mice.[36] Several lines of evidence implicate oxidative stress as a cause of ethanol-induced LPS hyper-responsiveness in macrophages. Adiponectin, which prevented steatotic change in CE, also exerts modulating effects on KpfCs, and was shown to downregulate LPS-responsive TNFα secretion in a fashion dependent on NFκB and the transcription factors EGR-1 and AP-1.[64]

Cyclic AMP.

Another line of evidence implicates ethanol-induced decreases in cyclic AMP as a mechanism for LPS hyper-responsiveness in macrophages. CE was shown to increase phosphodiesterase 4-B(PDE4B), which in turn degrades cyclic AMP. Treatment of human and murine macrophage cell lines with an inhibitor of PDE4B diminished the LPS-induced increase in TNFα. [65]

MAPK.

Other lines of evidence implicate oxidant stress pathways as mediators of LPS hyper-responsiveness in CE. Knockout of the Early Growth Response-1 (EGR-1) transcription factor conferred protection against the development of liver injury after CE feeding.[66] Following

lines of evidence that indicated that Extracellular-signal-regulated kinase-1 (ERK-1) promotes LPS hyper-responsiveness in macrophages stimulated with ethanol, potentially by upregulation of EGR-1, Thakur and coworkers examined the role of NADPH-derived reactive oxygen species (ROS) in macrophages. Treatment of macrophages with an inhibitor of NADPH oxidase (DPI) prevented TNFα secretion from macrophages in a p38-dependent manner. However, CE feeding prevented DPI from changing the ratio of phosphorylated p38 observed in pair-fed animals. Administration of DPI suppressed LPS-stimulated ERK phosphorylation, even in ethanol fed-animals, suggesting that ERK phosphorylation is indispensable to TNFα secretion in response to LPS, but that ethanol exerts actions through NADPH-oxidase-independent mechanisms that affect the p38 MAPK and NFκB pathways. [67]

Macrophage Iron

CE causes iron accumulates in hepatocytes and macrophages.[68] Ethanol upregulates the transferrin receptor in primary rat hepatocytes.[69] CE also may increase gut uptake of iron via downregulation of the iron transport hormonal mediator, hepcidin. Hepcidin, produced by hepatocytes, has been demonstrated to suppress iron uptake by the small bowel, and low levels of hepcidin have been observed in patients with ALD as well as in mouse models of CE feeding. [70] Additionally, alcohol disrupted iron-stimulated production of hepcidin from the liver, thus interrupting a negative feedback loop between serum iron and gut iron absorption.[71]

Iron accumulation in macrophages is associated with enhanced NFκB activation in ethanol feeding models.[72] Administration of iron dextran to CE-fed mice resulted in higher ALT and TNFα, and worsened liver inflammation.[73] Other investigators suggest a role for

endotoxin in increasing macrophage free iron, and propose a heme-oxygenase-1 dependent mechanism.[74]

Ethanol and Immunity

The liver has a well-characterized role in immunity, containing large numbers of tissue macrophages (KpfCs), plasmacytoid and myelocytoid dendritic cells (DC), T lymphocytes, natural killer (NK) cells, and natural killer-T cells (NKTs). Virtually all of these cell types have been demonstrated to be affected by CE.[75] Stellate cells have commanded significant interest due to evidence indicating their pivotal role in fibrotic change in the liver. [76, 77]

Broadly speaking, the central role of the endotoxin-mediated inflammatory cascade in ALD occurs in parallel with immunosuppressive effects of ethanol.[78] Ethanol is associated with increased susceptibility to bacterial infections, including salmonella, listeria, and others, particularly pulmonary infections.[79] Recognition of invading pathogens and initiation of innate and adaptive immune responses relies on the function of antigen presenting DCs, the function of which is impaired by ethanol.[80] DC populations in the liver are found in an immature phenotype, which may contribute to a tolerogenic environment.[80]

Ethanol Abuse and Antiviral Immunity

Alcohol abuse is a major cofactor for the development of cirrhosis and hepatocellular carcinoma in patients with chronic hepatitis B and C, and has been shown to be a predictor of negative outcomes in patients with chronic HCV or HBV.[81] Several lines of evidence implicate dysregulated cellular signaling events in the increased risk of disease progression in the setting of

viral exposure. Ethanol suppresses the effectivity of interferon therapy as a disease-modifying agent in HCV infection.[82] The molecular mechanisms of these effects remain unclear. Ethanol potentiates HCV viral replicon expression in vitro.[83] Ethanol activates the interferon-response element (ISRE), P38 and Jak/Stat signaling pathways in hepatocyte cell lines and fetal hepatocytes. AE inhibited HCV viral replication, but AE also suppressed the ability of IFN to inhibit HCV viral replication.[84] However, the application of these findings to CE are unclear. In Huh7 cells, co-expression of HCV core protein and alcohol induction of CYP2E1 additively increased mitochondrial ROS production and cellular death.[85] Taken in the aggregate, the weight of evidence suggests that ethanol impairs the host anti-viral response.

Alcohol and Autoimmune Host Response

Aside from the pathways of innate immunity described above, ethanol has significant effects on adaptive immunity that contribute to hepatic inflammation and dysfunction via several distinct, though potentially overlapping mechanisms. First, CE results in increased circulation of acetaldehyde and malondialdehyde, both of which can form antigenic adducts (singularly or in tandem) with native liver proteins.[86] Second, the prolonged inflammation, necrosis, and apoptosis present in ALD exposes damaged cellular material to immature antigen-presenting cells in the liver, which may cause autoantibody formation.[87] Supporting this, increased serum TNFα in patients with ALD was associated with higher prevalence of antibodies against oxidized cardiolipin and malondialdehyde-albumin adducts.[88] Autoantibodies were also demonstrated to be more prevalent in patients with ALD than non-drinking alcohol consumers.[89] This study

has been verified by others which have described increased IgG and IgA autoantibodies in patients with ALD versus moderate or non-alcohol consuming control subjects.[90]

60-80% of patients with alcoholic hepatitis or cirrhosis may have anti-phospholipid antibodies (aPl). A recent study by Vay et al. offers good evidence that aPl in ALD recognize oxidized phosphatidylserine residues on apoptotic cell membranes. Incubation of aPl serum from ALD patients with synthesized phosphatidyl serine micelles diminished their ability to bind apoptotic cells, and serum from ALD patients was able to target the plasma membrane of apoptotic HepG2 cells stimulated with ethanol.[87]

Anti-CYP2E1 antibodies are also highly prevalent in patients with ALD. In one study, up to 86% of cirrhotic patients had sera with positivity for immunoreactivity against CYP2E1.[91] Anti Cardiolipin antibodies are also reported to occur more frequently in patients with ALD than liver disease from other causes or healthy control subjects.[92] Antibodies are produced in the adaptive immune response by B lymphocytes. The effect of ethanol on B cells remains controversial. Although polyclonal hyperglobulinemia and increased circulating autoantibodies are found in alcoholics, recent investigations in a mouse model of chronic ethanol consumption demonstrates little effect of ethanol on B cell numbers.[93]

Summary and Conclusions

The disease-promoting effects of ethanol consumption on hepatic parenchymal and non-parenchymal cells is a complex phenomenon that incorporates changes at many different levels. On the one hand, the passage of ethanol through the metabolic pathways towards acetaldehyde or through the CYP2E1 system alters the cellular redox state, creates ROS, and alter lipid metabolic

pathways to favor lipid accumulation. While these changes are priming the hepatocyte to have increased susceptibility to TNFα-mediated apoptosis, ethanol is simultaneously inducing hyper-responsiveness to gut-derived endotoxin in hepatic Kupffer cells. The inflammatory effect of these changes induces recruitment of other cell types, including T cells, NK cells, and NKT cells, and the production of autoantibodies that further exacerbate liver injury. In the past decade, the use of transgenic mouse models, including cre-lox tissue specific knockout/knock-in models, has offered great insight into disease mechanisms. Future work promises additional insight towards the development of treatment strategies for the array of disease caused by alcohol use.

CHAPTER 1B.

Hypoxia Inducible Factors: Diverse Roles in Hepatic Health and Disease

The unique anatomical and functional niche occupied by the liver within the body profoundly affects its physiology and pathophysiology. Afferent blood flow to the liver derives from both highly oxygenated blood in the hepatic artery as well as oxygen-depleted blood in the hepatic portal vein. Furthermore, the directional flow of mixed oxygenated and deoxygenated blood towards the central vein of the hepatic lobule creates a physiological oxygen gradient.[94] This gradient has been reported to result in oxygen tensions from about 60-65mmHg in periportal blood, falling to about 30-35 mmHg in perivenous portions of the liver parenchyma; by comparison, physiological arterial oxygen concentration in most other body tissues is about 74-104 mmHg, and venous oxygen concentration is 34-46 mmHg.[94]

Hypoxia has profound consequences for the body tissues of an aerobic organism, and would rapidly lead to organ dysfunction and organismal death were it not for finely regulated homeostatic responses to low oxygen tension. In the past several decades, our knowledge of the homeostatic response to hypoxia has increased, expanding from reflexive neural regulation of physiological parameters, such as respiratory rate and heart rate, to humoral factors affecting the avidity of hemoglobin-oxygen binding, such as 2-3 bisphosphoglycerate, and finally to molecular genetic mechanisms. The Hypoxia Inducible Factors are a family of heterodimeric transcription factors that act as master regulators of a homeostatic transcriptional response to hypoxia in virtually all cells and tissues of the body. Active Hypoxia-Inducible Factor (HIF) consists of an alpha subunit and a beta subunit. Three alpha subunits, named Hypoxia Inducible Factor 1-α [HIF1α], Hypoxia Inducible Factor 2-α [HIF2α, also known as the Endothelial Per-

Arnt-Sim Domain-containing-1, EPAS1], or Hypoxia Inducible Factor 3α [HIF3α], have been described in humans, mice, and rats; all bind to a common β subunit named, alternatively, HIF1β , or the Aryl-Hyrdocarbon-Nuclear Receptor Translocator [ARNT].[95] Active HIF is named by its alpha subunit, hence, HIF1 is the active transcription factor consisting of HIF1α and ARNT, HIF2 is the dimer of HIF2α and ARNT, etc. HIF1 and HIF2 are the major hypoxia-inducible factors in humans, mice, and rats. Far less is known about the function of HIF3, which is thought to act as a dominant-negative suppressor of HIF activity in some systems.[95] (Figure 3). The hyroxylase mediated mechanism of oxygen-dependent HIF regulation is summarized in Figure 3.

Post-translational degradation by the proteasome is known to be a major pathway of HIF regulation. Under conditions of normoxia, and in the absence of other metabolic or molecular perturbations, the alpha subunits of HIF are rapidly hydroxylated by prolyl-hydroxylases (PHD1, PHD2, or PHD3) and scaffolded on a multimeric protein complex that includes the product of the Von Hippel Lindau tumor suppressor gene. Prolyl hydroxylation and presentation of HIF on the VHL scaffold leads to rapid ubiquitination and proteasomal degradation.[96] Under conditions of hypoxia, or perturbations in cellular redox state, HIFs escape hydroxylation and are free to form dimers with ARNT. Active HIF then translocates to the nucleus, where it binds to hypoxia-responsive elements (HREs) in the promoter region of target genes. HIF1 and HIF2 activate transcription of a broad range of target genes with some overlap between the two factors [97].

Oxygen and the liver

Numerous reports have offered evidence that the physiological gradient of oxygen tension across the hepatic lobule has profound effects on the function of hepatic parenchymal and nonparenchymal cells. Periportal hepatocytes and perivenous hepatocytes differ in their expression of many enzymes involved in glucose transport or metabolism, including insulin receptor, glucagon receptor, phosphoglycerate kinase (PGK1), L-type pyruvate kinase, and numerous others.[98-100] Consequently, periportal hepatocytes tend to sub-specialize in oxidative energy metabolism, glucose production, and synthesis of urea and bile, whereas perivenous hepatocytes are major sites of glucose uptake, glutamine formation and xenobiotic metabolism.[94]

Physiological exposure of hepatocytes to varying levels of oxygen tension also has consequences for the ability of hepatocytes to respond to hypoxic stress. Primary rat hepatocytes cultured in conditions approximating periportal oxygen tensions were able to survive transient anoxia with less cell death and cytokine release than hepatocytes cultured in conditions approximating perivenous oxygen tension. This suggests that in conditions of oxygen deprivation, such as increased hepatic metabolic demand, tissue ischemia, or other conditions, not only are the perivenous hepatocytes exposed to lower oxygen conditions, but despite chronic exposure to low oxygen tensions perivenous hepatocytes may be primed to increased injury when oxygen tension drops beneath a threshold level.[101] Indeed, centrilobular or perivenous hepatic necrosis is pathognomonic for ischemic hepatitis.

Figure 3. A General Schematic of HIF1α activation.

Under conditions of normoxia, HIF alpha subunits are rapidly hydroxylated at proline and asparagine residues by hydroxylase enzymes. Hydroxylation of HIF1α and assembly on a protein scaffold consisting of the VHL tumor suppressor, along with other co-factors, results in the rapid ubiquitination of the alpha subunit and subsequent degradation by the proteasome. Conversely, in conditions of hypoxia, HIF alpha subunits escape degradation and are free to dimerize with the binding partner, the Aryl Hydrocarbon Nuclear Translocator (ARNT). The HIF heterodimer is named by the alpha subunit (hence, HIF1α-ARNT heterodimer is the active HIF1 transcription factor) which translocates to the nucleus and affects transcription of target genes, typically by binding to a hypoxia response element in the upstream promoter region of the target gene.

Figure 3

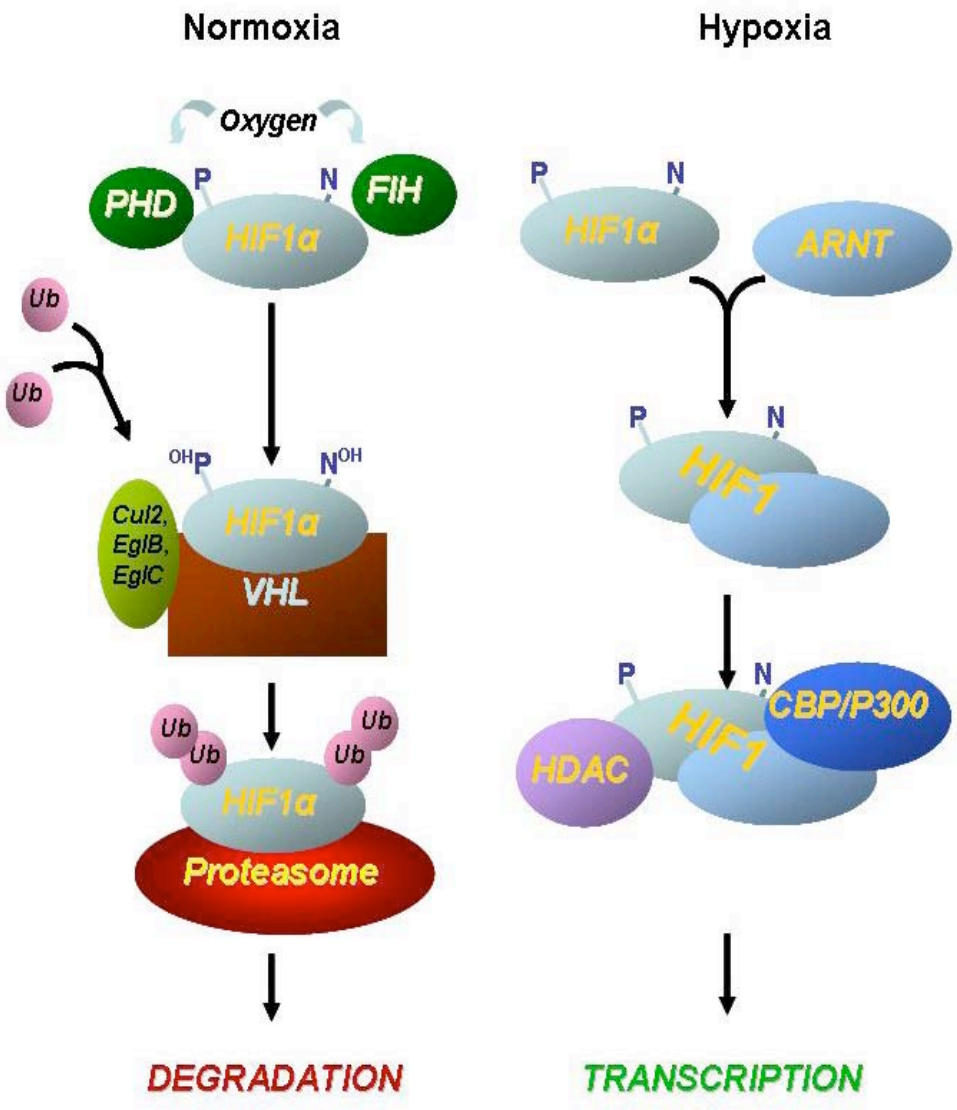
Normoxia
Hypoxia
Oxygen
PHD
FIH
P
N
HIF1α
Ub
Ub
OHP
NOH
Cul2,
EglB,
EglC
VHL
Proteasome
ARNT
HIF1
HDAC
CBP/P300
DEGRADATION
TRANSCRIPTION

Ischemia-Reperfusion Injury and Ischemic Hepatitis

The role of HIF1α in ischemia-reperfusion injury is controversial. Variable results have been reported in different tissues. For example, HIF1α siRNA pretreatment was able to protect against ischemia-reperfusion brain injury in rats.[102] In a different study, however, upregulation of HIF1α was associated with protection in cardiac post-conditioning, suggesting that HIF1α activation is an adaptive response.[103] Heterozygous HIF1α(+/-) mice were unable to respond to ischemic preconditioning.[104] Yet another group found that renal ischemia-reperfusion injury was prevented by acute inactivation of VHL (leading to HIF1α upregulation), prolyl hydroxylase inhibition, or by xenon preconditioning (again, with upregulation of HIF1α.) [105-107]

In liver, HIF1α induction was described as an early event, preceding apoptosis, in ischemia-reperfusion injury.[108] Others identified adenosine-dependent HIF1α activation as a protective event in late preconditioning.[109] Ischemia induced HIF1α and subsequent upregulation of the transferrin receptor, which may contribute to iron-species related liver injury in reperfusion.[110] Reperfusion, alternatively, was associated with decreased HIF1α DNA binding.[111] Delivery of a soluble VEGF antagonist was reported to reduce ischemia-reperfusion injury by inhibiting leukocyte migration and cytokine production, including TNFα and MCP-1, and indicating that HIF1α-dependent gene transcription may simultaneously be cytoprotective and pro-inflammatory in hepatic ischemia/reperfusion.[112]

A major concern in much of the work on HIFs in ischemia reperfusion injury is the reliance on HIF1α as the sole marker of hypoxia-dependent transcriptional activity. Further

work may reveal upregulation of other isoforms, such as HIF2α, that may have similar or divergent effects.

Hypoperfusion of the liver can also lead to hepatitis, a clinical entity described as ischemic hepatitis. In this condition, a rapid, though reversible, increase in serum ALT is accompanied by centrilobular necrosis.[113] In septic shock, ischemic hepatitis was described to occur in 13% of patients in one recent series. The development of ischemic hepatitis was associated with a significant increase in mortality.[114]

Ischemic hepatitis can arise as a complication of multiple primary disease processes, including hypovolemic shock in sepsis, cardiogenic shock, diabetic ketoacidosis, or hemorrhagic shock. In one series of 31 patients with ischemic hepatitis, cardiac factors were present in all patients, though cardiogenic ischemia was attributed as a causative factor in 77% of patients. The remainder of cases in that series were due to hypovolemia from hemorrhage, excessive dialysis or diuresis, or sepsis. 94% of patients in the study[113]had evidence of right sided heart failure, and most had relatively brief durations of hypotension (15-20 minutes.)[113] In a larger series of 142 patients, 56% of patients had congestive heart failure, and 14% had acute cardiac failure, with the remainder due to acute respiratory failure (13%) or circulatory shock (13%). [115]

Hypoxic hepatocytes have been reported have increased expression of Bcl2/adenovirus EIB Interacting Protein 3 (BNIP3). BNIP3 translocated into cytoplasm under conditions of low oxygen tension, including a murine model of ischemic liver injury, and knockdown of BNIP3 was able to ameliorate hepatocyte cell death in an *in vitro* model of hypoxic injury. [116]

Obstructive Sleep Apnea

An association has been described between obstructive sleep apnea (OSA) and non-alcoholic fatty liver disease and/or NASH, but remains controversial.[117] Several studies have linked OSA, and in particular, the incidence of apneic-hypopneic episodes, to elevation of liver enzymes and the histologic appearance of NASH.[118, 119] A major confounding factor is the frequent comorbidity of obesity and/or the metabolic syndrome; however, one recent study suggested that even among obese patients, nocturnal oxygen desaturation contributed to insulin resistance and liver injury, including fibrosis, inflammation and ballooning necrosis, but not the appearance of steatosis.[120] A study of 83 patients with OSA and matched controls suggested that there was a relationship between OSA and progression of steatosis to steatohepatitis, based on serum levels of type III procollagen.[121] In a larger study of 218 patients with OSA, severe OSA (defined as greater than 50 Apneic/Hypopneic episodes/hour, AHI) was associated with an increased liver enzymes (OR 5.9, $p<0.02$). Patients with AHI greater than 50/hour were also much more likely to have steatosis, lobular necrosis, and fibrosis by liver biopsy.[122]

Several studies in mouse models have offered some data to corroborate this observation. In one study, chow-fed mice were exposed to either room air or 12 hours of room air and 12 hours of chronic, intermittent hypoxia (CIH, approximately 5% oxygen for periods of 30 seconds followed by 21% oxygen for periods of 30 seconds). After 12 weeks on the CIH regimen, mice developed increased serum ALT, serum triglycerides, and serum cholesterol, as well as increased NFκB DNA- binding activity in liver nuclear extracts.[123] In mice genetically predisposed to obesity, CIH increased liver triglycerides and phospholipids, as well genes of lipid biosynthesis, including SREBP1c, Acetyl-coenzyme A Carboxylase, and Steroyl-

CoA Desaturases 1 and 2.[124] In a third study, WT mice were maintained on a high-fat diet and exposed to either room air (21% oxygen) or room air with period of intermittent hypoxia (as described above) for six months. At the conclusion of the study, CIH mice had a marked elevation in serum AST and ALT, some increase in inflammatory cytokines, and increased serum and liver malondialdehyde, myeloperoxidase, and alpha-1 collagen; however, liver triglycerides were unchanged, and only a mild enhancement of oil-red O staining was observed in CIH-treated mice.[125] The lack of an increase in steatosis (as quantified by increased oil-red O and liver triglyceride) in this model is surprising, but perhaps not unexpected given the significant metabolic stress induced by 6 months of high-fat-diet feeding.

Acetaminophen Poisoning

The model that is emerging from these studies suggests that milder periods of hypoxia, such as moderate OSA, are insufficient by themselves to cause progression to hepatitis/ steatohepatitis. However, when CIH is added to a primary insult, such as diet-induced steatosis, there is a predilection towards progression of liver injury. Corroborating evidence from other disease models includes the observation that sublethal acetaminophen poisoning resulted in fulminant liver failure when given in combination with CIH. [123] A more recent extended this work by combining CIH with daily injections of low-dose acetaminophen (APAP, 200mg/kg) in mice for 4 weeks. At the end of the study period, CIH/APAP mice had markedly elevated liver enzymes, including serum AST, ALT, GGT, and total bilirubin whereas no elevation was observed in mice with APAP alone, and only AST increased in mice with CIH alone.[126]

Some evidence related the HIF pathway and acetaminophen toxicity. HIF1α nuclear protein was observed to accumulate within 1 hour after a toxic dose (300mg/kg) of APAP; this increase in HIF1α was prevented by N-Acetylcysteine.[127] Pretreatment with Salidroside, an extract of an herbal compound used in Chinese medicine to ameliorate mountain sickness, was able to prevent ALT, AST, and serum TNFα in a mouse model of sublethal APAP toxicity when . Though HIF1α immunostaining was reported to be suppressed by salidroside pretreatment in that study, no immunoblots or mRNA data was presented.[128] It is unknown whether the role of HIF1α in APAP injury is protective or deleterious; for example, treatment of APAP-challenged mice with hyperbaric oxygen was able to improve survival, even though it increased HIF1 protein and the downstream target Glut1.[129]

Alcohol Mediated Liver Injury

As has been previously reviewed, chronic ethanol has diverse effects on cellular signaling and profoundly affects cellular metabolism and organ physiology.[130] The development of hypoxia in alcohol-exposed liver has also been reported and reviewed elsewhere.[131] Exposure of thin liver slices to acute ethanol was reported to increase oxygen consumption over three decades ago.[132] Acute ethanol causes a rapid increase in liver metabolism, including rapid induction of alcohol detoxifying enzymes and hepatic oxygen consumption within 2-3 hours.[133] More recently, acute ethanol was found to result in increased areas of staining using the hypoxia-specific marker pimonidazole; this effect appeared to be at least partially dependent on functional hepatic Kupffer cells.[134] This finding was replicated by the same group in a model of chronic continuous enteral alcohol treatment.[135]

The metabolism of alcohol in the liver is complex and proceeds by at least three mechanisms. First, and possibly best known, is the oxidation of alcohol to acetaldehyde by alcohol dehydrogenase (ADH) in a reaction that coordinately creates the reduced species NADH. Second, CYP2E1 catalyzes a hydroxylation of alcohol via an NADPH-dependent mechanism, primarily in the hepatocyte endoplasmic reticulum. Lastly, peroxisomal catalase enables oxidation of alcohol via an H_2O_2-dependent mechanism.[94] Each of these steps alters the cellular redox state and can result in the production of highly reactive oxygen intermediates.

Recent gene array data from ethanol-fed and pair-fed mice demonstrated upregulation of multiple genes in the glycolytic pathway, as well as genes in lipid metabolic pathways in the livers of chronically alcohol fed mice.[136] Although not explored in that publication, most, if not all of these genes may be regulated by HIF1α. An earlier report suggested an upregulation of HIF1α mRNA in the livers of chronic alcoholics.[137] One group offered some data to indicate that HIF1α mRNA is cyclically regulated with the urinary alcohol cycle in a model on continuous, intragastric ethanol feeding.[138] More recently, in the hypercholesterolemic ApoE(-/-) mouse, ethanol significantly increased HIF1α protein in liver, and a synergistic upregulation with tobacco smoke was observed.[139]

In addition to these mechanisms, it has been well established that alcoholic liver disease proceeds in part through a combination of prolonged metabolic insult coupled with activation of signaling through innate immune mechanisms. Given the role of HIFs in innate immunity as described further below, it is quite possible that the contribution of HIFs to alcoholic liver disease proceeds both through pathways of innate immunity as well as through pathways in the hepatocyte, including hepatic lipid accumulation.

Hypoxia inducible factors and immunity

In alcoholic liver disease (ALD) and non-alcoholic steatohepatitis (NASH), activation of Toll-like receptors by gut-derived endotoxin has been demonstrated to contribute to disease pathogenesis.[140] Several reports indicate that activation of HIF1α plays a pivotal role downstream of LPS signaling through TLR4. LPS upregulated hepatic HIF1α in rats, as well as HIF1α target gene aldolase.[141] In macrophages, LPS stimulation was able to upregulate HIF1α target genes, including VEGF, PAI-1, and iNOS, as well as HIF DNA binding and HIF1α mRNA and protein.[142] Using a cre-lox system of targeted HIF1α mutation to a transcriptionally inactive form, one group recently reported that knockdown of HIF1α transcriptional activity in cells of the myeloid lineage (LysMCre/$HIF^{flox/flox}$ mice) resulted in protection from LPS-induced sepsis. LysMCre/$HIF^{flox/flox}$ mice had lower levels of pro-inflammatory cytokines, including IL-6, IL-12, and TNFα, and maintained blood pressure and body temperature in the face of LPS challenge at levels that induced septic shock in wild-type mice.[143] Subsequent work indicated that LPS-induced HIF1α activity is dependent upon transcriptional regulation through the inflammatory master regulator group of proteins NFκB.[144] NFκB transcriptional activity is predominantly regulated through the inhibitory action of Inhibitor of κB proteins (IκB), which themselves are targeted for degradation by phosphorylation via the action of IκB Kinases (IKKα, IKKβ, the latter being the major isoform.) IKKβ deletion, then, renders cells unable to phosphorylate IκB and thereby inhibits NFκB signaling. Stimulation of bone-marrow-derived macrophages from mice in which IKKβ had been deleted by cre-lox mediated recombination (IKKβ-null mice) resulted in diminished HIF1α target gene

mRNAs. Additionally, HIF1α mRNA was suppressed in IKKβ-null mice prior to any stimulation, indicating that NFκB may regulate HIF1α at the transcriptional level.[145] Other investigators have found that virtually all NFκB subunits can transactivate the HIF1α promoter, that TNFα treatment recruited the NFκB subunits RelA and P65 to the HIF1α promoter, and that blockade of both IKKα and IKKβ proteins was required to suppress NFκB-induced HIF1α activation.[144]

Although a role for HIF1α activation in NASH has not been thoroughly investigated, pharmacological inhibition of IKK proteins, analogous to IKKβ-null strategies, was able to prevent steatosis and the development of NASH. IKK-inhibitor-treated animals on a high sucrose diet displaying lower levels of steatosis, hepatic triglyceride, and diminished secretion of pro-inflammatory cytokines including IL-6, and TNFα. Additionally, IKK-inhibitor treated animals were protected from the development of fibrosis.[14]

These data suggest that the activation of the pro-inflammatory cascade downstream of LPS-TLR4 signaling may be at least partially dependent upon functional HIF1α signaling. In contrast, in other cell types, some data suggests that HIF1α may suppress T-cell mediated inflammation. HIF1α knockout in T-lymphocytes prevented sepsis and mortality after cecal ligation and puncture (CLP), and T-Cell specific HIF1α(-/-) mice had significantly lower levels of serum ALT 72 hours after CLP challenge than WT mice.[146] Knockout of HIF1α in T-and ex-vivo stimulation of T-cells from T-cell specific HIF1α (-/-) mice resulted in higher levels of IL2 and IFNg, suggesting that the survival benefit of T-Cell specific HIF1α knockout may be at least partially due to a derepression of HIF1α inhibition of pro-inflammatory cytokine release. [146]

Hypoxia inducible factors: a common mechanism of lipid accumulation?

Multiple lines of evidence suggest that hypoxia and/or HIF may play a role in hepatic lipid accumulation. Numerous studies have implicated a role for hypoxia in altering lipid storage in various cell types. Rats exposed to chronic hypoxia accumulated foam cells in pulmonary alveoli.[147] Hypoxia was described to cause lipid-loading of macrophages, and this effect was prevented by HIF1α siRNA treatment.[148, 149] The differentiation of 3T3-L1 preadipocytes to an adipocytic phenotype was found to be partially dependent on HIF2α, which is transcriptionally regulated in adipocytic differentiation.[150] Forced expression of HIF1α in cardiomyocytes resulted in increased lipid accumulation, and was correlated to a suppression of peroxisome-proliferator-alpha DNA binding.[151] A recent study in breast cancer cell lines demonstrated an increase in HIF1 expression downstream of Akt signaling resulting in an increase in fatty acid synthase (FAS) which is over-expressed in several types of solid tumors. [152]

In hepatocytes, germline deletion of HIF2α resulted in neonatal death and a phenotype of severe steatosis.[153] Although this study suggests that the absence of HIF2α predisposes to steatosis, numerous other studies in vitro and in vivo have suggested that this observation does not apply to the role of HIFs in the adult liver. Hepatocyte specific deletion of the VHL gene is accompanied by a phenotype of hypervascularity and steatosis.[154] Simultaneous introduction of degradation-resistant transgenic constructs of HIF1α and HIF2α resulted in a similar phenotype of hepatic lipid accumulation; in that study, introduction of degradation-resistant HIF1α alone caused a mild phenotype of lipid accumulation, and introduction of degradation-resistant HIF2α alone caused a phenotype of hypervascularity, including the formation of

cavernous hemangioma, without lipid accumulation.[97] More recently, a different group described lipid accumulation in a murine model of liver-specific HIF2 activation.[155] In that study, mouse models with cre-lox mediated deletion of VHLH, HIF1α, and/or HIF2α resulted in mice in which both HIF1 and HIF2 or only one or the other isoform was active. HIF2 appeared to play a major role in regulating hepatic lipid by various mechanisms, including the upregulation of lipid biosynthetic pathways, the suppression of fatty acid β-oxidation, or upregulation of the lipid droplet surface protein ADFP.[155]

HIFs and metal accumulation in liver disease

Iron accumulation has a role in the pathogenesis of several hepatic diseases, including alcoholic liver disease, and hereditary hemochromatosis. Macrophage iron increased the severity of alcoholic liver disease in a rodent model.[73] In conditions of chronic iron deficiency, iron export is limited by production of hepcidin, which in turn degrades the iron efflux protein ferroportin. Using a model of hepatocyte specific HIF1α deletion, Peysonnaux and colleagues demonstrated that functional HIF1α is partially responsible for the downregulation of hepcidin in chronic iron deficiency.[156] In support of this, ARNT-knockout mice, which are completely defective in HIF signaling, accumulated high levels of iron.[157] Hypoxia Inducible factors have been implicated in gut iron absorption, where some recent data showed that deletion of HIF2α, but not HIF1α, in intestinal cells resulted in downregulation of serum iron and intestinal expression of the divalent metal ion transporter-1 (DMT1) .[158] A similar effect of HIF1α expression on DMT1 was observed in HEPG2 cells.[159]

Liver Fibrosis

Recent evidence also indicates a profound effect of HIF1 on cholestatic liver injury. Moon et al. recently described the effect of HIF1α deletion in bile-duct ligated mice, a model of cholestatic liver injury. Mice with a floxed HIF1α exon were mated to Mx-Cre mice. The Mx-Cre promoter enables near total excision of floxed genetic elements in cells of the immune system and the liver and partial deletion in other body tissues following serial injections of poly-I:C. Deletion of HIF1α was followed with bile duct ligation (BDL) or sham ligation. In WT mice, an increase of pimonidazole stained areas and accumulation of HIF1α was observed as early as 3 days following BDL. Both HIF1αflox/MxCre and WT mice displayed similar increases in ALT, AST, and serum bile acids, but HIF1αflox/MxCre mice were protected from increases in collagen synthesis and alpha-smooth muscle actin staining, both markers for tissue fibrosis, as well as profibrotic mediators including PAI-1 and Platelet-Derived Growth Factor (PDGF) A and PDGF-B.[160] In a series of *in vitro* experiments, the same group reported that production of profibrotic mediators was induced by culturing mouse hepatocytes in 1% oxygen. Using an siRNA approach, the authors demonstrated that the production of profibrotic mediators was completely prevented in ARNT-null cells, but only partially prevented in HIF1α-null cells, suggesting that other HIF isoforms (particularly, HIF2) play a role.[161]

These data in support of a role for HIF in liver fibrosis are rendered more compelling by evidence in other models of liver fibrosis. After five weeks of once-weekly diethylnitrosamine (DEN) injections (100mg/kg), pronounced collagen septa may be observed, and progression to cirrhosis is observed by 8 weeks. Collagen mRNA transcripts were increased in isolated hepatic stellate cells cultured under hypoxia. In DEN-treated mice, Vascular Endothelial Growth Factor

(VEGF) isoforms were increased with increasing time of treatment, becoming strongly positive by northern blot and immunohistochemical staining by 8 weeks of DEN treatment, and were correlated with increase in tissue hypoxia as observed by pimonidazole staining.[162]

In vitro models have been in concordance with the previous findings. Stellate cell activation has been described as an initiating factor in liver fibrosis. Exposure of the hepatic stellate cell line LX-2 to hypoxia stimulated HIF1α and VEGF mRNA accumulation by 8 hours, and was associated with evidence of increased signaling through the TGFb-SMAD dependent pathway. Comparison of a gene array using LX-2 cells in normoxia and hypoxia revealed several targets, including fibroblast growth factor-4, that have been implicated in fibrogenesis or [163]inflammation.[164] Another study also reported activation of HSC by hypoxia, and demonstrated that this activation was accompanied by secretion of proangiogenic cytokines, such as VEGF and ANG-1, which were able to stimulate HSC chemotaxis in an autocrine or paracrine fashion.

Viral Hepatitis

Several studies have illuminated the role of HIFs in the pathogenesis of viral hepatitis, including hepatitis B, hepatitis C, and hepatitis E. In a series of HCC cases secondary to primary HBV infection, Hepatitis B Virus X protein [HBx] was found to correlate with HIF1α expression, and transfection of HBx in HepG2 cells was found to increase HIF1α protein accumulation.[165] An earlier study similarly reported the stabilization of HIF1α protein in the presence of the HBx protein, and that this stability correlated with promoter activity of HIF1 at the Multi Drug Resistance-1 protein, an efflux drug transporter thought to be primarily

responsible for chemoresistance in HCC. HIF1α siRNA treatment was able to abolish the activation of an MDR-1-luciferase construct induced by HBx transfection.[166] These findings were confirmed and extended in another study that reported that HBx protein increased levels of Metastasis Associated Protein 1 (MTA1) and Histone Deacetylase 1 (HDAC1). These two proteins in turn physically associated with HIF1α, and contributed to HIF1α stability.[167]

The hepatitis E virus (HEV) open reading frame protein 3 (ORF3) is a viral protein thought to be required for infection. In an *in vitro* system of hepatocyte cell lines expressing HEV ORF3, upregulation of several glycolytic pathway enzymes was reported, and correlated with increased expression and DNA-binding activity of HIF1α. This expression was correlated with increased Akt phosphorylation as well as increased phosphorylation of the CBP/p300 transcriptional co-activator via an ERK-dependent mechanism.[168]

Hepatitis C infection may interact with the HIF1α pathway via multiple mechanisms. Huh7 cells expressing the HCV core protein were reported to have increased VEGF expression and increased HIF1α DNA binding by EMSA; this binding was partially abrogated in the presence of PD98059, an ERK inhibitor.[169] Transient HCV infection in Huh7 cells was associated with HIF1α stabilization by 3 days; furthermore, in Huh7 cells expressing subgenomic HCV replicons, HIF1α was also stabilized. This stabilization again appeared to be dependent on multiple kinase and transcriptional pathways, as functional ERK and PI3K inhibition was able to prevent HIF1α protein accumulation, as was Stat3 inhibition and NFκB inhibition. HIF1α stability was accompanied by production of functional VEGF. [169]

HIF in liver regeneration

HIF1α is rapidly induced in liver after partial hepatectomy, and remains upregulated for up to 24 hours.[170] Prolactin treatment was able to increase the proliferative response after partial hepatectomy, and was also able to upregulate HIF1α protein and VEGF.[171] However, in another study, hyperbaric oxygen pretreatment, which upregulates HIF1α protein, was unable to accelerate liver regeneration after partial hepatectomy; however, BRDU uptake, and indicator of cellular proliferation, was upregulated in hepatic sinusoidal endothelial cells.[172] Oncostatin M (OSM) is an IL-6-type cytokine secreted by leukocytes that has been described to have a role in liver regeneration, liver development, and angiogenesis.[173] A recent report offered data to demonstrate that OSM is able to up regulate HIF1α protein levels and HIF1α target genes, including PAI-1 and VEGF, in a Stat3 dependent mechanism. Further, the upregulation of HIF1 appeared to be at the transcriptional level.[173]

Hepatocellular Carcinoma

Significant evidence indicates that the HIFs play an important role in the pathogenesis and pathophysiology of hepatocellular carcinoma. HIF1α and VEGF were found to be expressed at higher levels in dysplastic nodules and implicated in malignant transformation.[174] This finding was confirmed in humans and extended by the description of HIF1 expression in chemically-induced preneoplastic lesions in mice.[175] Notably, this expression was independent of tissue hypoxia, as HIF1 positive areas did not differ from other regions of the liver in terms of needle-electrode measured oxygen tension and pimonidazole staining; however, HIF1 levels were effectively reduced by treatment with the PI3K inhibitor LY294002, raising the possibility of a PI3K-Akt dependent mechanism [175]. Recent data also suggest that inhibition of HIF may

have a role in cancer therapy. Nonresectable hepatocellular carcinomas may be treated by transarterial catheter embolization (TAE) in which tumor vessels are occluded via catheter-guided placement of a coil or other occluding agent. Drawbacks of this approach include an uncertain survival benefit, as well as a possible induction of tumor neovascularization following TAE. Following the observation that neovascularization of embolized tumors proceeds with upregulation of VEGF, delivery of antisense oligonucleotides against HIF1α in combination with TAE was able to improve efficacy of TAE in promoting tumor necrosis and preventing neovascularization. Furthermore, in that study, the ability of tumor cells to survive on glycolytic metabolism alone (the so-called Warburg effect) was inhibited through suppression of HIF1α glycolytic target genes, including the glucose transporter GLUT1 and Lactate Dehydrogenase A. [176]

The data from clinical studies paint a similar picture. In one series of cases, up to 50% of HBV-association hepatocellular carcinomas expressed high levels of HIF1α, and HIF1α expression correlated with metastases and decreased survival.[165] Poor prognosis was also associated with expression of Metastasis Associated Protein-1 (MTA-1), which is described as a stabilizer of HIF1α. Patients with MTA-1 positive cancer had larger tumors with increased incidence of microvessel invasion and nodal extension. The incidence of extrahepatic metastases was almost twofold higher (23% versus 12%, $p<0.001$) in patients with MTA positive lesions than in patients with MTA negative lesions. The prevalence of MTA-1 positive staining was higher in patients with HCC secondary to primary HBV infection than from other causes, including HCV infection or nonviral etiologies.[177]

Both HIF1α and HIF2α isoforms have been reported to be overexpressed in hepatocellular cancer. In one series of patients, HIF2α expression was found to be present in 52% of HCC, and correlated with tumor size, capsule infiltration, portal vein invasion, and necrosis.[178] A subsequent larger study found HIF2α expression in 69.5% of HCC cases, as well as 55% of adjacent tissue, but no expression in noncancerous tissue, suggesting that HIF2α expression may be a preneoplastic feature of tumors or a feature of tumor-associated stroma. In that study, high HIF2α expression was also correlated with vascular endothelial growth factor expression, microvessel density, and decreased survival.[179]

HIF1α inhibition may play a role in anticancer therapeutics. RNA-mediated inhibition of HIF1α was able to slow tumor growth.[180] The antitumor efficiency of doxorubicin was increased when combined with a HIF1α antisense oligonucleotide.[181] Rapamycin inhibits signaling by the Mammalian target of Rapamycin (mTOR) complex pathway, and has shown some efficacy against hepatocellular carcinoma. The prevention of HCC tumor growth by rapamycin in a rodent model was correlated to suppression of HIF1α by rapamycin.[182] Another compound, silibinin, was demonstrated to have some antitumor efficacy through phosphorylation of mTOR, and was also associated with suppression of HIF1α signaling.[183]

Summary

Hypoxia has been implicated in the pathogenesis of a wide range of hepatic disease. (Figure 4) In most of these models, some data exists to implicate a role for hypoxia inducible factors. Consideration of the role of HIFs in liver diseases should include multiple cell types, as HIF1α activity has been implicated in hepatocytes as well as myeloid (Kupffer cells) and

lymphoid (T-cells) lineage immune cells. Taken collectively, these findings strongly suggest that anti-HIF therapies will be greatly useful in the management of hepatic diseases of various etiologies.

With regards to alcoholic liver disease, there are several broad questions that remain unresolved. First, if HIFs are related to lipid accumulation, as some studies have suggested, a remaining question is whether an upregulation of HIF1α contributes to hepatic lipid accumulation in alcoholic liver disease. For example, much of the information we have that relates HIFs to lipid accumulation relies on the use of conditional knockouts of VHL or HIF overexpression systems, which may manifest steatosis as an artifact of transgene expression. Hence, the first group of experiments described below were designed to rigorously establish a role for HIFs in ALD by examining protein, mRNA, DNA binding, and expression levels of target genes. Though those studies, described below in Chapter 2, establish correlative evidence between the phenotype of alcoholic liver disease and detection of HIF isoform expression and activity, the question of the specific contribution of HIFs to steatosis in ALD remains unresolved. Three broad strategies were used to answer that question, first examining hepatocyte-specific HIF1α overexpression in a murine model of ALD, and determining that the presence of the HIF1α transgene was sufficient to drive increases in lipid accumulation. The effect of HIF1α on lipid accumulation was then replicated *in vitro,* using a model system of *in vitro* lipid accumulation in a hepatoma cell line along with plasmids that encoded active HIF-α isoforms or siRNAs targeting HIF-α subunits. These experiments offered further strong evidence that HIF1α activation leads to increased lipid accumulation. Following the finding that inhibition of the HIF1α subunit prevented lipid accumulation in vitro, we then sought to determine whether

limiting HIF1α activity would be able to prevent the development of ALD. Using a Cre-Lox system with a floxed HIF1α allele, and by expressing Cre recombinase under control of two different promoters, we investigated the effect of limiting HIF1α activity in hepatocytes or cells of the myeloid lineage.

The latter experiments, described in chapter 5, also begin to consider another remaining question on the development or progression of alcoholic liver disease, namely, what the relative contribution of cell types in the liver is to the development of ALD, and whether HIF1α expression is a determinant of ALD in hepatocytes, cells of the myeloid lineage, or both. As the progression of ALD appears to occur with repeated inflammatory attacks on a background of steatotic hepatocytes, one question is whether hepatocytes exposed to chronic ethanol actually participate in the inflammatory response, or whether it is solely a Kupffer cell mediated effect. In the latter case, in particular, steatotic hepatocytes may be more prone to cell death after proinflammatory stimulus. In the former case, chronic alcohol-exposed hepatocytes themselves may contribute to the inflammatory response. In support of that possibility, we report in chapter 5 that modifying HIF1α activity in hepatocytes has a profound effect on the secretion of cytokines after chronic alcohol exposure.

Figure 4. **Hypoxia Inducible Factors Across the Spectrum of Liver Diseases**

(**A.)** Normal livers have zonal oxygen gradients, and regions of relative hypoxia. HIF1a, HIF2a, and HIF3a mRNA is observed. **(B, C, D)** Chronic alcohol, Non-Alcoholic Fatty Liver Disease, and obstructive sleep apnea are all disease conditions that are related to steatosis. The phenotype of fatty liver has been recapitulated by HIF activation in mouse models. **(E, G)**. Both non-alcoholic and alcoholic steatohepatitis are marked by inflammatory processes downstream of TLR pathways, particularly TLR4; activation of TLR4 and subsequent release of TNFa may be influenced by HIF activation. **(F)** Cholestatic liver injury can result in fibrosis; inducible knock-out of HIF1a in a mouse model of bile-duct ligation was able to prevent fibrosis. **(G)** Fibrosis is also marked by stellate cell activation, which has been shown to have some dependence on hypoxia. **(H)** Chronic alcoholic steatohepatitis may also progress to fibrosis; the role HIF1a in this process is unknown, but may resemble HIF activation in other forms of fibrosis. **(I)** Ischemic hepatitis is marked by centrilobular necrosis and profound tissue hypoxia. **(J)** Viral proteins in several forms of viral hepatitis can activate HIF1a. **(K)** HIF1a is implicated in iron and copper metabolism, and thus may be related to the pathology observed in Wilson's Disease, Hemochromatosis, and chronic alcoholism. **(L)** HIF1a accumulation is an early event in acetaminophen-induced liver injury. **(M)** Some upregulation of HIF mRNA was reported in cirrhosis. **(N)** Hepatocellular cancer is often marked by HIF activation, which can be associated with aggressive phenotype and worse prognosis.

Figure 4

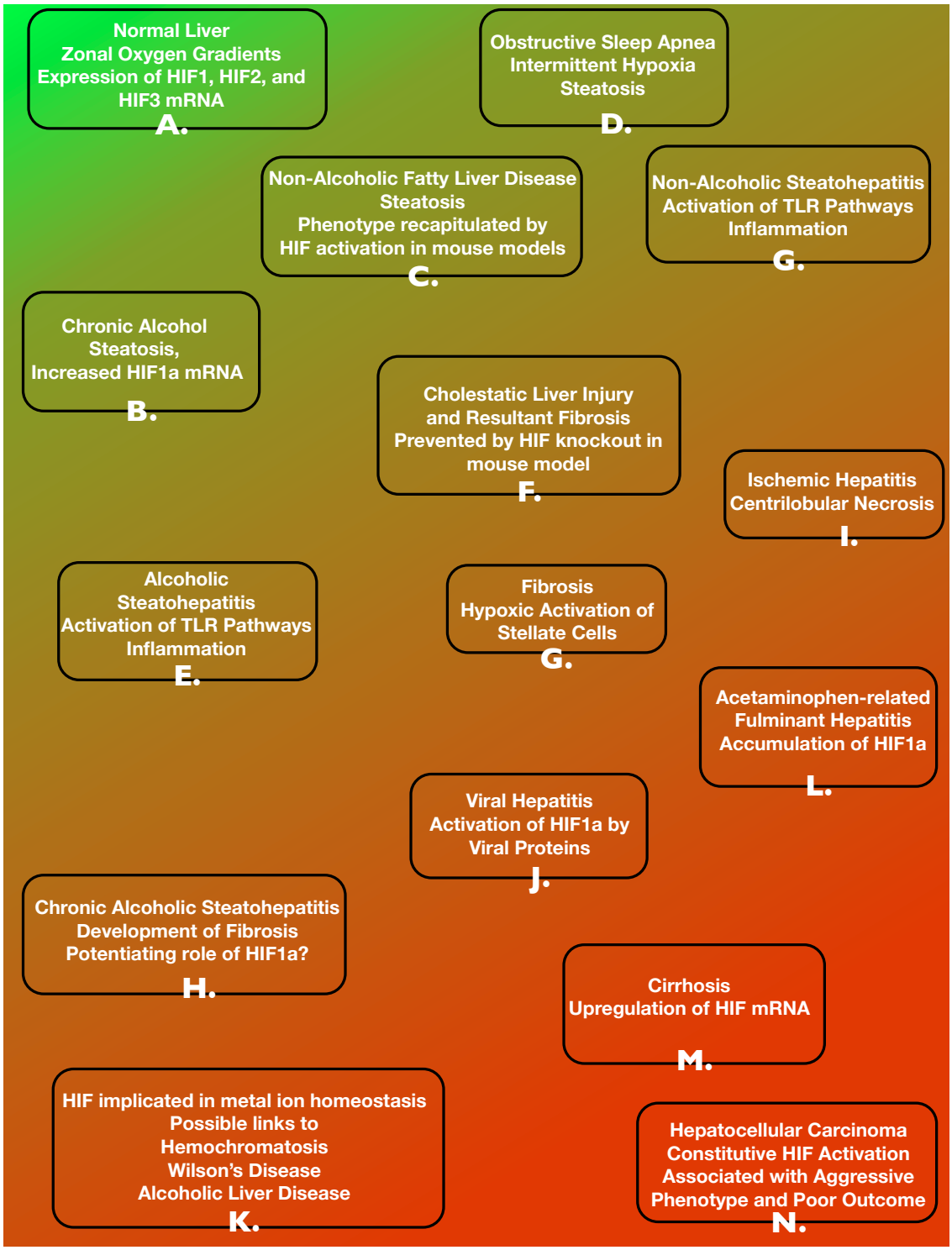
Normal Liver
Zonal Oxygen Gradients
Expression of HIF1, HIF2, and HIF3 mRNA
A.
Obstructive Sleep Apnea
Intermittent Hypoxia
Steatosis
D.
Non-Alcoholic Fatty Liver Disease
Steatosis
Phenotype recapitulated by HIF activation in mouse models
C.
Non-Alcoholic Steatohepatitis
Activation of TLR Pathways
Inflammation
G.
Chronic Alcohol Steatosis,
Increased HIF1a mRNA
B.
Cholestatic Liver Injury and Resultant Fibrosis Prevented by HIF knockout in mouse model
F.
Ischemic Hepatitis
Centrilobular Necrosis
I.
Alcoholic Steatohepatitis
Activation of TLR Pathways
Inflammation
E.
Fibrosis
Hypoxic Activation of Stellate Cells
G.
Acetaminophen-related Fulminant Hepatitis
Accumulation of HIF1a
L.
Viral Hepatitis
Activation of HIF1a by Viral Proteins
J.
Chronic Alcoholic Steatohepatitis
Development of Fibrosis
Potentiating role of HIF1a?
H.
Cirrhosis
Upregulation of HIF mRNA
M.
HIF implicated in metal ion homeostasis
Possible links to
Hemochromatosis
Wilson's Disease
Alcoholic Liver Disease
K.
Hepatocellular Carcinoma
Constitutive HIF Activation
Associated with Aggressive Phenotype and Poor Outcome
N.

CHAPTER 2

HYPOXIA INDUCIBLE FACTORS IN A MURINE MODEL OF ALCOHOLIC LIVER DISEASE

Summary

Chronic ethanol consumption leads to a spectrum of liver pathology that begins with hepatic lipid accumulation, or steatosis, and may progress with prolonged inflammatory insult to steatohepatitis and cirrhosis; the latter being a major risk factor for hepatocellular carcinoma. The liver in chronic alcohol abuse develops regions of hypoxia, and scattered data have suggested that hypoxia-inducible factors may be upregulated in the livers of patients with alcoholic liver disease. In the studies that follow, we offer evidence for the activation of hypoxia inducible factors in a murine model of chronic alcohol feeding. We establish that HIF1α and HIF2α are upregulated at the protein and the mRNA level. We further offer evidence that HIF protein is functional, based on increased HIF DNA binding using the electrophoretic mobility shift assay (EMSA). We analyze expression of several genes that are downstream targets of HIF1, and demonstrate that some, but not all, HIF1 target genes are upregulated by chronic alcohol feeding.

Acknowledgements

The author is grateful to Istvan Hritz for the provision of tissue samples from chronic ethanol fed mice that were used for preliminary studies related to this project, and to Donna Catalano, who assisted with mouse feedings.

Introduction

Alcoholic liver disease [ALD] can be viewed as a spectrum of disorders ranging from the mild and reversible (e.g., steatotic accumulation) to the life-threatening and irreversible (cirrhosis). The cellular and molecular mechanisms that contribute to damage in ALD continue to be elucidated, and over the past several decades, numerous paradigms have been proposed, including the pivotal inflammatory role of tumor necrosis factor alpha (TNF-alpha) signaling downstream of Toll-like-Receptor-4 (TLR4) stimulation by gut-derived endotoxin.

The Hypoxia Inducible factors (HIFs) are a family of heterodimeric transcription factors that promote a homeostatic transcriptional response to low oxygen tension. Mature HIF is composed of one of three isoforms of an alpha- subunit (HIF1α, HIF2α, or HIF3α) and a β subunit, the major isoform of which is termed HIF1β or the Aryl-Hydrocarbon Receptor Nuclear Translocator (ARNT). Under conditions of normal oxygen tension, the alpha subunits of HIF are rapidly degraded in the cytoplasm. The major pathway of degradation involves scaffolding of the alpha subunits on the protein product of the Von-Hippel Lindau tumor suppressor gene, where they are hydroxylated on specific proline residues. Proline hydroxylation of HIF alpha subunits leads to their ubiquitination and degradation by the proteasome. Under conditions of low oxygen tension, HIF alpha subunits escape hydroxylation and dimerize with HIF1B/ARNT, translocate to the nucleus and activate hypoxia response elements (HRE) in the genome. HIFs are named by their alpha subunit, with HIF1 and HIF2 having a wide, overlapping but non-identical set of transcriptional targets. Recent investigation with a murine model of hepatocyte specific HIF activation demonstrated that simultaneous activation of HIF1 and HIF2 results in a phenotype of hepatomegaly with macrovesicular lipid accumulation.[97] In that stud, activation

of HIF1 alone resulted in minimal lipid accumulation, while activation of HIF2 alone resulted in gross vascular changes without any appreciable increase in hepatic lipid. However, the relationship of this phenotype to human diseases characterized by steatosis, e.g., alcoholic steatosis or non-alcoholic fatty liver disease, remains to be elucidated.

Scattered data from the research literature support a role for hypoxia-inducible factors in the spectrum of ALD. Liver hypoxia has been documented in rats on a continuous ethanol diet, and some investigators suggest that a process analogous to ischemia-reperfusion injury may be implicated. Others have postulated an increase in HIF1 mRNA as a mechanism of ethanol-induced liver injury. However, the direct contribution of HIF1 to alcoholic liver injury is unknown.

We hypothesized that HIF1s protein would be upregulated in the livers of mice after chronic ethanol feeding. As HIF1α is primarily regulated by post-translational hydroxylation and degradation though the ubiquitin-proteasome pathway, we postulated that changes in HIF1 levels might not correlate with changes in HIF1α mRNA. Because both HIF1α and HIF2α were required for maximal lipid accumulation in a mouse model of constitutive activation of HIF isoforms, we postulated that both HIF1 and HIF2 protein would be increased with chronic ethanol feeding. Finally, we hypothesized that an increase in HIF1 protein would be accompanied by an increase in the mRNA of HIF1 target genes.

In this chapter, we present evidence that HIF1α is upregulated in an oral, ad libitum model of ethanol-induced liver injury. C57Bl6 mice were maintained on the Lieber-DeCarli ethanol-containing diet for four weeks. In order to demonstrate that functional HIF1 is increased in the livers of ethanol-fed mice, we utilize western blotting to show increased HIF1α protein

and EMSA to demonstrate increased HIF DNA binding. This increase in HIF1 expression correlated with the expression of some, but not all, HIF1 target genes. In addition to HIF1, we present evidence that HIF2α protein is increased in the livers of mice maintained for four weeks on the Lieber De Carli ethanol-containing diet. Finally, we offer evidence that the hepatic regulation of HIF1α and HIF2α with chronic alcohol is not only at the post-translational level, but that significant upregulation of HIF1α mRNA is also observed.

Methods

Animal Studies

All animals received care in compliance with protocols approved by the Institutional Animal Use and Care Committee of the University of Massachusetts Medical School. For all mouse studies, mice were gradually habituated to a Lieber-DeCarli liquid diet with 5% ethanol (volume/volume) over a period to two weeks, then maintained on the 5% diet for four weeks. Consumption was recorded daily, and isocaloric amounts of a non-alcohol containing diet (in which dextran-maltose replaced calories from ethanol) were dispensed to pair-fed animals. Weights were recorded before the introduction of the diet and weekly thereafter. Wild-type mice (C57/Bl6) were purchased from Jackson Laboratories (Bar Harbor, Maine). At the conclusion of the feeding, mice were weighed and euthanized. Livers were excised and weighed, and divided and portions were snap frozen in liquid nitrogen for protein and biochemical assays, preserved in 10% neutral-buffered formalin for histopathological analysis, or soaked in RNALater (Qiagen GmbH, Hilden, Germany) for RNA extraction. Blood was collected and serum separated for biochemical analysis.

Biochemical Analysis

Serum alanine aminotransferase (ALT) was determined using a commercially available reagent (Advanced Diagnostics Inc, Plainfield, NJ). Briefly, 15ul of serum was mixed with 100ul of reagent diluted according to the instructions of the manufacturer, and UV absorbance at 37 degrees celsius was measured over three minutes. The average change in absorbance per minute interval is then multiplied by a conversion factor to yield ALT levels.

For liver triglyceride levels, liver whole-cell lysates were prepared as described below and lipids separated by isopropanol precipitation of non-lipid components. A commercially available kit (Wako Chemicals USA Inc., VA) was used to determine the triglyceride concentration.

Protein concentrations were determined by adding 1uL of whole-cell lysate or nuclear extract to Bradford reagent (BioRad) and by measuring the difference between absorbance at 650nM and 595nM on a 96 well plate using a plate reader. Concentrations were determined using a standard curve of bovine serum albumin.

RNA analysis

RNA was purified using the RNeasy Mini kit (Qiagen Sciences, Maryland, USA) with on-column DNA digestion (ProMega). cDNA was prepared using random hexamer primers and the Reverse Transcription System kit (Promega Corp., Madison WI). Real-time quantitative polymerase chain reaction was performed using an iCycler (Bio-Rad laboratories Inc., Hercules, CA), using specific primers. Primer sequences are shown in Table 1. Fold-change in gene

Table 1: Mouse Real-Time PCR Primers.

PAI-1
F: 5’-ATG CCA TCT TTG TCC AGC GG-**3’**
R: 5’-TTG GTA TGC CTT TCC ACC CAG-**3’**

ADRP
F: 5’ CTG TCT ACC AAG CTC TGC TC-**3’**
R: 5’-CGA TGC TTC TCT TCC ACT CC-**3’**

DEC1
F: 5’ CAT TTG CAC TTC AGG GAT T-**3’**
R: 5’ GCA CTT TCT CCA GCT GAT CC-**3’**

VEGF
F: 5’ CAT CTT CAA GCC GTC CTG TGT-**3’**
R: 5’ CAG GGC TTC ATC GTT ACA GCA-**3’**

HIF1a-
F: 5’- CAA GAT CTC GGC GAA GCA A-**3’**
R: 5’- GGT GAG CCT CAT AAC AGA AGC TTT-**3’**

HIF2a-
F: 5’-CCC AAG ACG GTG ACA TGA TCT-**3’**
R: 5’-CGC AAG GAT GAG TGA AGT CAA A-**3’**

EGLN3
F: 5’-AGG CAA TGG TGG CTT GCT ATC-**3’**
R: 5’-GCG TCC CAA TTC TTA TTC AGG T-**3**’

expression was determined by normalizing to a house keepig gene (18S mRNA) and calculating gene expression by the ΔΔCt method.

Histopathological Analysis

Sections of formalin-fixed livers were stained with hematoxylin/eosin and analyzed by microscopy.

Whole Cell Lysate

60mg of liver tissue was washed and subsequently homogenized in lysis buffer (9.5ml RIPA buffer, 1mM NaF, 2mM Na3VO4, 1 protease inhibitor tablet, 500ul PMSF) using rotor-stator homogenization. After 10 minutes of incubation on ice, homogenates were centrifuged at 10,000RPM for 10 minutes at 4 degrees C. The supernatant was collected and stored in aliquots at -80 degrees C.

Nuclear Extraction

60mg of snap-frozen liver tissue was washed in 10-fold excess volume TKM-0.32 buffer (0.32 molal sucrose, 50mM Tris-HCl, 25mM KCl, 5mM MgCl, 5mM PMSF, with protease inhibitor tablets (1 per 10ml of buffer, Sigma) and homogenized using a rotor-stator homogenizer (Ika). Homogenates were transferred to microcentrifuge tubes and centrifuged (10mins/1000rpm/4 degrees C.) Pelleted material was resuspended in TKM-2.0 buffer (2 molal sucrose, 50mM Tris-HCl, 25mM KCl, 5mM PMSF) and homogenized again by rotor-stator. Pellets were collected by centrifugation (60mins/14000rpm/4 degrees C) and resuspended in 400ul Buffer A (10mM

Hepes/KOH, pH 7.9, 2mM MgCl, 1mM EDTA, 10mM KCl, 1mM DTT, 5mM PMSF, 1 protease inhibitor tablet/5ml buffer). Pellets were again collected by centrifugation (2mins/ 14000rpm/4 degrees C) and resuspended in 50ul Buffer B (10mM Hepes/KOH pH 7.9, 2mM MgCl, 1mM EDTA, 50mM KCl, 300mM NaCl, 2mM DTT, 5mM PMSF, 1 protease inhibitor tablet (Sigma) per 5mL buffer, 10% glycerol). Resuspended material was frozen at -80 degrees overnight, thawed with gentle agitation at 4 degrees C. Supernatant containing nuclear extract was collected after centrifugation (10mins/14000rpm/4 degrees C) and assayed for protein concentration.

Electrophoretic Mobility Shift Assay

A consensus double-stranded Hypoxia Response Element (HRE) (Santa Cruz Biotech, CA) oligonucleotide was used for EMSA. End-labeling was accomplished by treatment with T4 kinase in the presence of [32P]ATP. Labeled oligonucleotides were purified on a polyacrylamide copolymer column (BioRad). Five micrograms of nuclear protein was added to a binding reaction mixture containing 50 mM Tris-HCl, pH 7.5, 5 mM MgCl2, 2.5 mM EDTA, 2.5 mM DTT, 250 mM NaCl, 20% glycerol, 20 μg/ml BSA, 2 μg poly(dI–dC) and 30,000 c.p.m. of 32P-labeled NFB oligonucleotide. Samples were incubated at room temperature for 30 min. Reactions were run on a 5% polyacrylamide gel and the dried gel was exposed to an X-ray film at –80°C overnight. Cold competition was done by adding a 20-fold excess of specific unlabeled double-stranded probe to the reaction mixture. Band density was quantified using Labworks 4.0 image analysis.

Western Blotting

30-50ug of nuclear extract was resolved on 10% polyacrylamide gels and transferred overnight to nitrocellulose support. Membranes were blocked overnight with blocking buffer (5% bovine serum albumin in Tris-Borate-SDS with 0.01% Tween 20) with refrigeration, and subsequently probed overnight with anti-HIF1α (R&D Biosciences) or anti-HIF2α (Chemicon) mouse monoclonal antibodies. Detection was performed using an anti-mouse horseradish-peroxidase conjugated secondary antibody and chemiluminescent substrates. Band density was quantified using Labworks 4.0 image analysis.

Results

Liver pathology in ethanol fed mice

We first undertook to reproduce liver pathology in an oral, ad libitum murine model of chronic alcohol-mediated liver injury. Six-to-eight week-old C57/Bl6 mice were gradually habituated to a liquid diet, and subsequently randomized into alcohol-fed or pair-fed groups. In the alcohol fed groups, the liquid diet was gradually supplemented with increasing percentages of 100% ethanol until a final ethanol concentration of 5% (v/v) was achieved. Consumption was recorded daily, and a control liquid diet that was isocaloric by volume to the ethanol-containing diet was prepared and dispensed to pair-fed animals. Over the five-week course of the feeding, weights were recorded weekly, and revealed similar weight-gain between pair-fed and ethanol-fed animals. (Figure 5A).

At the conclusion of the feeding, mice were sacrificed and livers and sera were collected. Because chronic ethanol consumption is known to induce steatosis, we first examined the weight

of excised livers and expressed this weight as a ratio to the sacrifice weight of the animal. We confirmed that ethanol fed mice had hepatomegaly as evidenced by higher liver-weight to body-weight ratios than pair-fed mice (Figure 5B). Hepatomegaly in chronic ethanol alcohol related liver injury is secondary to steatosis. Thus we sought to quantify the triglyceride content in liver tissue, as liver triglycerides are known to accumulate in response to chronic ethanol feeding. Lysates were prepared from portions of snap-frozen liver and analyzed for triglyceride content using a biochemical assay. In order to correct for inequalities between different initial tissue weights and sample-to-sample error in processing, final triglyceride concentration is expressed as a ratio to the protein concentration in each sample. As expected, triglyceride concentration in liver tissue from ethanol-fed mice was elevated significantly over that observed in pair-fed mice. (Figure 5C) Chronic ethanol feeding is also known to result in elevation of liver enzymes through hepatocyte injury. Using a biochemical assay, we found an increase in serum alanine aminotransferase (ALT) levels (Figure 5D).

We then examined the livers of ethanol-fed and pair-fed mice by histopathology. Formalin fixed tissue samples were processed onto slides and stained with hematoxylin and eosin. Microscopy revealed significant macrovesicular steatosis, with accumulation of large lipid droplets, in ethanol fed animals; pair-fed animals displayed minimal lipid accumulation. (Figure 6)

Expression of Hypoxia Inducible Factors with chronic alcohol feeding

We then turned to examine whether wild-type mice had increased expression of hypoxia-inducible factors using three different strategies. First, liver nuclear extracts were prepared and

Figure 5. Parameters of Liver Injury with Chronic Ethanol Feeding in Wild-Type Mice. 6-8 week old C57/Bl6 mice were maintained on the Lieber-DeCarli ethanol-containing diet for 5 weeks. All mice tolerated the diet well, and similar weight gain was observed between pair-fed and ethanol-fed animals (A). Despite the similar weight gain to pair-fed animals, ethanol-fed animals had significant upregulation in liver-weight to body-weight ratio (B). Serum ALT was measured using a biochemical assay, and it was found that ethanol fed animals had higher serum ALT values in comparison with pair-fed animals (C). Whole-liver lysates were prepared and analyzed for protein and triglyceride concentration. Ethanol-fed animals had higher levels of hepatic triglycerides (D) than pair-fed animals.

Figure 5

A. Weight Gain

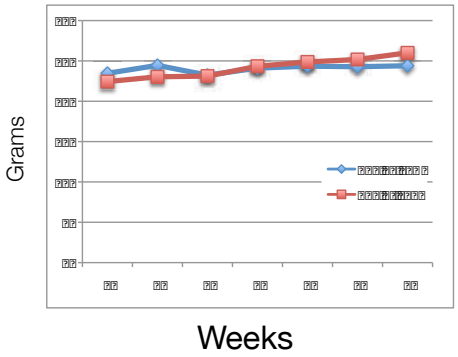

B. Liver Weight/Body Weight

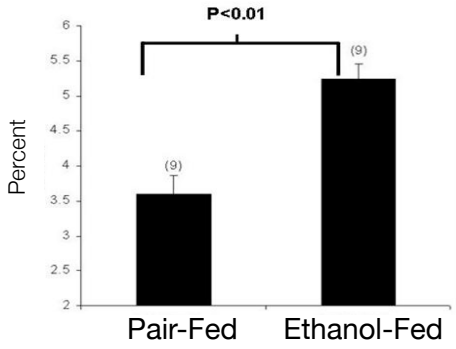

C. Hepatic Triglycerides

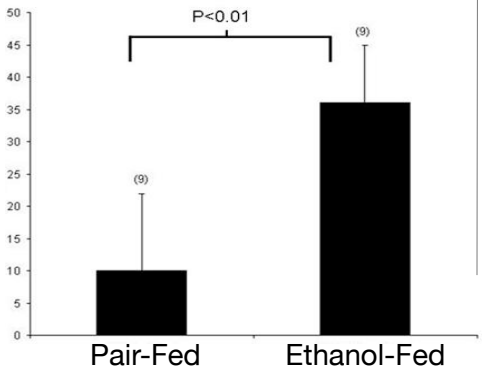

D. Serum ALT

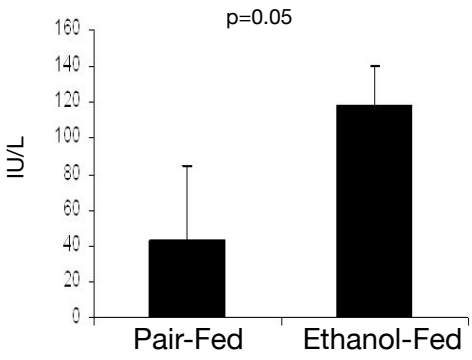

Figure 6. Liver Histology from pair-fed and ethanol-fed wild-type mice, H&E section. Pair-fed animals displayed minimal accumulation of hepatic lipid (Panels A and B, 200x and 400x, respectively). Ethanol fed animals displayed significant lipid accumulation in the form of macrovesicular steatosis (Panels C and D, 200x and 400x, respectively).

Figure 6

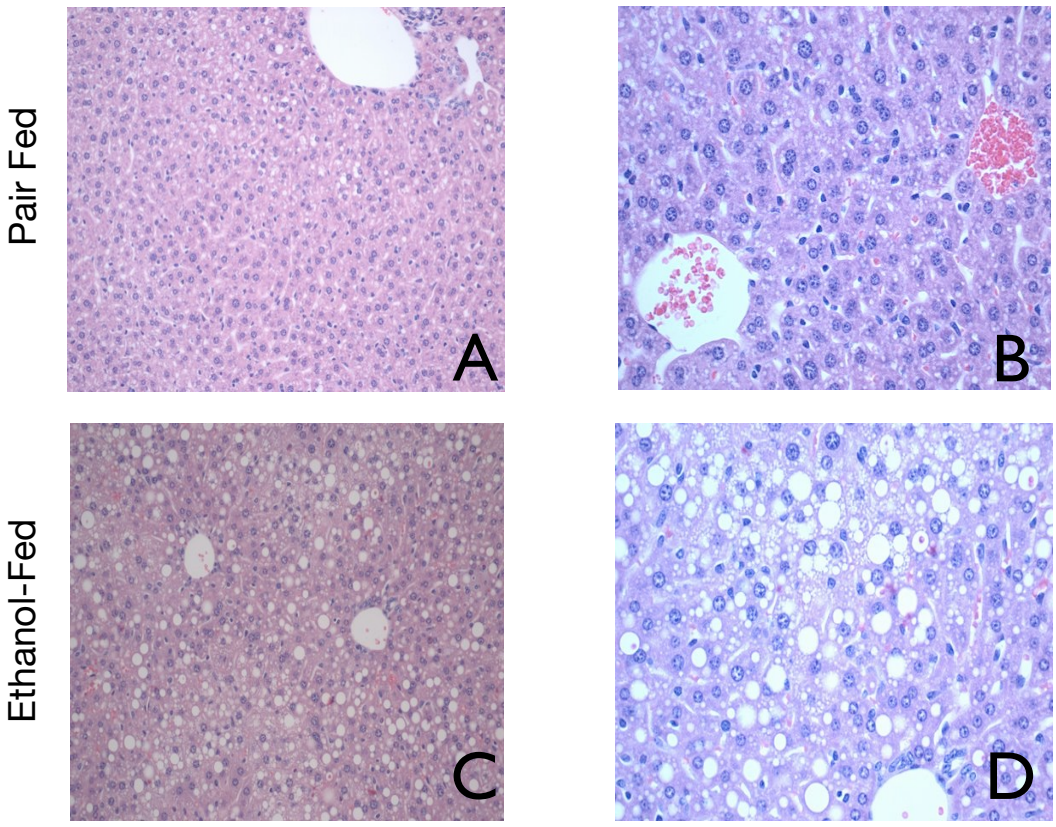

assayed for HIF1α nuclear protein and HIF2α nuclear protein by immunoblotting. Both HIF1α and HIF2α protein were significantly upregulated in ethanol-fed animals (Figure 7A-B, D-E). We then turned to examine mRNA levels for HIF1α and HIF2α. HIFs are primarily known to be degraded by post-translational hydroxylation and subsequent degradation of the alpha subunits by the ubiquitin/proteasomal system. However, we found that HIF1α and HIF2α mRNA were both significantly upregulated by ethanol feeding in wild-type mice (Figure 7C and 7F). To confirm that HIF1α and HIF2α protein were indeed transcriptionally active, we performed an electrophoretic mobility shift assay (EMSA) using a commercially available HRE oligonucleotide. We found a significant upregulation of HIF DNA-binding activity in ethanol-fed animals versus pair-fed animals (Figure 8).

Functional significance of HIF expression with chronic alcohol feeding

We then sought to determine whether HIF target gene expression was altered with chronic ethanol feeding. We identified two groups of target genes: (1) by cross-referencing HIF1α target genes with genes known to be upregulated in chronic alcohol liver injury, we identified several candidate genes that were likely to be upregulated by chronic ethanol, with or without a HIF1α specific contribution: these included PAI-1 and inducible nitric oxide synthase (iNOS). We then identified a subset of genes that were known to be upregulated by hepatic HIF1 or HIF2 expression, but were not known to be upregulated in alcoholic liver disease, including Vascular Endothelial Growth Factor and Differentially Expressed in Chrondrocytes-1 (DEC1). We examined the levels of mRNA of these and other target genes in ethanol-versus pair-fed wild-type mice. We confirmed that expression of PAI-1 and iNOS was increased with chronic ethanol feeding.

Figure 7. Hypoxia Inducible Factors 1α and 2α are upregulated in the livers of chronic-ethanol-fed mice. In hepatic nuclear extracts, an upregulation of HIF1α protein was observed (Panel A). Band density was quantified and normalized to the density of a loading control on the same gel. (Panel B.) mRNA was quantified by real-time PCR, and we detected an elevation in HIF1 mRNA (Panel C). Additionally, we found an upregulation in hepatic HIF2α in hepatic nuclear extracts (Panel D). Similar quantification and normalization against loading control revealed a significant change in hepatic HIF2α protein concentration. (Panel E). A similar extent of mRNA induction was also observed (Panel F).

Figure 7

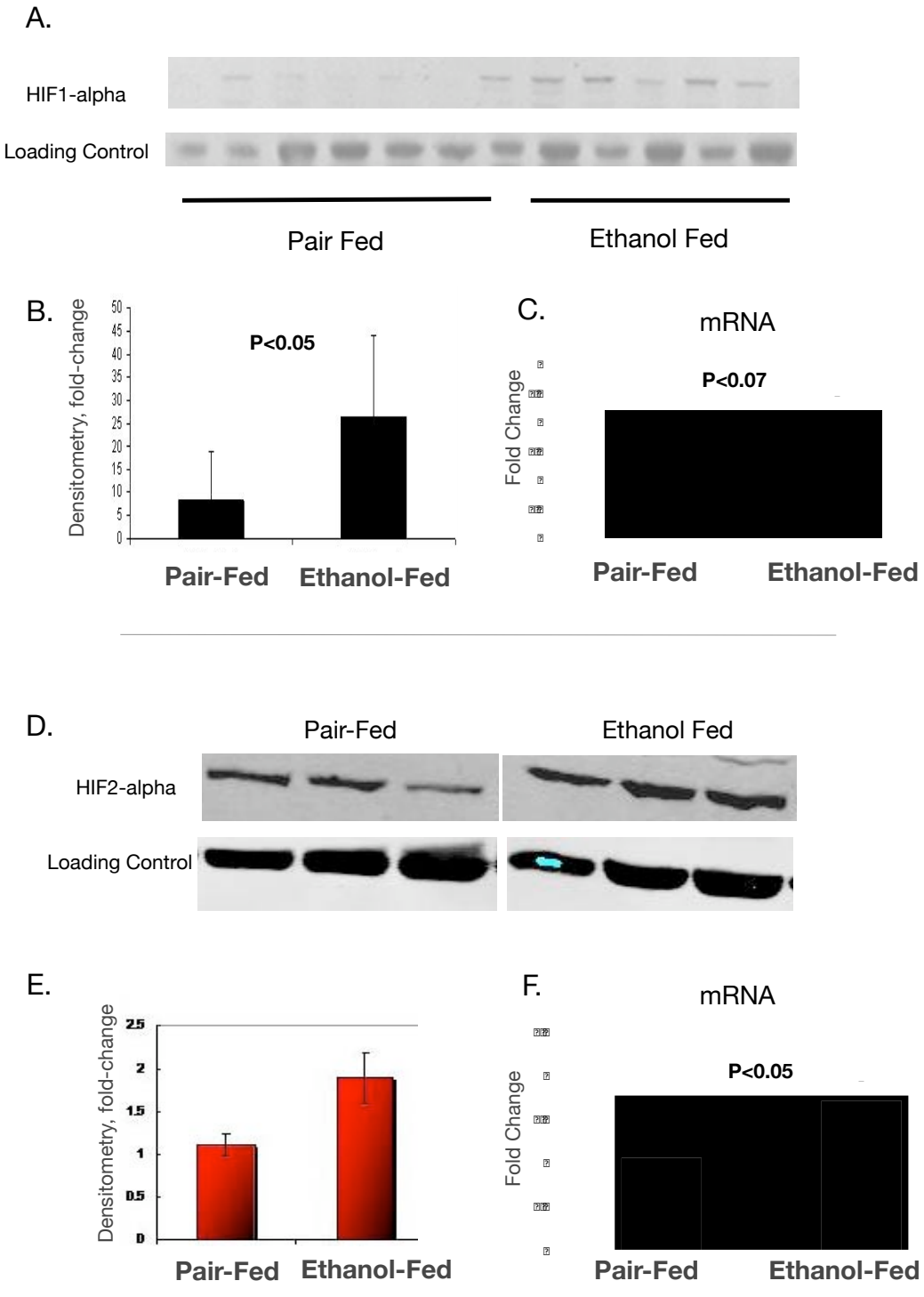
A.
HIF1-alpha
Loading Control
Pair Fed
Ethanol Fed
B.
Densitometry, fold-change
P<0.05
Pair-Fed
Ethanol-Fed
C.
mRNA
Fold Change
P<0.07
Pair-Fed
Ethanol-Fed
D.
Pair-Fed
Ethanol Fed
HIF2-alpha
Loading Control
E.
Densitometry, fold-change
Pair-Fed
Ethanol-Fed
F.
mRNA
Fold Change
P<0.05
Pair-Fed
Ethanol-Fed

Figure 8. Hepatic HIF DNA binding activity is increased by chronic ethanol. Hepatic nuclear extracts were prepared and hybridized to radiolabelled DNA probe containing a HIF consensus sequence, or hypoxia-response element. We found that chronic ethanol feeding resulted in an upregulation of HIF DNA binding activity in hepatic nuclear extracts (A). Comp= competition lane; 10x unlabeled DNA probe was added to confirm specificity of binding. Bands were quantified by densitometry (B).

Figure 8

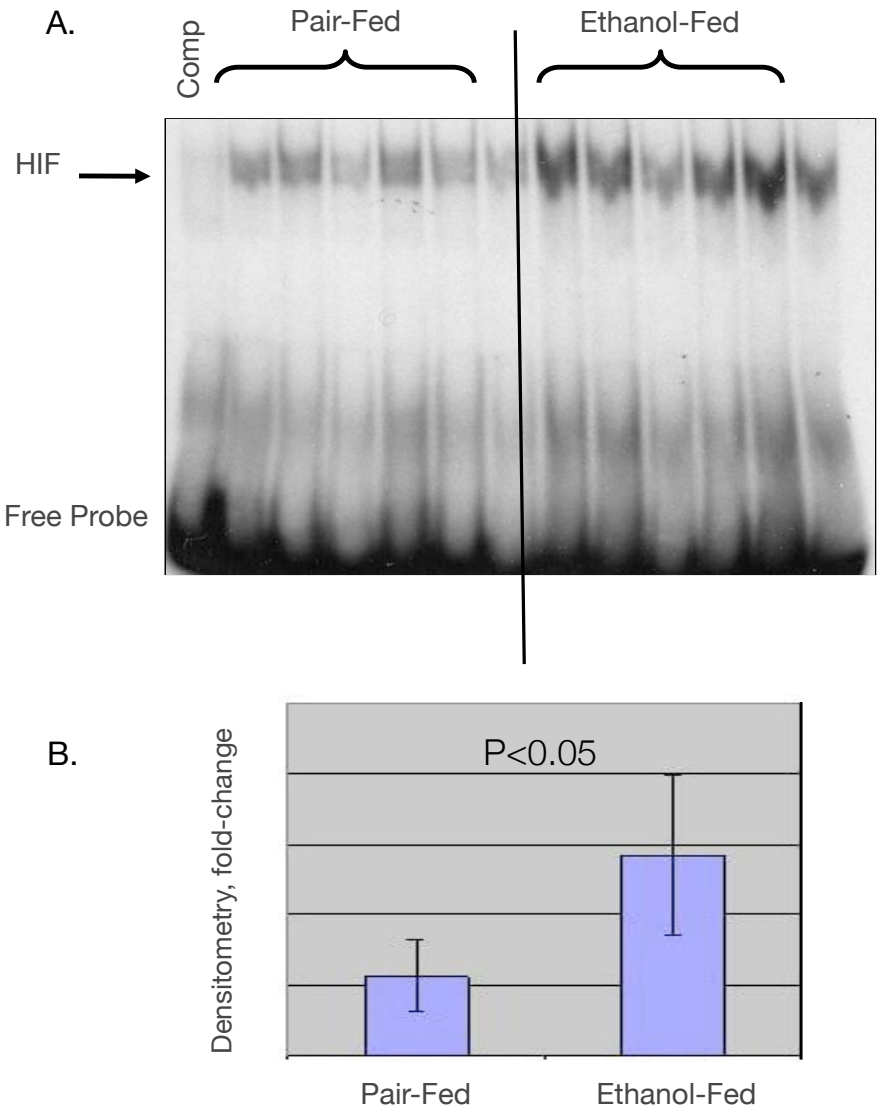
A.
Comp
Pair-Fed
Ethanol-Fed
HIF
Free Probe
B.
Densitometry, fold-change
P<0.05
Pair-Fed
Ethanol-Fed

(Figure 9) To our surprise, we found that expression of Vascular Endothelial Growth Factor was not significantly changed with alcohol feeding (Figure 9C). The HIF target gene DEC1 was also upregulated with chronic ethanol (Figure 9D).

Discussion

Chronic alcohol feeding in C57/Bl6 mice results in an increase in liver steatosis as quantified by liver weight/body weight ratio, as well as increases in serum ALT and hepatic triglyceride as quantified through biochemical assays. Several different mouse models of chronic alcohol have been used experimentally, including the Lieber DeCarli ethanol diet, chronic and continuous feeding through intragastric cannula, as well as alcohol supplementation in drinking water.[184-186] For these and subsequent studies, we chose the Lieber DeCarli alcohol-containing diet, which allows mice an *ad libitum* access to alcohol, accurately matches caloric consumption between pair-fed and ethanol-fed groups, and avoids the stress and encumbrance of continuous intragastric feeding models. In our hands, this model led to a reproducible model of liver injury observed through steatosis, quantification of liver weight/body weight ratio, and serum ALT levels after five weeks of feeding.

Liver hypoxia is an established feature of alcoholic liver disease, and has been documented in chronic intragastric models of alcohol feeding.[135] We sought to determine whether HIF activation is observed in the Lieber DeCarli ethanol feeding model, and hypothesized that HIF activity would be increased with chronic ethanol in mouse livers. Consistent with our hypothesis, we found upregulation of HIF DNA binding in livers from chronic ethanol fed mice. We also found increased accumulation of both HIF1α and HIF2α

Figure 9. Selective HIF target gene upregulation with chronic ethanol feeding.

Total RNA was prepared from whole liver. Quantitative PCRs were performed using gene-specific primers and normalized to 18S controls. (A) Inducible Nitric Oxide Synthase showed a trend towards increased expression in WT ethanol fed mice. (iNOS) (B) Plasminogen Activator Inhibitor-1 mRNA was significantly increased in WT, ethanol-fed mice. (C) Little difference was observed in Vascular Endothelial Growth Factor (VEGF) after chronic ethanol feeding. (D) Differentially Expressed in Chondrocytes-1 (DEC-1), another HIF1α target gene, was significantly upregulated in livers of chronic ethanol-fed mice.

Figure 9

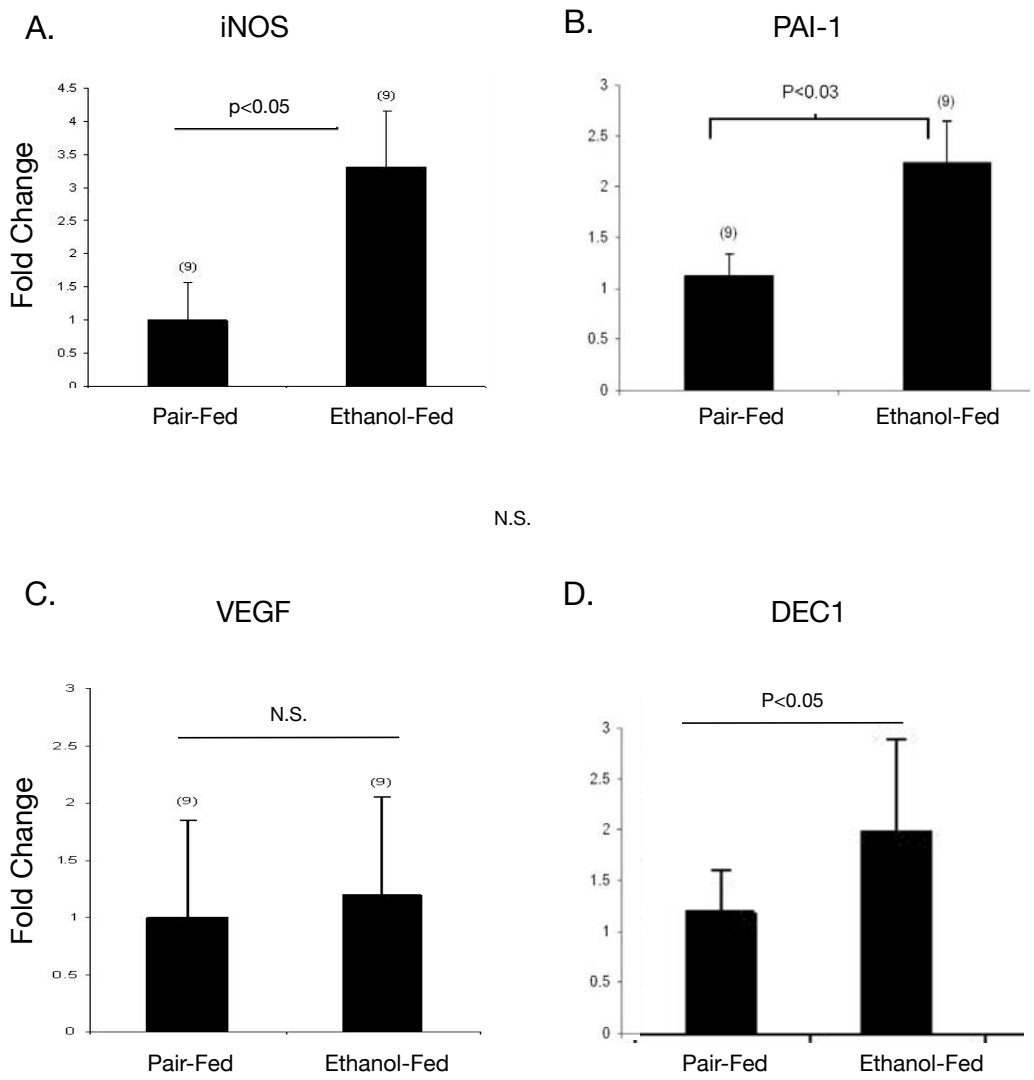
A.
iNOS
Fold Change
p<0.05
(9)
(9)
Pair-Fed
Ethanol-Fed
B.
PAI-1
P<0.03
(9)
(9)
Pair-Fed
Ethanol-Fed
N.S.
C.
VEGF
Fold Change
N.S.
(9)
(9)
Pair-Fed
Ethanol-Fed
D.
DEC1
P<0.05
Pair-Fed
Ethanol-Fed

isoforms in nuclear extracts from chronic ethanol-fed animals. Downstream targets of HIF, including PAI-1 and iNOS were upregulated with chronic ethanol feeding. Though those targets were already known to be upregulated by chronic alcohol, our analysis indicated that additional HIF targets, including DEC1, were upregulated by alcohol, though VEGF was not consistently upregulated by chronic ethanol in our model, suggesting other counter-regulatory mechanisms.

Although our data provide convincing evidence for the upregulation of HIFs in the livers of chronically ethanol-fed mice, many questions about the functional significance of this remain. Based on work done in other mouse models, HIF activation could have a role in hepatic lipid accumulation. Activation of HIF1α in hepatocytes resulted in a phenotype of mild lipid accumulation, whereas simultaneous activation of HIF1 and HIF2 in a murine model resulted in macrovesicular steatosis; conversely, in other models, knockout of HIF1α in combination with VHL knockout resulted in steatosis. The complexity of the role of HIF in the liver, however, is supported by the observation that in a whole-body knockout of HIF2, gross hepatomegaly and steatosis was present.[187] Additionally, HIF activation could have a role in the pathogenesis of liver injury with chronic ethanol through pro-inflammatory mechanisms, rather than pure effects on hepatic lipid accumulation. These effects could be through recruitment and activation of leukocytes, and could be mediated through either hepatocytes or cells of other lineages. In the following chapter, we explore the contribution of HIF1α to alcoholic liver disease by utilizing a mouse model of hepatocyte-specific constitutive HIF1α activation.

CHAPTER 3

EFFECT OF ETHANOL FEEDING IN A MODEL OF HEPATOCYTE-SPECIFIC, CONSTITUTIVELY ACTIVE HYPOXIA INDUCIBLE FACTOR 1α

Summary

Functional HIF1 is increased in the livers of mice on the Lieber-deCarli diet, as is expression of some, but not all, HIF1 target genes. To further determine the role of HIF1, we used a cre-lox model of hepatocyte-specific, degradation resistant HIF1α. HIF1dPA mice were maintained on the Lieber-DeCarli ethanol-containing diet for up to four weeks. We determined that the presence of this transgene conferred a susceptibility to increased hepatic lipid accumulation versus non-transgene bearing littermate controls. The presence of several HIF1α downstream genes, including PAI-1, iNOS, and KC was significantly upregulated in ethanol-fed HIF1dPA mice compared to control mice. Using the EMSA technique to assay DNA binding, HIF1dPA pair-fed mice had HIF DNA binding activity approximately equal to ethanol-fed control mice. Hepatic triglyceride in HIF1dPA pair-fed mice was approximately equal to that in control ethanol-fed mice, and increased dramatically in ethanol fed HIF1dPA mice. Liver weight to body weight ratio showed a similar trend, with HIF1dPA pair-fed and control ethanol-fed mice having approximately equal liver weight to body weight ratios, and HIF1dPA ethanol fed mice having a significant elevation of liver weight to body weight ratios over HIF1dPA pair-fed mice. We conclude that constitutively active, hepatocyte-specific HIF1α increases the propensity to lipid accumulation and liver injury with chronic ethanol feeding. These data support a role for HIF1α in ethanol induced steatosis.

Acknowledgements

The LSL-HIF1dPA mice used in these experiments were the kind gift of Dr. William Kim, University of North Carolina, Chapel Hill, who developed them as a postdoctoral research fellow in the lab of Dr. William Kaelin, Dana Farber Cancer Center, Harvard University, Boston MA.

The author is grateful for the assistance of Donna Catalano with mouse feedings associated with the work reported in this chapter.

Multiplex cytokine array data was collected in collaboration with Karen Kodys, with equipment generously made available to us by the Flotte lab, and the assistance of Christian Mueller, PhD.

Introduction

Much of our knowledge of the function of hypoxia inducible factors has been gained through innovative approaches using Cre-Lox recombinant DNA technology. In this system, short (13bp) palindromic sequences of DNA known as *LoxP* sites are engineered to flank a target stretch of DNA of interest. A target stretch of DNA flanked by *LoxP* sites is described as 'floxed.' The Cyclization Recombination protein (Cre), is an enzyme that catalyzes homologous recombination between palindromic sequences of DNA known as *LoxP* sites, resulting in excision of the DNA sequence between the *LoxP* sites. The Cre-recombinase protein may be expressed under the control of promoters with varying types of specificity, including tissue specific (e.g., Albumin-cre for hepatocyte-specific expression) or inducible (e.g., Mx-Cre, which is inducibly expressed after stimulation with poly inosinic:polycytidylic acid in immune cells and liver tissue) promoters, with the resultant ability to tightly control levels of expression of the transgene of interest within specific tissues or the whole organism.

Investigators in several laboratories have developed different approaches using Cre-Lox technology to study the function of HIFs. One approach was the engineering of a mouse strain in which the Von Hippel Lindau tumor suppressor gene was flanked by *LoxP* sites (floxed VHL). Cre-mediated recombination resulted in tissue specific disruption of expression of the VHL protein (pVHL).[154] As HIF alpha subunits are targeted for degradation by ubiquitination on a pVHL scaffold, pVHL deficiency leads to HIF activation in the target tissue of interest. VHL inactivation in hepatocytes led to a phenotype of hypervascularity and steatosis. However, a significant limitation of this approach was the possibility that other functions of pVHL are lost and contribute to the observed phenotype. Thus, another approach was to engineer degradation-

resistant mutants of HIF1α and HIF2α. The signal for ubiquitination and degradation of HIF1α and HIF2α is hydroxylation at specific proline residues. By site-directed mutagenesis, HIF1α and HIF2α alleles in which the degradation target proline residues were mutated to alanine residues (HIF1dPA or HIF2dPA) were engineered and introduced into murine embryonic cells. In order to create tissue-specificity, a stop element flanked by *loxP* sites was placed upstream of the HIF1dPA or HIF2dPA transgenes. Upon co-expression of the Cre-recombinase, excision of the stop element occurs, with subsequent expression of the degradation resistant mutant. Experiments with these mutants revealed that hepatocyte-specific HIF1dPA expression resulted in a phenotype of mild lipid accumulation, whereas hepatocyte-specific HIF2dPA expression resulted in a phenotype of hypervascularity with little to no observed lipid accumulation. Co-expression of both HIF1dPA and HIF2dPA in hepatocytes resulted in a phenotype of marked lipid accumulation and the formation of cavernous hemangiomas, i.e., recapitulation of the phenotype of hepatocyte-specific pVHL loss.[97]

More recently, an alternate approach to study the specific functions of HIF1α or HIF2α has been described. In this approach, Cre recombinase was expressed under control of the albumin promoted in mice with floxed VHL and floxed HIF1α and/or floxed HIF2α. In the resultant offspring, the lack of pVHL enabled HIF alpha subunits to escape degradation and active downstream gene targets, and the simultaneous mutation of either HIF1α, HIF2α, or both HIF1α and HIF2α enabled dissection of their phenotypes. Intriguingly, in this model, the compound mutant pVHL(flox/flox)/HIF1α (flox/flox) had the greatest degree of lipid accumulation, suggesting that of the two alpha subunits, HIF2α is primarily responsible for the phenotype of lipid accumulation.[155]

It is difficult to reconcile the divergent results of these two carefully executed studies. One suggests that activation of both HIF isoforms is required for lipid accumulation, whereas another suggests that activation of merely HIF2α is sufficient, and would appear to explicitly refute the claim that activation of HIF1α is sufficient. Complicating matters further, generation of a whole-organism HIF2α knockout was reported to result in a phenotype of neonatal lethality with extensive hepatic lipid accumulation.[153] The approach that utilizes simultaneous introduction of degradation resistant HIF1α and HIF2α has the advantage that other functions of pVHL are retained. The relevance of these various genetic models to human disease conditions in which lipid accumulates in the liver, such as NAFLD and ALD, is unclear.

As described in chapter 2 of this dissertation, we previously found that that HIF1α and HIF2α protein accumulated in the nuclear fraction of livers of chronically ethanol-fed mice, and that this protein accumulation was accompanied by an upregulation of HIF1α and HIF2α mRNA, HIF DNA binding, and activation of HIF target genes. In order to further dissect the function of HIF proteins in ALD, we utilized the degradation-resistant HIF1dPA mouse model. By co-expressing HIF1dPA with a Cre allele under the control of the albumin promoter, we generated mice with constitutive HIF1α in hepatocytes. These mice were maintained on the Lieber De Carli ethanol diet for up to four weeks. We found that constitutive activity of HIF1α dramatically increased hepatic lipid accumulation with alcohol feeding versus littermate controls. Furthermore, the expression of downstream targets that have been implicated in the pathogenesis of alcoholic liver disease, including PAI-1, TNFα, iNOS, and KC, was dramatically increased in HIF1dPA mice.

Methods

Animal Studies

All animals received care in compliance with protocols approved by the Institutional Animal Use and Care Committee of the University of Massachusetts Medical School. HIF1dPA mice were the kind gift of Dr. William Kim, UNC. Alb-Cre mice were purchased from Jackson Laboratories (Bar Harbor, ME). Litters were tagged by ear notching, and tail snips were collected. DNA was isolated from tail snips using the Extract-N-Amp SYBR Green DNA isolation kit (Sigma). Genotyping was performed by real-time PCR and verified by resolution of DNA fragments by agarose gel electrophoresis. Due to mixed genetic background, littermates expressing Alb-Cre but lacking the HIF1dPA transgene were utilized as controls (Alb-Cre mice). For all mouse studies, mice were gradually habituated to a Lieber-DeCarli liquid diet with 5% ethanol (volume/volume) over a period to two weeks, then maintained on the 5% diet for four weeks. Consumption was recorded daily, and isocaloric amounts of a non-alcohol containing diet (in which dextran-maltose replaced calories from ethanol) were dispensed to pair-fed animals. Weights were recorded before the introduction of the diet and weekly thereafter. At the conclusion of the feeding, mice were weighed and euthanized. Livers were excised and weighed, and divided and portions were snap frozen in liquid nitrogen for protein and biochemical assays, preserved in 10% neutral-buffered formalin for histopathological analysis, or soaked in RNALater (Qiagen GmbH, Hilden, Germany) for RNA extraction. Blood was collected and serum separated for biochemical analysis.

Biochemical Analysis

Serum alanine aminotransferase (ALT) was determined using a commercially available reagent (Advanced Diagnostics Inc, Plainfield, NJ). Briefly, 15ul of serum was mixed with 100ul of reagent diluted according to the instructions of the manufacturer, and UV absorbance at 37 degrees celsius was measured over three minutes. The average change in absorbance per minute interval is then multiplied by a conversion factor to yield ALT levels.

For liver triglyceride levels, liver whole-cell lysates were prepared as described below and lipids separated by isopropanol precipitation of non-lipid components. A commercially available kit (Wako Chemicals USA Inc., VA) was used to determine the triglyceride concentration.

Protein concentrations were determined by adding 1uL of whole-cell lysate or nuclear extract to Bradford reagent (BioRad) and by measuring the difference between absorbance at 650nM and 595nM on a 96 well plate using a plate reader. Concentrations were determined using a standard curve of bovine serum albumin.

RNA analysis

RNA was purified using the RNeasy Mini kit (Qiagen Sciences, Maryland, USA) with on-column DNA digestion (ProMega). cDNA was prepared using random hexamer primers and the Reverse Transcription System kit (Promega Corp., Madison WI). Real-time quantitative polymerase chain reaction was performed using an iCycler (Bio-Rad laboratories Inc., Hercules, CA), using specific primers. Primer sequences are shown in Table 1. Fold-change in gene expression was determined by normalizing to 18S mRNA.

Histopathological Analysis

Sections of formalin-fixed livers were stained with hematoxylin/eosin and analyzed by microscopy.

Whole Cell Lysate

60mg of liver tissue was washed and subsequently homogenized in lysis buffer (9.5ml RIPA buffer, 1mM NaF, 2mM Na3VO4, 1 protease inhibitor tablet, 500ul PMSF) using rotor-stator homogenization. After 10 minutes of incubation on ice, homogenates were centrifuged at 10,000RPM for 10 minutes at 4 degrees C. The supernatant was collected and stored in aliquots at -80 degrees C.

Nuclear Extraction

60mg of snap-frozen liver tissue was washed in 10-fold excess volume TKM-0.32 buffer (0.32 molal sucrose, 50mM Tris-HCl, 25mM KCl, 5mM MgCl, 5mM PMSF, with protease inhibitor tablets (1 per 10ml of buffer, Sigma) and homogenized using a rotor-stator homogenizer (Ika). Homogenates were transferred to microcentrifuge tubes and centrifuged (10mins/1000rpm/4 degrees C.) Pelleted material was resuspended in TKM-2.0 buffer (2 molal sucrose, 50mM Tris-HCl, 25mM KCl, 5mM PMSF) and homogenized again by rotor-stator. Pellets were collected by centrifugation (60mins/14000rpm/4 degrees C) and resuspended in 400ul Buffer A (10mM Hepes/KOH, pH 7.9, 2mM MgCl, 1mM EDTA, 10mM KCl, 1mM DTT, 5mM PMSF, 1 protease inhibitor tablet/5ml buffer). Pellets were again collected by centrifugation (2mins/ 14000rpm/4 degrees C) and resuspended in 50ul Buffer B (10mM Hepes/KOH pH 7.9, 2mM MgCl, 1mM EDTA, 50mM KCl, 300mM NaCl, 2mM DTT, 5mM PMSF, 1 protease inhibitor tablet (Sigma) per 5mL buffer, 10% glycerol). Resuspended material was frozen at -80 degrees

overnight, thawed with gentle agitation at 4 degrees C. Supernatant containing nuclear extract was collected after centrifugation (10mins/14000rpm/4 degrees C) and assayed for protein concentration.

Electrophoretic Mobility Shift Assay

A consensus double-stranded Hypoxia Response Element (HRE) (Santa Cruz Biotech, CA) oligonucleotide was used for EMSA. End-labeling was accomplished by treatment with T4 kinase in the presence of [32P]ATP. Labeled oligonucleotides were purified on a polyacrylamide copolymer column (BioRad). Five micrograms of nuclear protein was added to a binding reaction mixture containing 50 mM Tris-HCl, pH 7.5, 5 mM MgCl2, 2.5 mM EDTA, 2.5 mM DTT, 250 mM NaCl, 20% glycerol, 20 μg/ml BSA, 2 μg poly(dI–dC) and 30,000 c.p.m. of 32P-labeled NFB oligonucleotide. Samples were incubated at room temperature for 30 min. Reactions were run on a 5% polyacrylamide gel and the dried gel was exposed to an X-ray film at –80°C overnight. Cold competition was done by adding a 20-fold excess of specific unlabeled double-stranded probe to the reaction mixture. Band density was quantified using Labworks 4.0 image analysis.

Western Blotting

30-50ug of nuclear extract was resolved on 10% polyacrylamide gels and transferred overnight to nitrocellulose support. Membranes were blocked overnight with blocking buffer (5% bovine serum albumin in Tris-Borate-SDS with 0.01% Tween 20) with refrigeration, and subsequently probed overnight with anti-HIF1α (R&D Biosciences) or anti-HIF2α (Chemicon) mouse

monoclonal antibodies. Detection was performed using an anti-mouse horseradish-peroxidase conjugated secondary antibody and chemiluminescent substrates. Band density was quantified using Labworks 4.0 image analysis.

Results

Liver Pathology in HIF1dPA mice with chronic ethanol

We began by introducing HIF1dPA and control mice to the ad libitum murine model of chronic alcohol feeding as previously described. Briefly, six-to-eight week-old HIF1dPA and control mice were habituated to a liquid diet containing a final ethanol concentration of 5% (v/v). Consumption was recorded daily, and an isocaloric amount of control diet was dispensed to pair-fed animals. Weights were recorded weekly, and revealed similar weight-gain between pair-fed and ethanol-fed animals. (Figure 10A). Animals were sacrificed after 2 and 4 weeks of feeding with 5% alcohol-containing diet. Analysis of liver-weight/body-weight ratios revealed increased liver weight/body weight in HIF1dPA mice versus controls at 4 weeks. Specifically, HIF1dPA-pair-fed mice and control ethanol-fed mice had a statistically significant upregulation of LW/BW versus pair-fed controls after 4 weeks of ethanol feeding (Figure 10B). Ethanol-fed HIF1dPA mice had the highest LW/BW ratios ($p<0.02$ versus HIF1dPA pair-fed animals.)

Serum ALT was assessed as a measure of liver injury (Figure 10C). HIF1dPA pair-fed mice had elevations in serum ALT similar to control mice fed ethanol, and significantly upregulated over control mice ($p<0.05$, HIF1dPA pair-fed versus control pair-fed.) No further upregulation was observed with ethanol feeding in HIF1dPA mice.

We then examined liver triglycerides from whole-liver extracts prepared from ethanol fed and pair-fed HIF1dPA mice and control mice (Figure 10D). Ethanol caused an upregulation of triglyceride in hepatic extracts in control mice at 2 and 4 weeks. At both 2 and 4 weeks, triglyceride levels were higher in pair-fed HIF1dPA mice versus pair-fed control mice, ($p<0.05$ for HIF1dPA pair-fed versus control pair-fed at both 2 and 4 weeks) indicating an effect of constitutive HIF1α on lipid accumulation in the absence of any other stimulus. At 4 weeks, HIF1dPA mice fed ethanol had the highest average hepatic triglyceride content ($p<0.05$ versus all other groups).

Formalin-fixed livers were sectioned and stained with H&E as well as Oil-Red O for histological analysis. HIF1dPA mice on the control diet accumulated a significant degree of lipid as evidenced by macrovesicular steatosis in liver tissue sections; this lipid accumulation appeared to be further enhanced by ethanol feeding (Figure 11, E-H). In contrast, control mice accumulated less lipid with ethanol feeding, and almost no visible lipid droplets on the control diet (Figure 11, A-D).

HIF protein, mRNA, and DNA-binding activity

We then turned to examine expression of HIF alpha subunit isoforms by western blotting (Figure 12). Both HIF1α and HIF2α isoforms were present in the livers of HIF1dPA mice, with and without ethanol feeding. HIF2α was strongly upregulated in control mice with alcohol feeding, in accordance with previous results. HIF1α expression was variable in control mice.

In agreement with these findings, HIF DNA binding activity was strongly upregulated in HIF1dPA mice versus control mice. (Figure 13) With ethanol, there was a trend towards upregulation in HIF1dPA and Alb-Cre mice; by densitometry, this was not significant.

Figure 10. Parameters of ethanol feeding and liver injury in HIF1dPA mice. HIF1dPA and control mice were maintained on the Lieber-DeCarli ethanol-containing diet for up to 4 weeks. All mice tolerated the diet well, and similar weight gain was observed between pair-fed and ethanol-fed animals (A). Ethanol-fed animals had significant upregulation in liver-weight to body-weight ratio (B). Serum ALT was measured using a biochemical assay, and it was found that ethanol fed animals had higher serum ALT values in comparison with pair-fed animals. HIF1dPA pair-fed mice had similar serum ALT levels to control ethanol-fed mice (C). Whole-liver lysates were prepared and analyzed for protein and triglyceride concentration. Ethanol-fed animals had higher levels of hepatic triglycerides (D) than pair-fed animals; at 4 weeks, HIF1dPA mice had accumulated the greatest amount of triglyceride.

Figure 10

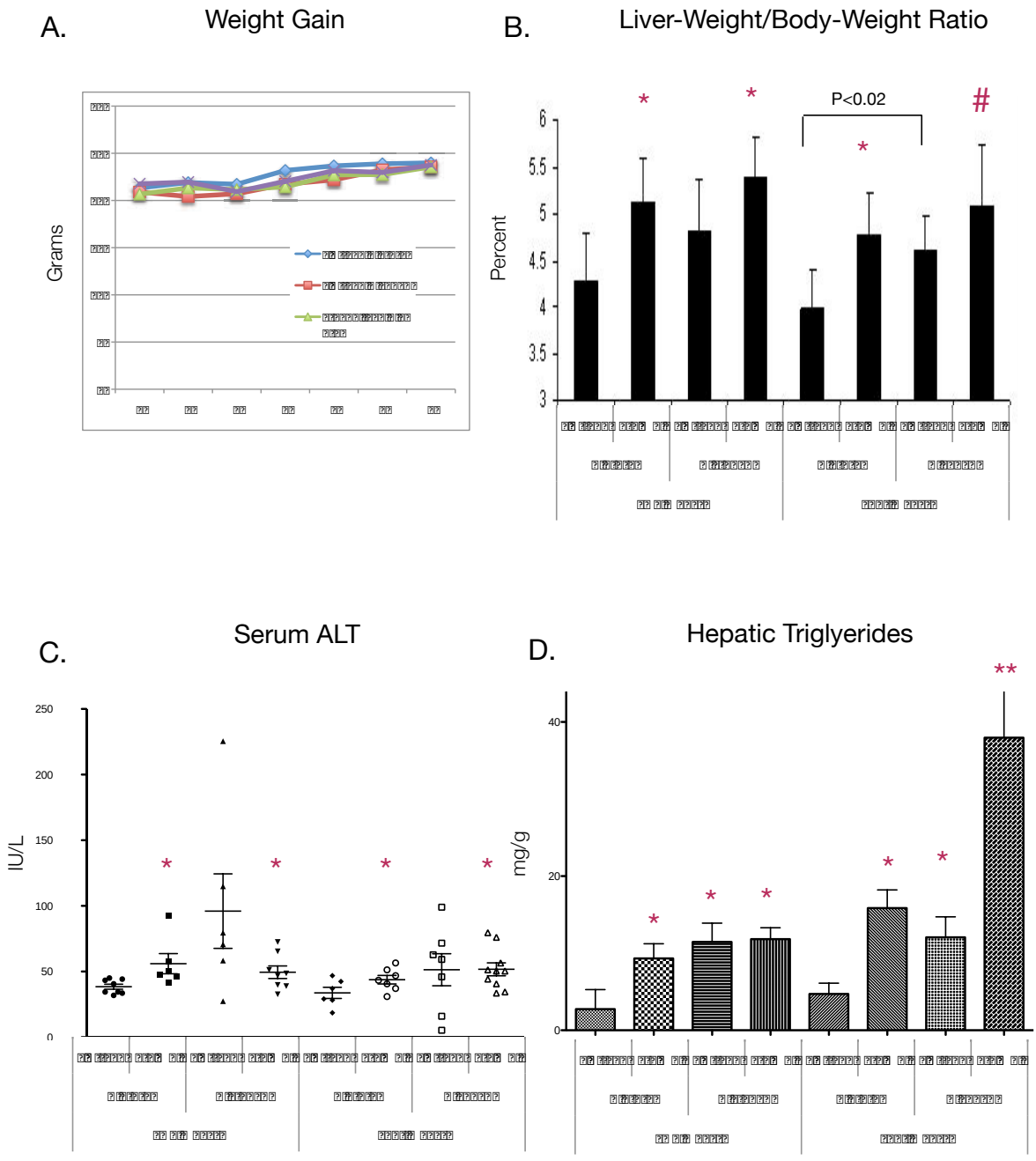
A.
Weight Gain
Grams
B.
Liver-Weight/Body-Weight Ratio
Percent
P<0.02
C.
Serum ALT
IU/L
D.
Hepatic Triglyerides
mg/g

Figure 11. Histology, HIF1dPA and control mice with Ethanol and Pair-Feeding. Panels **A-D** show Alb-Cre mice, whereas panels **E-H** show HIF1dPA mice. Little lipid vacuolization is observed in Alb-Cre pair-fed mice (**A** and **C**), even after 4 weeks. In contrast, ethanol-fed Alb-Cre mice accumulated some lipid, which was more apparent histologically by 4 weeks of ethanol feeding (**D**). In HIF1dPA mice, on the other hand, prominent lipid vacuolization was observed after 2 weeks on both the pair-fed and the ethanol fed diet. By 4 weeks of ethanol feeding, gross steatosis and lipid accumulation was observed in most hepatocytes in HIF1dPA mice (**H**).

Figure 11

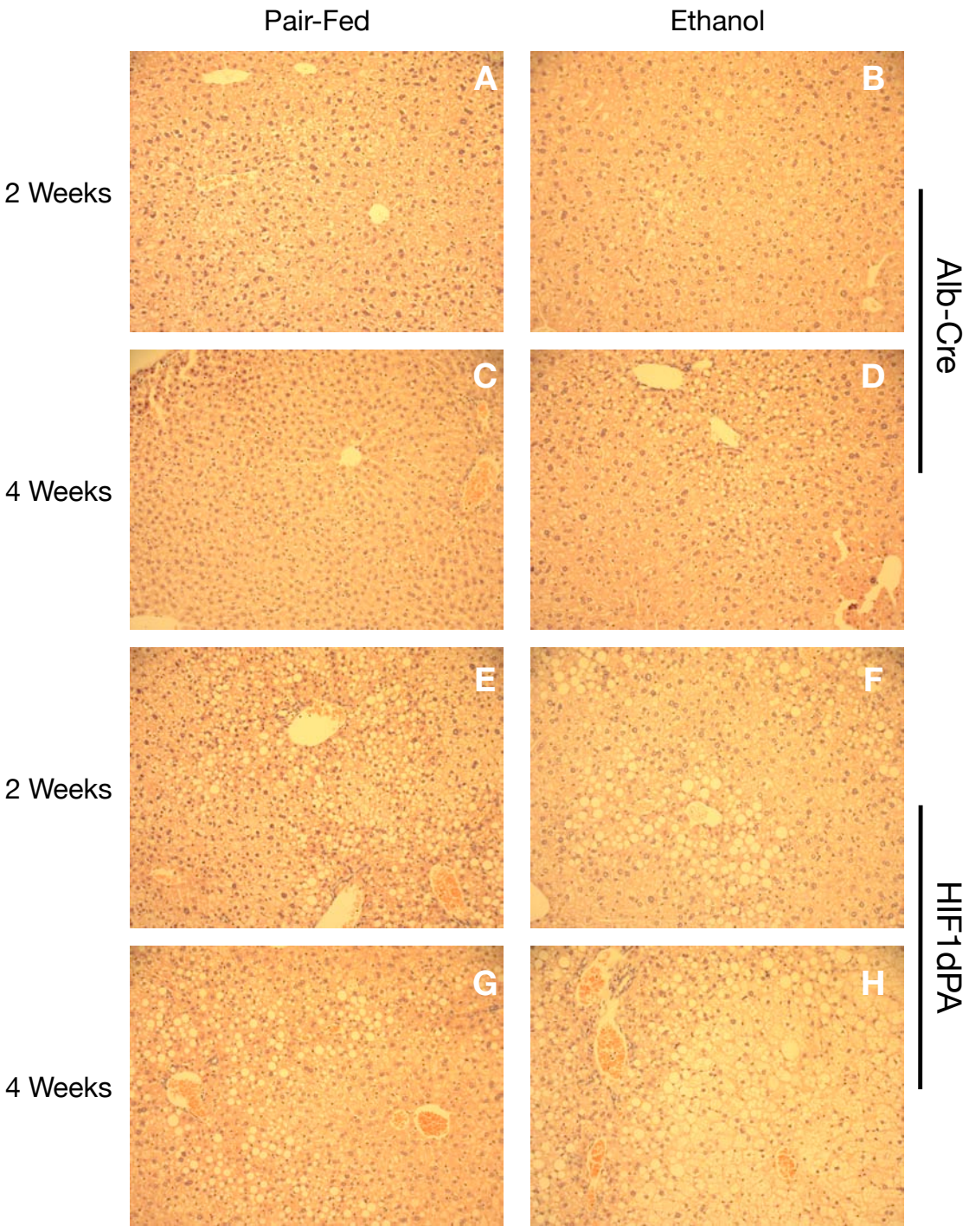
Pair-Fed
Ethanol
2 Weeks
4 Weeks
2 Weeks
4 Weeks
A
B
C
D
E
F
G
H
Alb-Cre
HIF1dPA

Figure 12. HIF1α and HIF2α subunit Western Blot. (A and B) Nuclear HIF1α was prominently expressed in HIF1dPA mice, both under the pair-fed and ethanol-fed conditions. HIF2α was also expressed in HIF1dPA mice under all conditions. HIF2α was also expressed in albumin-cre ethanol fed mice, but was not detected in Alb-Cre pair-fed mice. The expression of HIF1α was variable in Alb-Cre ETOH-fed and pair-fed mice.

Figure 12

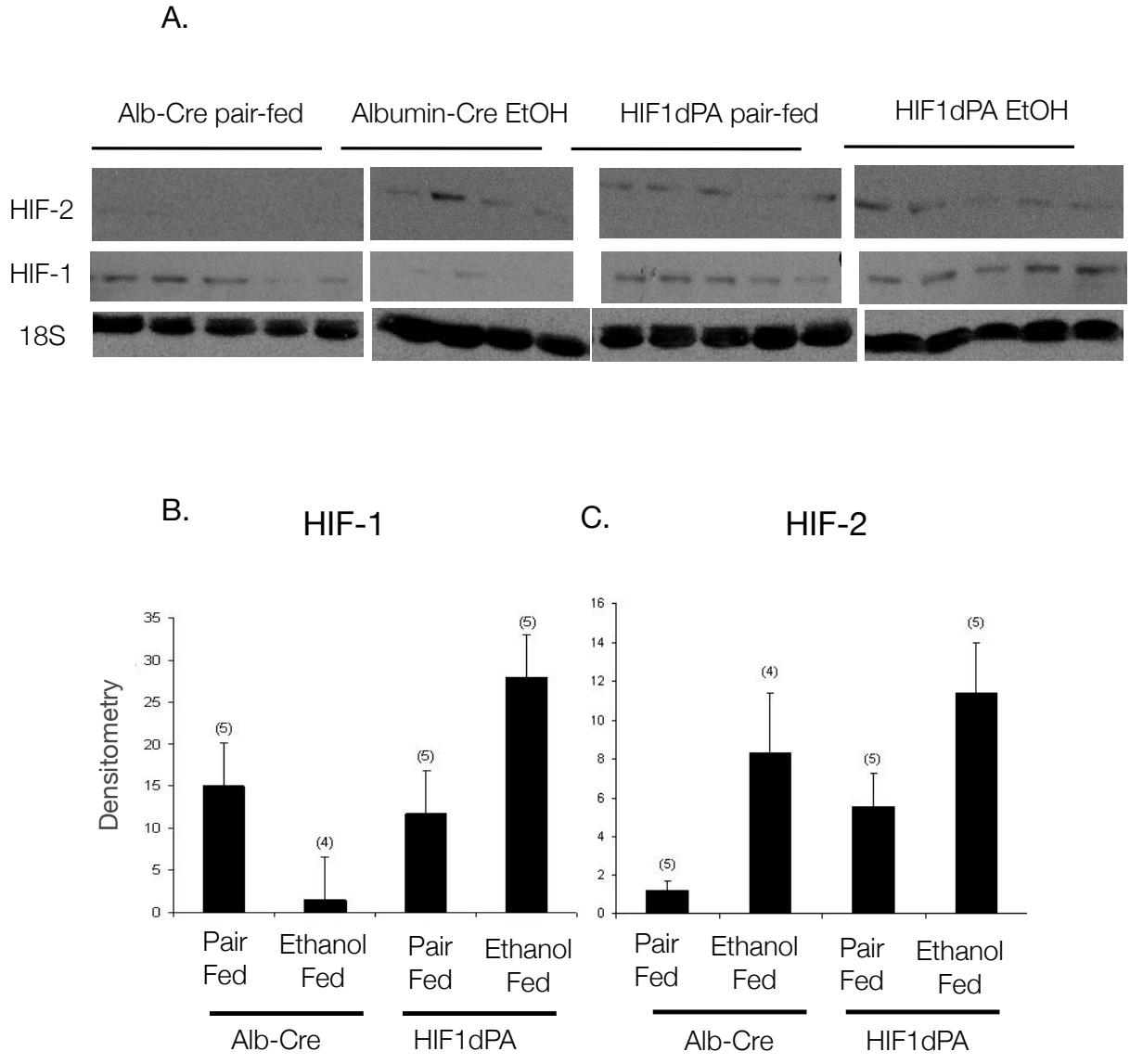
A.
Alb-Cre pair-fed
Albumin-Cre EtOH
HIF1dPA pair-fed
HIF1dPA EtOH
HIF-2
HIF-1
18S
B.
HIF-1
Densitometry
35
30
25
20
15
10
5
0
(5)
(4)
(5)
(5)
Pair Fed
Ethanol Fed
Pair Fed
Ethanol Fed
Alb-Cre
HIF1dPA
C.
HIF-2
16
14
12
10
8
6
4
2
0
(5)
(4)
(5)
(5)
Pair Fed
Ethanol Fed
Pair Fed
Ethanol Fed
Alb-Cre
HIF1dPA

Figure 13. HIF1dPA DNA binding by EMSA, HIF1dPA and control mice. A. Liver nuclear extracts were prepared from wild-type mice fed ethanol or control diets and assayed by EMSA. Ethanol-fed wild-type mice showed increased HIF DNA binding. **B.** Nuclear extracts from ethanol-fed or pair-fed HIF1dPA or Alb-Cre mice were prepared and assayed for HIF1 DNA binding by EMSA. Significant upregulation of DNA binding was observed in HIF1dPA pair-fed mice versus Alb-Cre pair-fed mice ($P<0.01$, HIF1dPA Pair-Fed versus Alb-Cre Pair-fed), indicating that the HIF1dPA transgene was active. Further trends towards upregulation in ethanol fed Alb-Cre and HIF1dPA mice were apparent, but not significant by densitometry. Lane marked with a ‘x’ was loaded incorrectly and is excluded from analysis.

Figure 13

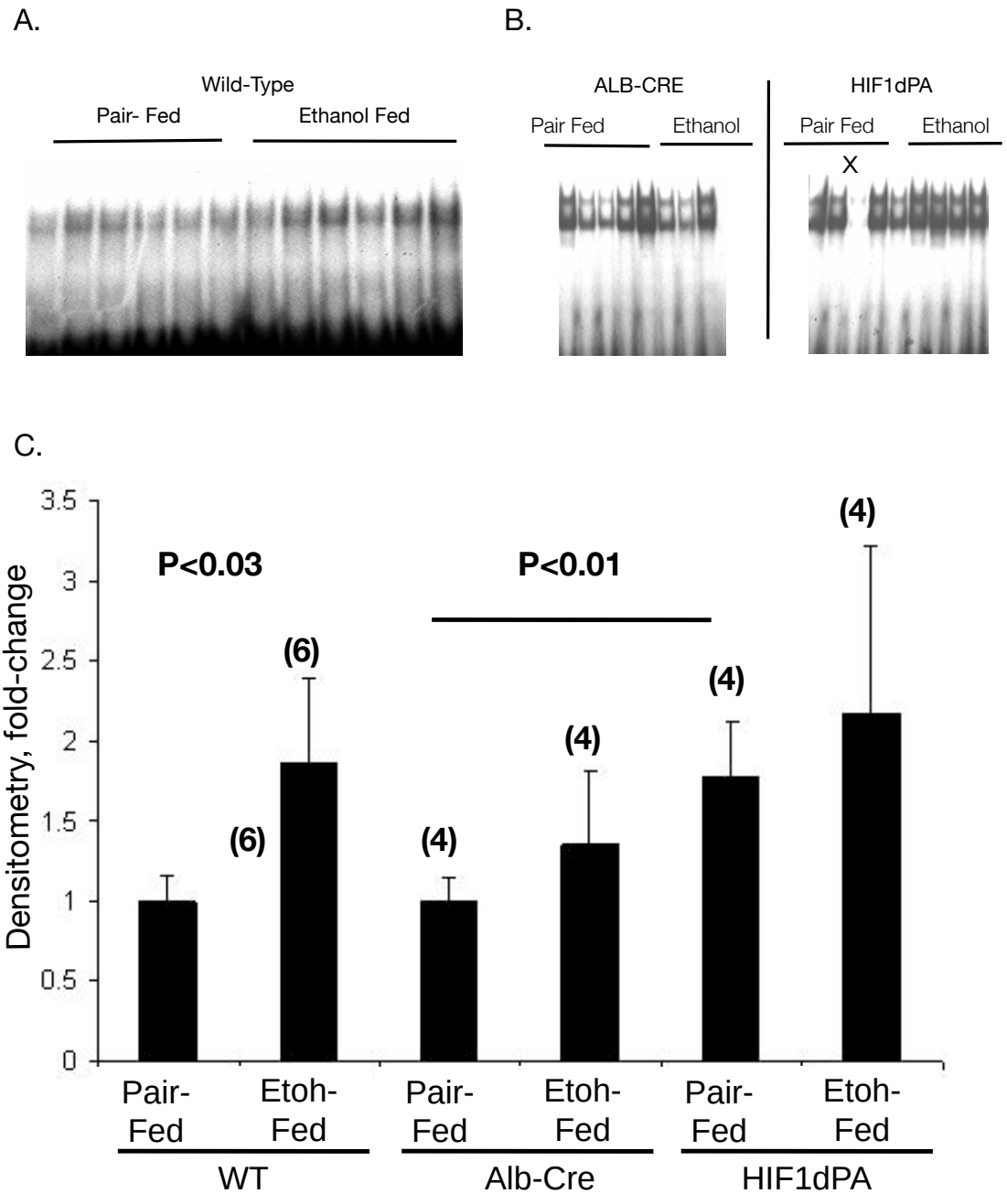
A.
Wild-Type
Pair- Fed
Ethanol Fed
B.
ALB-CRE
Pair Fed
Ethanol
HIF1dPA
Pair Fed
Ethanol
X
C.
Densitometry, fold-change
3.5
3
2.5
2
1.5
1
0.5
0
P<0.03
P<0.01
(6)
(6)
(4)
(4)
(4)
(4)
Pair-Fed
Etoh-Fed
Pair-Fed
Etoh-Fed
Pair-Fed
Etoh-Fed
WT
Alb-Cre
HIF1dPA

Functional Significance of HIF1dPA expression

Given the functional increase of HIF1α DNA binding in HIF1dPA mice and the aggravated phenotype of hepatic injury, we then turned to examine genes downstream from HIF, to determine whether alcohol feeding had any effect on their expression and to correlate any changes with pathology. MRNA for EGLN-3, a prolyl hydroxylase that is upregulated by HIF in an autoregulatory loop, was specifically upregulated in HIF1dPA mice. Alcohol had differential effects on this gene at 2 and 4 weeks, causing a mild upregulation at 2 weeks but a mild suppression at 4 weeks. EGLN3 expression served as an internal confirmation of HIF1dPA transgene expression. (Figure 14A)

Plasminogen activator inhibitor-1 has been correlated with alcoholic liver disease by other investigators.[188] We have confirmed higher expression levels of PAI-1 with ethanol feeding in earlier experiments using C57/BL6 mice. PAI-1 expression was much higher in HIF1dPA mice than in control mice. A trend towards upregulation was observed with ethanol feeding in HIF1dPA mice. (Figure 14B)

Inducible Nitric Oxide Synthase (iNOS) is another gene that has been reported to be regulated by HIF and which has a role in alcoholic liver disease. We examined iNOS mRNA expression, and found that HIF1dPA mice robustly increased expression of iNOS, with a similar trend towards upregulation observed in ethanol-fed HIF1dPA mice.(Figure 14C)

Vascular Endothelial Growth Factor was upregulated in HIF1dPA mice, but no change was observed with ethanol feeding, consistent with our earlier work in C57/Bl6 mice. (Figure 14D)

Other gene targets examined include Tumor Necrosis Factor-Alpha (TNFα) which was also upregulated in HIF1dPA mice. Although there was some further upregulation with chronic ethanol feeding, this difference did not prove to be statistically significant. (Figure 14E)

Upregulation of serum chemokine KC in HIF1dPA mice

The chemokine IL8 is a neutrophil chemoattractant that is upregulated in alcoholic liver disease.[189] Murine and rat homologues of this chemokine are termed KC and CINC, respectively, and are also reportedly upregulated in models of alcoholic liver disease.[189] We utilized a multiplex cytokine bead array and determined serum levels of MCP-1, MIP1B, IL-6, and KC.(Figure 15A). We found that ETOH-fed HIF1dPA mice had higher serum KC than ETOH-fed control mice ($p<0.02$) and pair-fed HIF1dPA mice ($p<0.02$), suggesting that the combination of HIF1α activity and ETOH may cooperatively upregulate KC. No upregulation of MIP1b, MCP-1, or IL-6 was observed in HIF1dPA mice. We also observed an increase in KC mRNA in HIF1dPA mice (Figure 15B).

Discussion

As we had previously found an upregulation of HIF1α protein and mRNA in livers from chronic ethanol-fed mice, we hypothesized that HIF1α activation in hepatocytes would accelerate the pathogenesis of alcoholic liver disease. Utilizing a murine model of hepatocyte-specific expression of a degradation-resistant mutant of HIF1α , we demonstrated that both ethanol and HIF1dPA expression induce lipid accumulation. Furthermore, alcohol fed HIF1dPA mice had increased triglyceride content in their livers, and more severe steatosis by

Figure 14. Real-Time PCRS for HIF1 downstream targets. A. The HIF1α downstream target EGLN3 was selected as a marker of HIF1α transgene expression, and was significantly upregulated in HIF1dPA mice versus Alb-Cre mice, which showed essentially flat expression of EGLN3. (*=$p<0.03$ versus controls, $n>5$ for each condition.). **B.** Plasminogen Activator Inhibitor-1 (PAI-1) was upregulated in HIF1dPA mice versus Alb-Cre controls. ($p<0.01$, HIF1dPA ET-fed or Pair-fed versus Alb-Cre controls. **C.** Inducible Nitric Oxide Synthase (iNOS) mRNA was upregulated several fold in HIF1dPA mice versus controls. ($P<0.01$, HIF1dPA ethanol or pair-fed versus Alb-Cre ethanol or pair-fed.) **D.** Vascular Endothelial Growth Factor was also significantly upregulated in HIF1dPA ethanol-fed mice versus Alb-Cre ethanol-fed mice. A strong trend towards significance in HIF1dPA ethanol-fed mice was significant versus Alb-Cre pair-fed mice at a level of significance of $P<0.07$. **E.** Tumor necrosis factor-alpha (TNFα) was significantly upregulated in HIF1dPA mice versus Alb-Cre mice, with a trend towards further upregulation with ethanol feeding. ($P<0.01$, HIF1dPA mice versus corresponding group of Alb-Cre mice.)

Figure 14

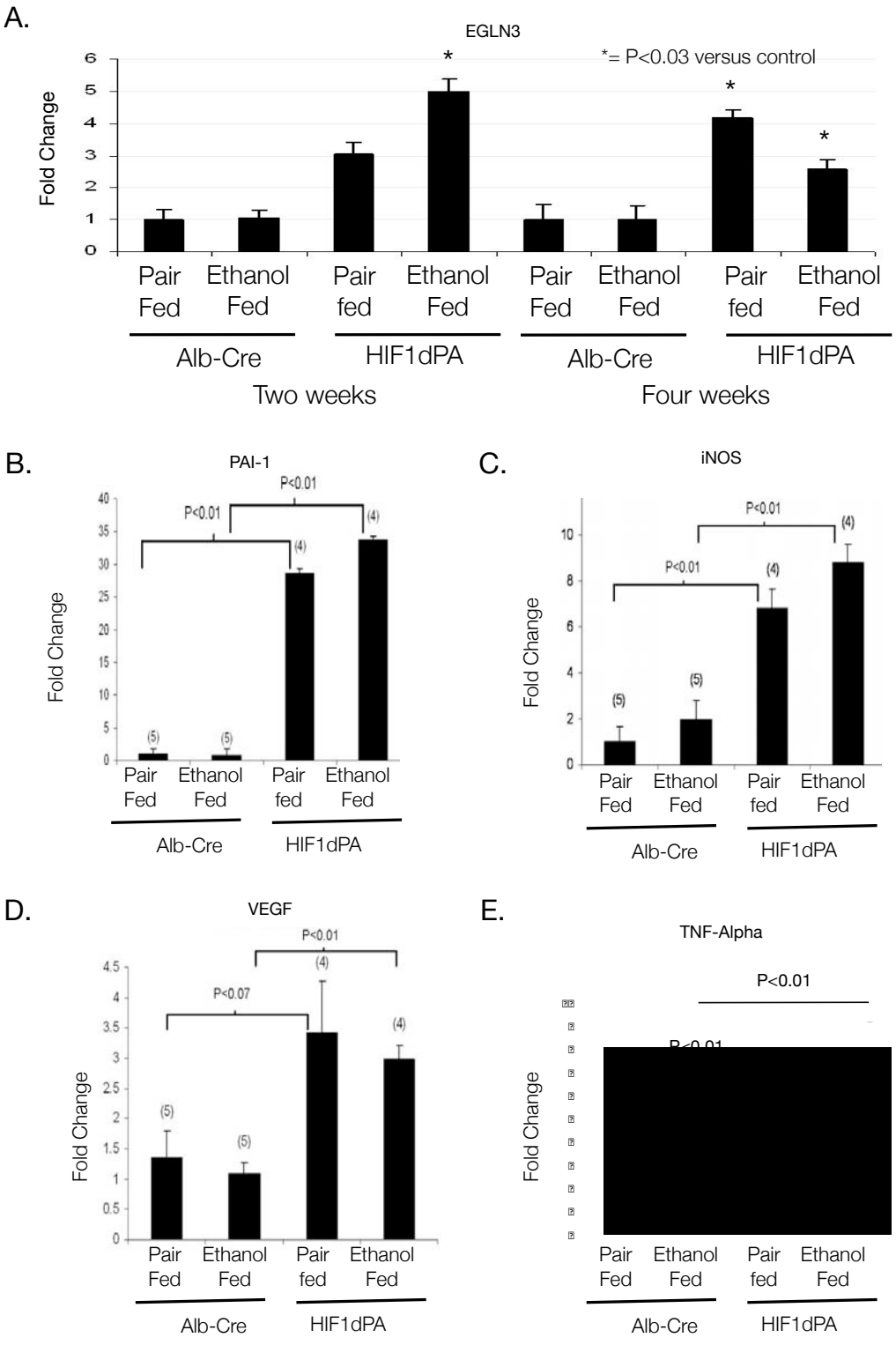
A.
EGLN3
*= P<0.03 versus control
Fold Change
Pair Fed
Ethanol Fed
Pair fed
Ethanol Fed
Alb-Cre
HIF1dPA
Two weeks
Four weeks
B.
PAI-1
P<0.01
C.
iNOS
D.
VEGF
P<0.07
E.
TNF-Alpha

Figure 15. Serum cytokine levels in HIF1dPA and control mice with ethanol feeding. Serum levels of the cytokines MIP1b, MCP-1, IL-6, and KC were determined using a multiplex bead array(**A**). Serum MCP-1 was significantly upregulated in ethanol-fed wild-type mice versus pair-fed controls. (*=P<0.05 versus wild-type pair-fed group.) Other changes in wild-type mice (in IL-6, KC, and MIP1B) were not significant. KC was significantly upregulated in HIF1dPA ethanol-fed mice. (*=p<0.05 versus Alb-Cre pair- or ethanol-fed or HIF1dPA pair-fed groups.) (A). A corresponding increase in KC mRNA was observed in HIF1dPA mice (**B**)

Figure 15

A.

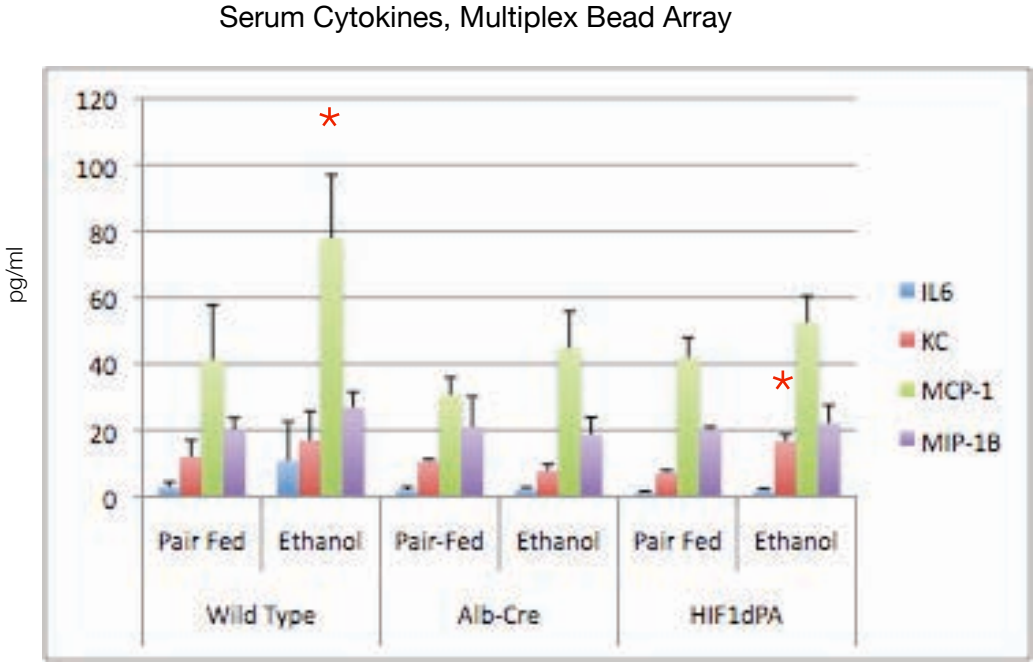
Serum Cytokines, Multiplex Bead Array
pg/ml
120
100
80
60
40
20
0
*
*
IL6
KC
MCP-1
MIP-1B
Pair Fed
Ethanol
Pair-Fed
Ethanol
Pair Fed
Ethanol
Wild Type
Alb-Cre
HIF1dPA

B.

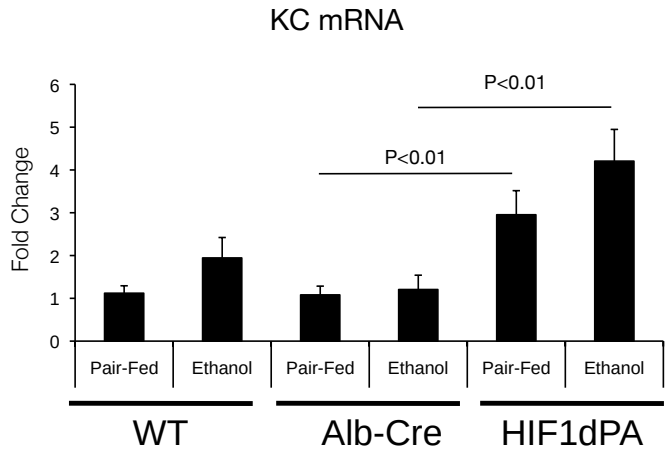
KC mRNA
Fold Change
6
5
4
3
2
1
0
P<0.01
P<0.01
Pair-Fed
Ethanol
Pair-Fed
Ethanol
Pair-Fed
Ethanol
WT
Alb-Cre
HIF1dPA

histopathology in comparison with ethanol-fed Alb-Cre control mice, suggesting an additive effect in the development of steatosis.

In the original work of Kim et al, constitutive activation of HIF1α using a HIF1dPA transgene resulted in mild lipid accumulation, whereas simultaneous activation of HIF1α and HIF2α caused significant lipid accumulation as well as pronounced vascular defects. Drawing on this work, we hypothesized that hypoxia-inducible factors had a role in the pathogenesis of alcoholic liver disease, which is marked by hepatic lipid accumulation and inflammation. Our results differed from the results of Kim et al, mainly in that in our experiments the HIF1dPA mice accumulated significant amounts of lipid. This difference is readily attributable to the extended length of our feeding, in which mice were maintained on a calorically-dense diet with or without alcohol for up to five weeks (including the acclimatization period) and at sacrifice were several months (20 weeks) old. In contrast, Kim et al observed these mice on a chow diet and sacrificed them at a much younger age. We speculate that the difference we observe may be due to a cooperative effect of HIF1α expression on lipid accumulation with the effects of the diet with or without alcohol.

Alcohol feeding of HIF1dPA mice resulted in some increased parameters of liver injury when compared to Alb-Cre littermate controls. Notably, HIF1dPA mice and Alb-Cre mice all had increased liver-weight/body-weight ratios with ethanol feeding. By four weeks of feeding, HIF1dPA pair-fed mice had LW/BW ratios comparable to ethanol-fed Alb-Cre mice, suggesting that ethanol-feeding and HIF1α activation had approximately equal effects on the development of hepatomegaly. Alcohol feeding to HIF1dPA mice resulted in a further increase in hepatomegaly versus HIF1dPA pair-fed mice by four weeks. This predisposition to lipid

accumulation in HIF1dPA mice was confirmed by histology and quantification of hepatic triglyceride content.

Ethanol feeding caused a slight increase in serum ALT levels in ethanol-fed Alb-Cre mice. Although HIF1dPA pair-fed mice had levels of serum ALT that were comparable to Alb-Cre ethanol-fed mice, ethanol feeding of HIF1dPA mice did not result in a significantly increased serum ALT level. We speculate that the level of serum ALT elevation we observed was limited by the absence of LPS stimulation, an omission in our study. It is possible that activation of HIF1α may confer some protection to steatotic hepatocytes; our prediction is that further injury, such as that caused by LPS stimulation, would likely overcome that protective effect and result in greater liver injury in HIF1dPA mice. Inclusion of such a group would be expected to reveal greater differences among ethanol-fed and pair-fed mice, and may have revealed further predisposition to injury in the HIF1dPA mice.

Interestingly, HIF1α and HIF2α subunit expression was detected in all HIF1dPA mice; additionally, HIF2α protein was detected in Alb-Cre ethanol fed mice. These findings coincide with those of Kim et al, reporting that constitutive activation of both HIF1 isoforms induced lipid accumulation.

When downstream gene expression was examined, several-fold upregulation of several genes including PAI-1, iNOS, VEGF, and TNF-a was observed in HIF1dPA livers versus control livers. The expression of these genes, several of which have been reported as upregulated in alcoholic liver injury, may relate to the higher level of lipid accumulation and liver injury observed in ethanol-fed HIF1dPA mice. For example, the use of PAI1(-/-) mice or pharmacological PAI-1 inhibition resulted in prevention of steatosis with chronic ethanol in one

mouse model.[190] However, numerous questions remain about the relationship of HIF1α downstream genes to lipid accumulation. We also observed some differences in gene expression between Alb-Cre control mice and C57/Bl6 mice. Notably, the gene expression levels of iNOS and PAI-1 were relatively unchanged with ethanol feeding in Alb-Cre mice, whereas a statistically significant upregulation of these targets was observed with alcohol feeding in C57/Bl6 mice. There are two possibilities that might explain this observation. The first possibility is that the Alb-Cre mouse has a phenotype that confers some resistance to alcohol-mediated liver injury. In support of this possibility, the serum ALT levels attained with chronic ethanol feeding in Alb-Cre mice were also lower than that observed in C57/Bl6 mice, although these differences may also be due to other experimental variability, including batch variation of the ALT reagent or other conditions. The mechanism of this resistance might be due to integration of the Alb-Cre transgene within a gene locus whose transcription is crucial for the development of ALD, or, alternatively, it may be due to a survival-promoting effect of expression of the site-specific recombinase on cellular function--for example, inhibitory interaction of the recombinase with transcription-factor binding sites implicated in inflammation, apoptosis, or an array of other possibilities. As we did observe increased triglyceride accumulation and an elevation in liver-weight/body-weight ratio, as well as some elevation of serum ALT, in Alb-Cre mice, we were able to conclude that ethanol feeding had an observable effect on these mice and judge the effect of the HIF1dPA transgene thereby. A second possibility is that the elevation of HIF target genes such as PAI-1 and iNOS observed with chronic ethanol owes more to alcohol-induced hyper-responsiveness of innate immune signaling pathways. In support of this theory, when chronic alcohol-fed mice are challenged with an intraperitoneal injection of LPS, they

attain much higher fold-increase in levels of PAI-1 and iNOS. Thus, the moderate increases we observe without exogenous LPS challenge might be indicative of a chronic-low-level LPS stimulation. Subtle variations in the Alb-Cre mice, such as the composition of their gut flora, might account for differences in their portal venous levels of gut derived endotoxin. Importantly, whereas C57/Bl6 mice were purchased from an outside vendor, the Alb-Cre littermate mice we used in out study were bred and raised within our facility, which suggests a possible rationale for suspecting differences in their enteric bacterial composition.

Induction of pro-inflammatory cytokines, or a priming effect of HIF1dPA transgene expression on cytokine induction, plays a role in the pathogenesis of alcoholic liver disease. In support of this hypothesis, we found that the pro-inflammatory cytokine KC, the murine homolog of IL8, was upregulated by chronic ethanol and HIF1dPA transgene expression. We also found higher levels of TNFα mRNA, which also has been related to hepatic lipid accumulation. Other cytokines, including MCP-1, MIP1B, and IL-6 were not significantly altered in HIF1dPA mice. Again, it is possible that the addition of LPS stimulation would have revealed a difference in the expression of these cytokines, or that, if these cytokines are related to HIF1α expression, some cytokines act upstream of HIF1α activation, whereas others (such as KC) may be induced by HIF1α. Another possibility, alluded to previously, is that the Alb-Cre transgene interfered with the inflammatory response in these mice. Lending support to that theory, ethanol-fed Alb-Cre mice maintained lower levels of cytokines and gene expression of targets such as TNFα than we observed in wild-type mice. The addition of LPS, again, may have clarified these findings.

With regards to the differential gene regulation we observed between C57/BL6 mice and HIF1dPA and/or Alb-Cre mice, a few disparities should be addressed. For one thing, although we have postulated the increase in HIF1α as a mechanistic possibility for the pathogenesis of ALD, the classic HIF1α target gene VEGF is not upregulated, either within the Alb-Cre mice or C57/Bl6 mice, with chronic ethanol feeding. As HIF1α is a transcriptional regulator of both inflammation and angiogenesis, it stands to reason that there would be some scenarios in which it would be evolutionarily advantageous to decouple these two broad responses. We have observed a situation, namely chronic ethanol, in which upregulation of HIF1α is not accompanied by upregulation of VEGF. This suggests that the proinflammatory and the proangiogenic functions of HIF1α can indeed be decoupled. There are several possible mechanisms whereby this decoupling may occur For one, as HIF1α activity is known to depend upon the recruitment of co-factors, competition for co-factor recruitment by proinflammatory transcription factors, such as NFκB, might inhibit some, but not all, functions of HIF1α; in particular, those functions of HIF1 that also depend upon NFκB, such as the induction of proinflammatory cytokines, might be preserved while others that are NFκB-independent might be prevented. Other mechanisms include transcriptional suppression via other DNA binding proteins, or epigenetic regulation e.g., histone protein modification and chromatin remodeling.

Another remaining question is the differential regulation of the chemokine MCP-1 between HIF1dPA mice, Alb-Cre mice and C57/BL6 mice. The explanations that we have suggested for differential VEGF regulation are not sufficient in this case, as MCP-1 is an inflammatory cytokine and hence would not be expected to be decoupled from other functions of HIF1α in the manner we have proposed above. One possibility is that MCP-1 is induced

upstream of HIF1α activation, and further stimulation of HIF1α signaling pathways, (for example, via introduction of the HIF1dPA transgene) does not result in further upregulation of MCP-1.

Both direct effects of HIF1 transgene expression on lipid metabolic pathways as well as induction of pro-inflammatory cytokines may have effects on hepatic lipid accumulation and the progression of liver disease. In the next chapter, we explore the contribution of MCP-1 in an *in vitro* model of lipid accumulation, and the relationship of that lipid accumulation to the activation of HIF1α.

CHAPTER 4

IN VITRO STUDIES ON HIF1 AND LIPID ACCUMULATION

Summary

Our previous studies correlated HIF1α expression to hepatic lipid accumulation in ethanol-fed mice. We sought to test the hypothesis that HIF1α could be related to lipid accumulation in hepatocytes. A recent *in vitro* study using the human hepatoma cell line Huh7 demonstrated that lipid accumulation could be induced in this cell line with MCP-1 treatment. MCP-1 levels were synergistically upregulated in wild-type mice with ethanol feeding and LPS injection, thus we tested HIF1α induction using MCP-1 in an *in vitro* hepatocyte cell line system. MCP-1 treatment upregulated HIF1 nuclear protein and HIF DNA binding in Huh7 cells. Using an siRNA-mediated approach, we demonstrate that HIF1 or HIF2 siRNA pretreatment is sufficient to block MCP-1-induced triglyceride accumulation in Huh7 cells. HIF1 siRNA treatment also limited lipid accumulation as identified by Oil-Red O staining. Finally, transfection of Huh7 cells with HIF1dPA or HIF2dPA plasmids resulted in an increase in triglyceride accumulation. We conclude that MCP-1-induced lipid accumulation in the Huh7 cell line occurs at least in part via a HIF dependent mechanism, and that HIF overexpression in the Huh7 cell line is sufficient to induce lipid accumulation.

Acknowledgements

The HIF1dPA and HIF2dPA plasmids were the kind gift of Dr. William Kim, University of North Carolina, Chapel Hill, who developed them as a postdoctoral research fellow in the lab of Dr. William Kaelin, Dana Farber Cancer Institute, Harvard University, Boston MA.

The author is grateful to Ivan Levin MD for assistance with cell culture studies, and for generation of data in figure 20, panel A.

pcDNA3.1 encoding GFP was the kind gift of Seema Paliwal, PhD, from the lab of Steven Grossman MD PhD.

Introduction

Hepatic lipid accumulation, or steatosis, is an early and reversible feature of hepatic pathology observed after chronic ethanol stimulation. Multiple lines of evidence suggest that hepatic lipid accumulation as the result of chronic ethanol treatment proceeds via mechanisms that involve the hepatocyte as well as other cell types in the liver (Reviewed in [130]). In this regard, numerous similarities exist between alcoholic liver disease and non-alcoholic fatty liver disease (NAFLD). Notably, the progression of both NAFLD and ALD to NASH and alcoholic hepatitis, respectively, appears to be at least partially dependent upon activation of innate immune pathways, including signaling through the Toll-like Receptor family of pattern recognition receptors.

Monocyte Chemoattractant Protein-1 (MCP-1) is a member of the C-C group of chemokines, identified by the conserved motif of two adjacent cysteine residues. Four MCP isoforms are known in humans. MCP-1 is known to exert effects through binding its receptor, CCR2, in either a dimeric or a monomeric form. The CCR2 receptor is a G-protein coupled receptor whose activation results in the activation of phospholipase C, the formation of inositol triphosphate, and ultimately, protein kinase C activation leading to activation of the master regulator of inflammation, NFκB.[191]

MCP-1 has been implicated by various lines of evidence in the pathogenesis of liver disease. MCP-1 has been demonstrated to be secreted by various cell types in the liver, including hepatocytes, macrophages (Kupffer cells, KpfCs) as well as hepatic stellate cells. One study demonstrated that KpfCs secreted nitric oxide and MCP-1 in response to LPS stimulation. [192] Hepatocyte and whole liver mRNA and protein levels of MCP-1 were increased in

response to homocysteine treatment, mimicking the liver injury seen in hereditary hyperhomocysteinemia.[193] MCP-1 expression in adipose tissue was reported to increase hepatic steatosis. [203] Blockade of the MCP-1 receptor was reported to decrease hepatic steatosis and improve insulin sensitivity in db/db mice, which are deficient in the leptin receptor and are predisposed to obesity.[204] Furthermore, increased serum MCP-1 was observed in nonalcoholic steatohepatitis.[205] TLR4 is known to play a role in both ALD as well as NAFLD, and hepatic MCP-1 RNA was partially, though not completely, suppressed in TLR4(-/-) mice fed a high-fat, high cholesterol diet (atherogenic diet). [194] Another study demonstrated that hepatic stellate cells secrete MCP-1 in response to TLR9 receptor stimulation (via the bacterial unmethylated CpG DNA motif), and that TLR9 (-/-) mice were protected from hepatic fibrosis after bile-duct ligation.[195] Similarly, anti-MCP-1 gene therapy diminished hepatic fibrosis after diethylnitrosamine challenge.[196]

Clement and colleagues described the finding that treatment of human hepatoma cell line Huh7 with the chemokine Monocyte Chemoattractant Protein-1 (MCP-1) resulted in lipid accumulation.[197] We and others report elsewhere that MCP-1 is synergistically upregulated by alcohol and lipopolysaccharide injection.[1] MCP-1 is a chemokine that is reported to be upregulated in visceral adipose tissue in metabolic disease; it is thus positioned as a target of interest in two different models of fatty liver disease, namely Non-Alcoholic Fatty Liver Disease (NAFLD) as well as alcoholic steatohepatitis.

Some literature exists on crosstalk between hypoxia-inducible factors and MCP-1 stimulation. MCP-1 has been implicated in angiogenesis. Earlier work described an

---

[1] *Vide infra.* We report the upregulation of MCP-1 with ethanol and LPS stimulation in Chapter 5.

upregulation of HIF1α in aortic endothelial cells stimulated with MCP-1, and subsequent production of VEGF-A.[198] Other investigators reported that a transcription factor, MCP-1 Induced Protein, acts downstream of MCP-1 stimulation in monocytes to stimulate VEGF-A and HIF1α upregulation.[199]

We undertook to determine whether *in vitro* evidence could suggest a link between hepatic steatosis, MCP-1 treatment, and HIF1α activation. Using the Huh7 cell line, we report that HIF1α protein is upregulated by MCP-1 treatment, and that upregulation of MCP-1 is associated with hepatic lipid accumulation. Treatment of the Huh7 cell line with siRNA targeting HIF1α or HIF2α prevented hepatic lipid accumulation as observed by Oil-Red O staining or by triglyceride assay, whereas treatment with scrambled siRNA conferred no such protection. Finally, treatment of Huh7 cells with a HIF1dPA or HIF2dPA plasmid directly induced hepatic lipid accumulation as measured by triglyceride assay. We conclude that MCP-1 induced lipid accumulation in the Huh7 cell line is dependent upon hypoxia inducible factor activation.

Methods

Cell Culture Studies

All studies were performed using the human hepatocellular carcinoma cell line Huh7. Cells were maintained in complete growth medium (Dulbecco's Modified Eagle Medium (DMEM) supplemented with 10% fetal bovine serum (FBS), 2% Penicillin/Streptomycin, and 1% 100X amino-acid supplement mixture.) Cells were passaged in T75 flasks at 70% confluence by washing once with phosphate-buffered saline followed by 5 minute incubation with TryplE express trypsin analogue. Trypsinized cells were resuspended in complete growth medium. For

in vitro assays, cells were plated on 10cm plates, and then transfected with plasmid DNA or siRNA and/or treated with recombinant monocyte chemoattractant protein-1 (MCP-1, R&D Systems).

Plasmid transfections

The HIF1dPA and HIF2dPA plasmids were the kind gift of Dr. William Kim (UNC). Plasmid DNA was transfected into Huh7 cells using Fugene transfection reagent according to the manufacturers instructions. Briefly, Huh7 cells on 10cm plates at 50-60% confluence were transfected with 5ug plasmid DNA (HIF1dPA or HIF2dPA transgenes encoded into pcDNA3.1) with 15ul Fugene 6 and 160ul serum free media. For verification of plasmid transfection, pcDNA3.1 encoding GFP was used and cells imaged 24 hours post-transfection with a fluorescent microscope.

siRNA transfections

HIF1α siRNA, HIF2α siRNA, or scrambled (scr) siRNA were purchased from Santa Cruz Biotechnology. Transfection was achieved using siPORT Amine transfection agent (Applied Biosystems) according to the protocol of the manufacturer. Briefly, for a 10cm-plate, 17ul siPORT Amine reagent at room temperature was added to 333ul Opti-MEM serum-free medium and incubated at room temperature for 10 minutes. 7.5ul of 10um HIF1α, HIF2α, or scr siRNA was diluted in 142ul Opti-MEM and incubated for 10 minutes at room temperature.

Subsequently, both the transfection reagent and the siRNA mixture were mixed and transfection complexes allowed to form after a 10 minute incubation at room temperature. The

mixture (500ul) was dispersed on a 10cm plate, and overlaid with 7x105 cells in a final volume of 7ml. After 24 hours, medium was aspirated and replaced with 10ml complete culture medium for subsequent treatment with MCP-1 or other assays.

Real Time PCR

For RNA analysis from cell culture, medium was aspirated from plates and plates were washed with 5ml PBS. 500ul of Buffer RLT (Qiagen) was added, the plate surface scraped and collected, and passed through a QiaShredder column and stored at -80 until subsequent RNA purification using the RNeasy mini kit (Qiagen). Primer sequences are listed in table 2. Protein concentrations were determined by adding 1uL of whole-cell lysate or nuclear extract to Bradford reagent (BioRad) and by measuring the difference between absorbance at 650nM and 595nM on a 96 well plate using a plate reader. Concentrations were determined using a standard curve of bovine serum albumin.

Oil Red O Staining

Media was removed from cultured and treated cells and plates were washed with 2ml PBS. 2ml of 10% formalin was added to each plate and plates were incubated for 10 minutes. Subsequently, formalin solution was replaced with fresh 10% formalin (2%), plates were tightly wrapped with parafilm and stored at room temperature overnight. Formalin was then removed, and cells were washed twice with ddH_2O and then washed for 5 minutes with 60% isopropanol. Plates were dried, and then 1ml of Oil Red O working solution was added and plates were

TABLE 2. Human PCR primers

HIF1a F: 5’-ATC CAT GTG ACC ATG AGG AAA TG-3’

HIF1a R: 5’-CTC GGC TAG TTA GGG TAC ACT T-3‘

HIF2a F: 5‘-GTC TCT CCA CCC CAT GTC TC-3’

HIF2a R: 5’-GGT TCT TCA TCC GTT TCC AC-3’

incubated for 10 minutes. Oil Red O solution was removed and plates were immediately destained with 4 washes of ddH_2O. Plates were then photographed with photomicroscopy.

Nuclear Extraction

Cells were scraped into ice-cold PBS and washed at 1700RPM for 10 minutes at 4 degrees. Cells were resuspended in 400ul ice-cold Buffer A (10mM HEPES pH 7.9, 10mM KCl, 0.1mM EDTA, 0.1mM EGTA, 1mM DTT, 1mM PMSF, plus 1 Complete Mini protease inhibitor tablet/ 10ml buffer.) Cells were lysed by adding 20ul non-idet P40 substitute and vortexing briefly. Lysates were centrifuged for 30 seconds at 12,500RPM/4 degrees C, and supernatants removed. Pellets were washed twice in 300ul Buffer A, and resuspended and then frozen at -80 degrees C in 50ul Buffer B (20% glycerol, 20mM HEPES pH7.9, 400mM KCl, 1mM EDTA, 1mM EGTA, 1mM DTT, 1mM PMSF, plus 1 Complete Mini Protease Inhibitor Tablets/5ml Buffer B.) Lysates were thawed and rocked for 30 minutes at 4 degrees C. Supernatants were collected after centrifugation at 12500RPM for 10 minutes and used for downstream analysis.

Electrophoretic Mobility Shift Assay

A consensus double-stranded Hypoxia Response Element (HRE) (Santa Cruz Biotech, CA) oligonucleotide was used for EMSA. End-labeling was accomplished by treatment with T4 kinase in the presence of [32P]ATP. Labeled oligonucleotides were purified on a polyacrylamide copolymer column (BioRad). Five micrograms of nuclear protein was added to a binding reaction mixture containing 50 mM Tris-HCl, pH 7.5, 5 mM MgCl2, 2.5 mM EDTA, 2.5 mM DTT, 250 mM NaCl, 20% glycerol, 20 μg/ml BSA, 2 μg poly(dI–dC) and 30,000 c.p.m. of 32P-

labeled NFB oligonucleotide. Samples were incubated at room temperature for 30 min. Reactions were run on a 5% polyacrylamide gel and the dried gel was exposed to an X-ray film at –80°C overnight. Cold competition was done by adding a 20-fold excess of specific unlabeled double-stranded probe to the reaction mixture. Band density was quantified using Labworks 4.0 image analysis.

Western Blotting

30-50ug of nuclear extract was resolved on 10% polyacrylamide gels and transferred overnight to nitrocellulose support. Membranes were blocked overnight with blocking buffer (5% bovine serum albumin in Tris-Borate-SDS with 0.01% Tween 20) with refrigeration, and subsequently probed overnight with anti-HIF1α (R&D Biosciences) mouse monoclonal antibodies. Detection was performed using an anti-mouse horseradish-peroxidase conjugated secondary antibody and chemiluminescent substrates. Band density was quantified using Labworks 4.0 image analysis.

Results

MCP-1 induces lipid accumulation in Huh7 hepatoma cells.

MCP-1 is increased in chronic alcohol feeding, and others have shown that lipid accumulation is induced in Huh7 cells with MCP-1 treatment. We first undertook to reproduce the finding that MCP-1 treatment induces lipid accumulation in the cell line Huh7. Huh7 cells were cultured and plated on 10cm plates. At 50%-70% confluence, recombinant MCP-1 was added at 100ng/ml. We found that MCP-1 treatment induced an increase in triglyceride content within 24 hours.

(Figure 16A) We also stained culture plates with Oil Red O, and found increased Oil Red O staining in MCP-1 treated Huh7 cells after 24 hours. (Figure 16B).

We then sought to determine whether MCP-1 treatment had any effect on the accumulation of HIF1α protein. Cultured Huh7 cells were treated with MCP-1 as described, and nuclear extracts were prepared from cells collected at several time points (Figure 17A). HIF1α protein in nuclear extracts and HIF1 DNA binding were increased by MCP-1 treatment (Figure 17C). Band intensity was quantified by densitometry, (Figure 17B and D)

Activation of HIF1 or HIF2 induces hepatic lipid accumulation

Since MCP-1 treatment induced lipid accumulation and HIF1α activation, we then sought to determine whether HIF1α activation alone could recapitulate the phenotype of lipid accumulation. HIF1dPA and HIF2dPA plasmids are degradation resistant mutants of HIF1α and HIF2α, and were the kind gift of Dr. William Kim, UNC. We transfected HIF1dPA, HIF2dPA, or GFP control into Huh7 cells using the Fugene transfection reagent. GFP-positive cells confirmed that transfection was successful in Huh7 cells.(Figure 18A) HIF1dPA and HIF2dPA transfection was confirmed by specific upregulation of HIF1α or HIF2α mRNA.(Figure 18B and 18C) HIF1dPA or HIF2dPA transfection also increased HIF1 DNA binding.(Figure 18E and 18F). HIF1dPA or HIF2dPA transfection resulted in increased triglyceride (Figure 18D.) Finally, we observed increased lipid accumulation in HIF1dPA or HIF2dPA treated Huh7 cells using Oil Red O staining and microscopy. (Figure 19)

Figure 16. MCP-1 treatment and triglyceride accumulation. Huh7 cells were treated with MCP-1. Intracellular triglyceride was increased using a biochemical assay **(A).** MCP-1 treated cells accumulation more lipid as demonstrated by increased intensity of Oil Red O staining.**(B)** The first two columns show conventional light microscopy of the culture plates, with Oil-Red O visible as red stain; the second two columns show the same images with inverted contrast in order to heighten the visibility of Oil-Red O positive areas, which appear as blue regions.

Figure 16

A.

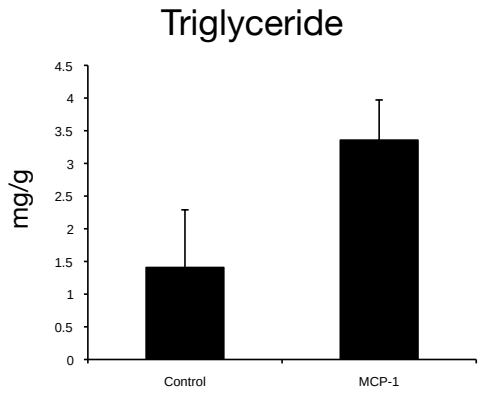
Triglyceride
mg/g
4.5
4
3.5
3
2.5
2
1.5
1
0.5
0
Control
MCP-1

B.

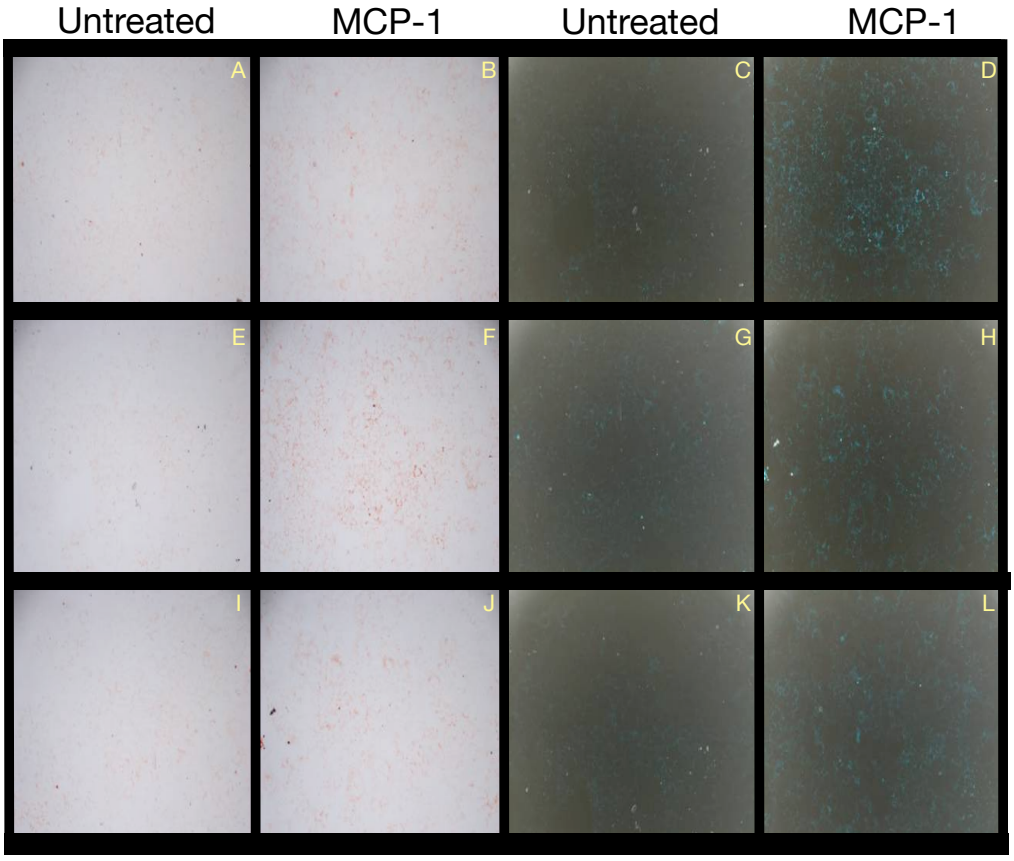
Untreated
MCP-1
Untreated
MCP-1
A
B
C
D
E
F
G
H
I
J
K
L

Figure 17. MCP-1 Treatment and HIF activation. Huh7 cells were treated with MCP-1. Nuclear extracts were prepared, and western blotting was performed with an anti-HIF1α antibody. Significant upregulation of HIF1α was observed with MCP-1 treatment (20A). Densitometry appears in panel B. Increased HIF DNA binding was observed using a HIF specific oligonucleotide. (20C) Densitometry appears in panel C.

Figure 17

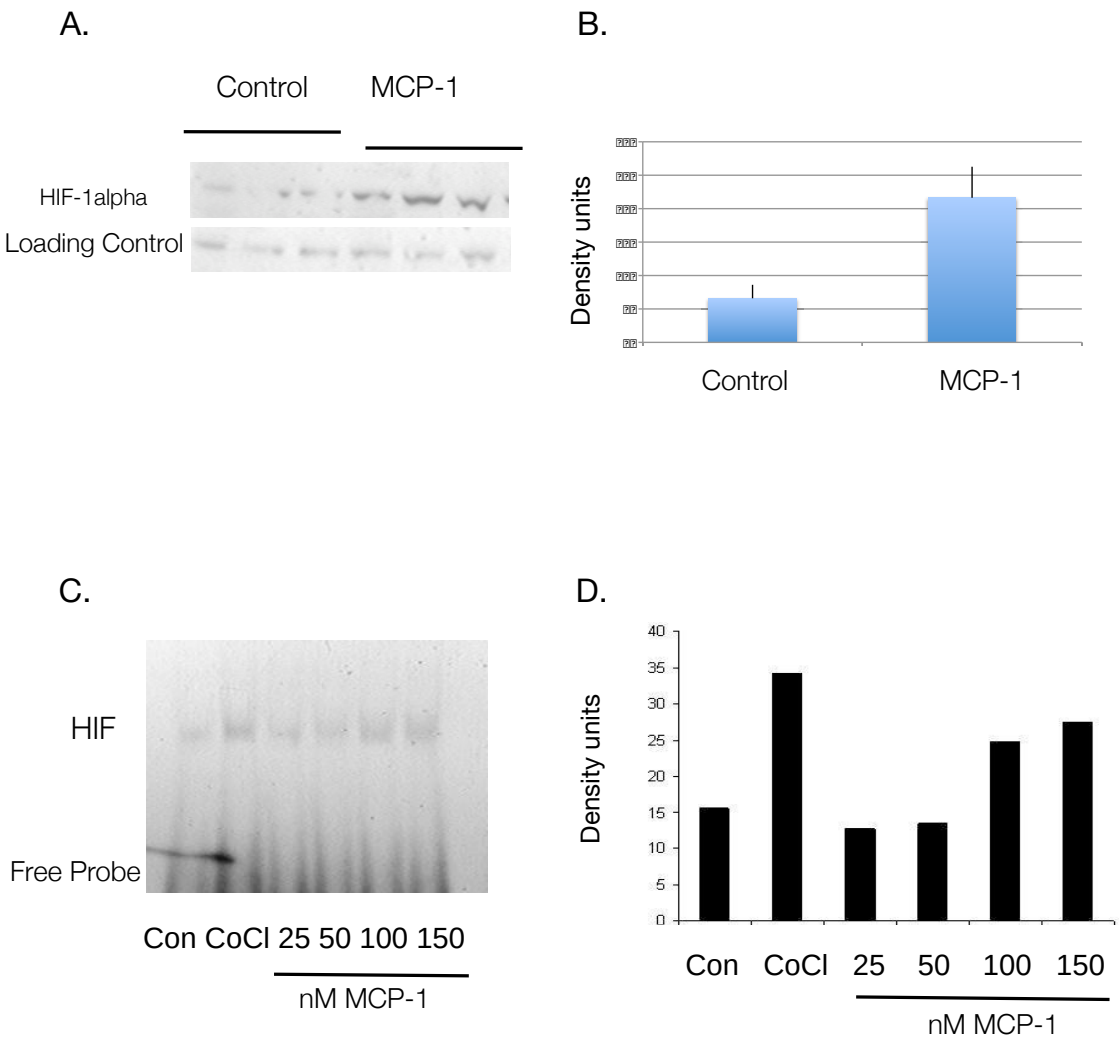
A.
Control
MCP-1
HIF-1alpha
Loading Control
B.
Density units
Control
MCP-1
C.
HIF
Free Probe
Con CoCl 25 50 100 150
nM MCP-1
D.
Density units
40
35
30
25
20
15
10
5
0
Con
CoCl
25
50
100
150
nM MCP-1

Figure 18. HIF1dPA and HIF2dPA plasmid transfections.

Transfection was confirmed using plasmid encoding GFP (A), which was also used as a negative control in subsequent experiments. HIF1dPA plasmid transfection or HIF2dPA plasmid transfection was confirmed using RT-PCR (**A and B**). HIF1dPA or HIF2dPA plasmid transfection resulted in an increase in intracellular triglyceride.(**C**) Both HIF1dPA and HIF2dPA plasmid transfection increased HIF DNA binding (**E**), densitometry appears in (**F.**)

Figure 18

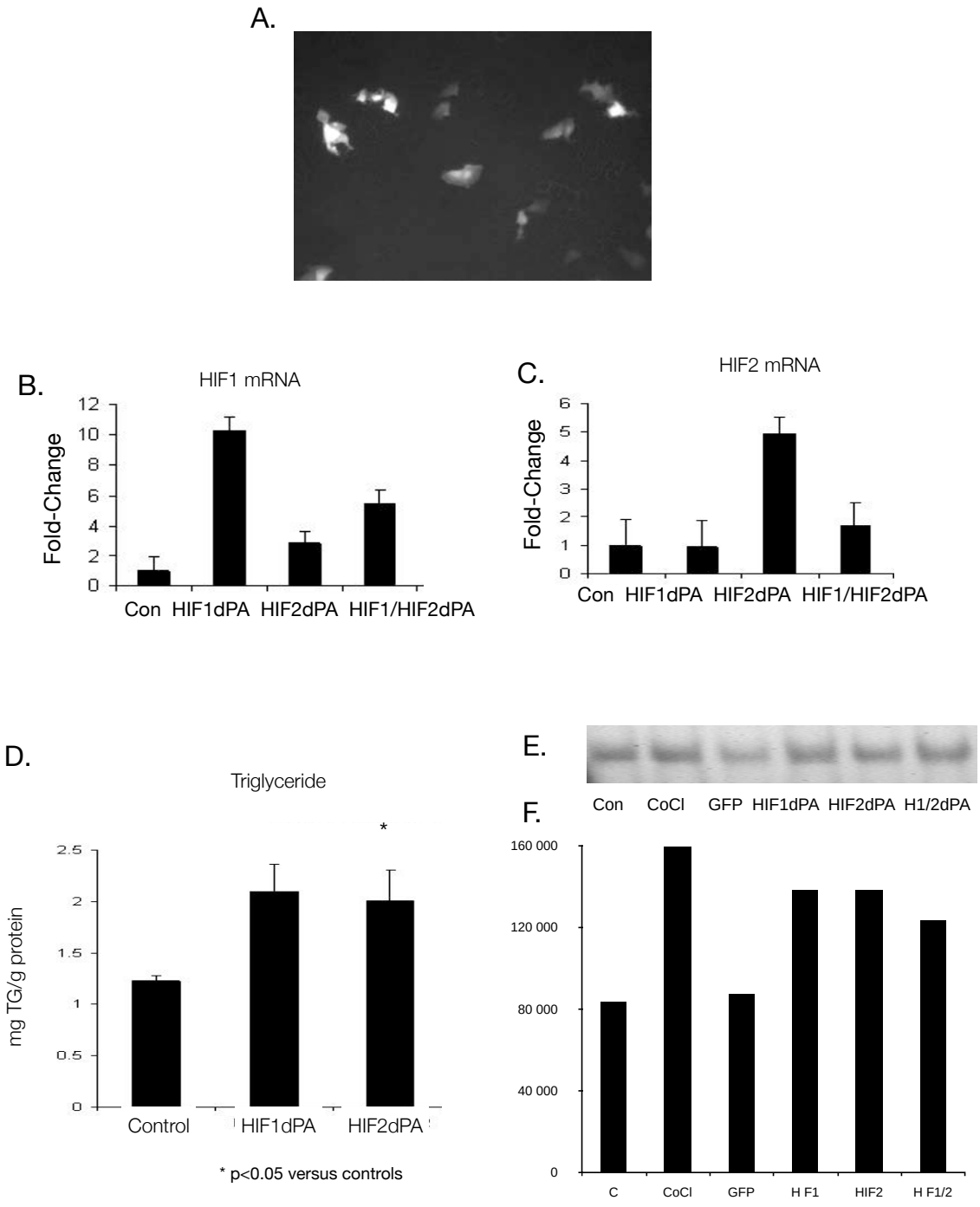
A.
B.
HIF1 mRNA
Fold-Change
12
10
8
6
4
2
0
Con
HIF1dPA
HIF2dPA
HIF1/HIF2dPA
C.
HIF2 mRNA
Fold-Change
6
5
4
3
2
1
0
Con
HIF1dPA
HIF2dPA
HIF1/HIF2dPA
D.
Triglyceride
mg TG/g protein
2.5
2
1.5
1
0.5
0
*
Control
HIF1dPA
HIF2dPA
* p<0.05 versus controls
E.
Con
CoCl
GFP
HIF1dPA
HIF2dPA
H1/2dPA
F.
160 000
120 000
80 000
40 000
0
C
CoCl
GFP
H F1
HIF2
H F1/2

Figure 19. Oil-Red O staining, HIF1dPA/HIF2dPA plasmid transfection. Huh7 cells transfected with HIF1dPA or HIF2dPA plasmid were stained with Oil Red O and photographed by microscopy. (**A**) Huh7 cells without any treatment. Little lipid accumulation is visible. (**B**) Huh7 cells treated with MCP-1. Lipid accumulation is visible as red refractile particles (arrowhead). (**C**) Cells treated with reagent only (Fugene 6). (**D)** Cells treated with empty vector. (**E**) Cells treated with HIF1dPA plasmid. (**F)** Cells treated with HIF2dPA plasmid. Lipid is indicated by arrowhead.

Figure 19

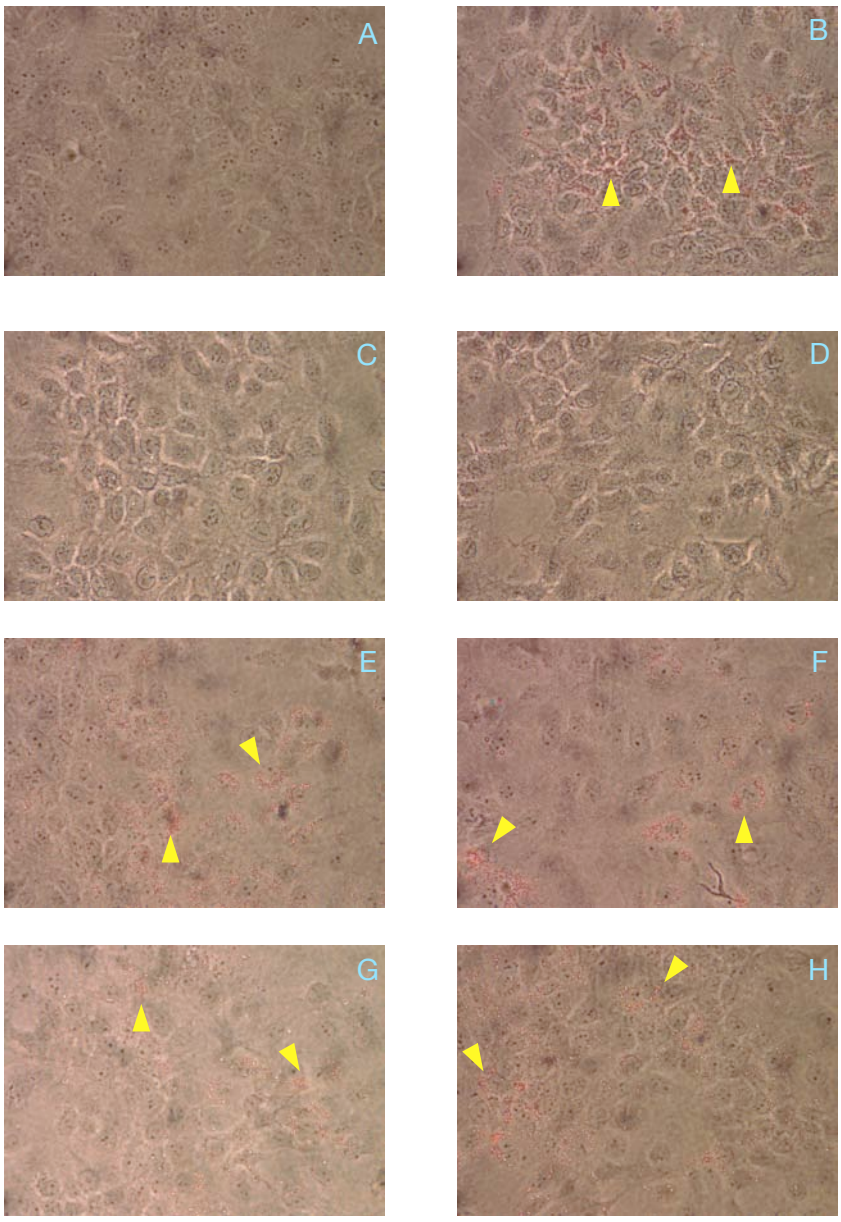

Prevention of MCP-1 induced lipid accumulation by treatment with HIF1α or HIF2α siRNA

Since we had demonstrated that HIF1α was upregulated by MCP-1 treatment, and that HIF1dPA plasmid transfection caused increased lipid accumulation in Huh7 cells, we then wondered whether knockdown of HIF1α or HIF2α (via an siRNA approach) would be sufficient to prevent lipid accumulation in the Huh7 cell line. HIF1α, HIF2α siRNA, or scrambled control was transfected into Huh7 cells using SiPORT NeoFX transfection reagent. We confirmed knockdown of HIF1α or HIF2α cellular mRNA using qRT-PCR. (Figure 20A) Scrambled siRNA did not alter HIF1α or HIF2α mRNA levels.(Figure 20A) We then designed an approach to determine whether HIF1α knockdown could prevent MCP-1 induced lipid accumulation. Briefly, cells were transfected with siRNA for HIF1α, HIF2α, or scrambled control, and after 24 hours, treated with MCP-1. After an additional 24 hours, cells were assayed for intracellular lipid accumulation using a triglyceride assay (Figure 20B) or via Oil Red O staining. (Figure 20C) We determined that HIF1α or HIF2α siRNA prevented MCP-1 induced lipid accumulation in the Huh7 cell line.

Discussion

The chemokine MCP-1 is secreted by visceral adipose tissue and induces lipid accumulation in the hepatocyte cell line Huh7 *in vitro.* We found a synergistic upregulation of MCP-1 by chronic alcohol and lipopolysaccharide injection *in vivo* (see chapter 5, below), underscoring the potential relevance of this cytokine to the pathogenesis of alcoholic liver disease. We were able to reproduce the results of Clement et al, demonstrating an increase in Oil Red O staining in Huh7 cells treated with recombinant MCP-1. Additionally, we were able to demonstrate an

Figure 20. HIF1α or HIF2α siRNA prevents MCP-1 induced lipid accumulation in the Huh7 cell line.

A. Huh7 cells were treated with HIF1α or HIF2α siRNAs or scrambled siRNA control sequence and specific knockdown of HIF1α and HIF2α mRNA was determined.(*=P<0.05 versus untreated control). **B.** Cells with transient knockdown of HIF1α or HIF2α were then treated with MCP-1. We found that knockdown of HIF1α or HIF2α prevented lipid accumulation as assayed by triglyceride assay **C.** HIF1α siRNA or scrambled control cells were treated with MCP-1, and culture plates were stained with Oil Red O for intracellular lipid. Pretreatment with HIF1α siRNA inhibited the lipid accumulation observed with MCP-1 treatment. Panel 1, cells with MCP-1; Panel 2, cells with transfection reagent and MCP-1; panel 3, scrambled siRNA and MCP-1; panel 4, HIF1α siRNA and MCP-1. Similar results were obtained with HIF2α siRNA and MCP-1 (not shown).

Figure 20

A.

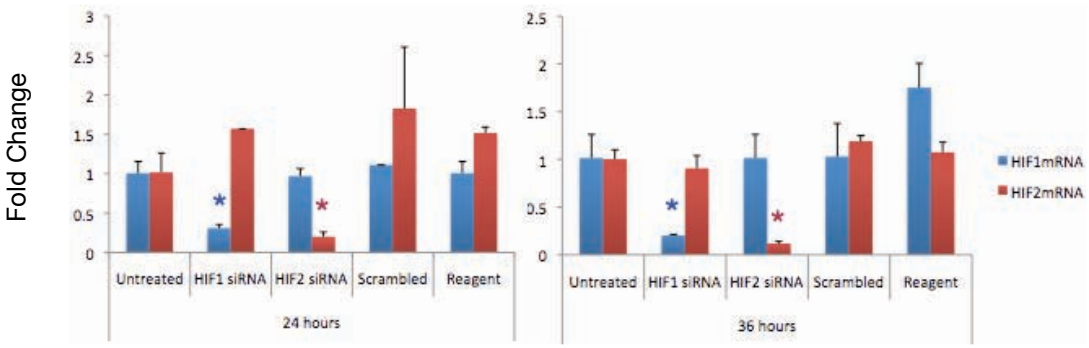

B.

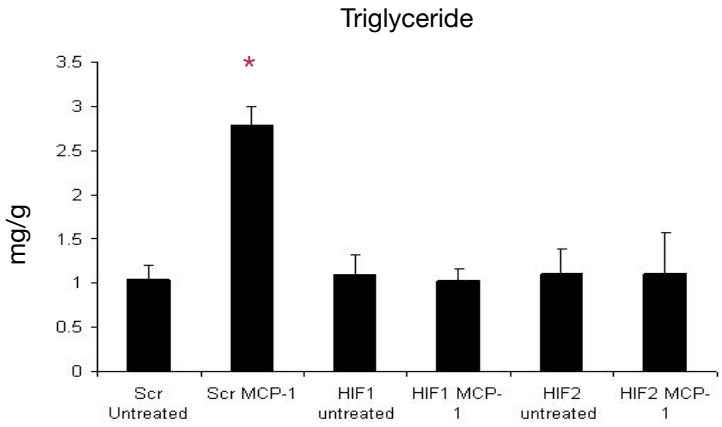

C.

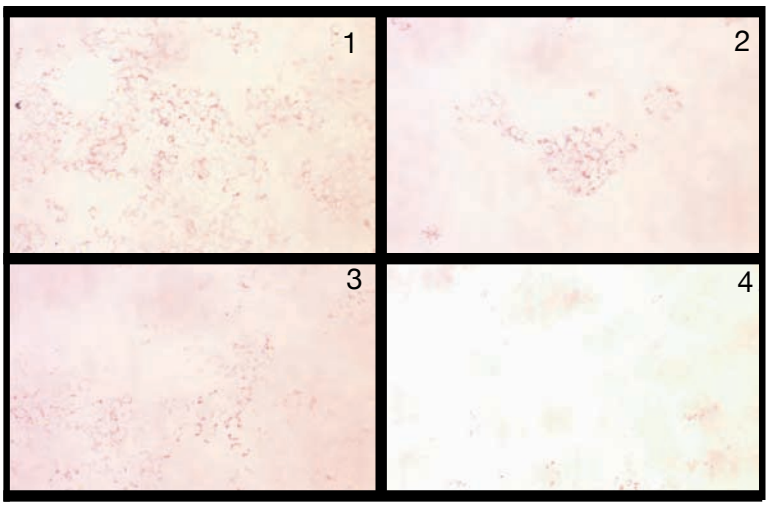

increase in triglyceride using a biochemical assay. In this group of studies, we extended these findings by demonstrating that MCP-1 treatment results in induction of HIF1α activity, and that HIF1α activity alone is sufficient to induce hepatic lipid accumulation.

Given that the hepatocyte specific HIF1α degradation resistant mutant (HIF1dPA) was able to induce lipid accumulation in hepatocytes in a mouse model, and that we were able to demonstrate increased triglyceride accumulation in ethanol-fed HIF1dPA mice versus controls, we wondered whether HIF1 activation could be related to MCP-1 induced lipid accumulation. We verified MCP-1-induced upregulation of HIF1α protein by western blot, and further verified upregulation of HIF1α DNA binding using EMSA. In order to determine whether HIF1 alone could induce lipid accumulation in this cell line, we transfected Huh7 cells with the HIF1dPA plasmid, and were able to detect triglyceride accumulation using a biochemical assay. Finally, we wondered whether inhibition of HIF would be able to prevent MCP-1 induced lipid accumulation. Using an siRNA approach, we transfected Huh7 cells with HIF1 siRNA or scrambled control. HIF1α siRNA pretreated cells did not accumulate lipid when treated with recombinant MCP-1, whereas scrambled siRNA treated cells accumulated lipid in a similar fashion to untreated cells.

Of note, we observed similar effects with HIF2dPA plasmid treatment and HIF2 siRNA mediated approaches. Other work has suggested that both HIF isoforms may have a role in modulating lipid accumulation *in vivo*. Given that HIF1dPA plasmid transfection showed a small but significant effect on HIF2α mRNA levels, it is possible that HIF1α-mediated silencing of hepatic lipid accumulation still depends on intact HIF2α signaling; alternatively, both isoforms may have redundant effects.

A significant remaining question is the mode of upregulation of HIF1α-by MCP-1 treatment. MCP-1 stimulation of the CCR2 receptor is known to result in NFκB activation; NFκB activation, in turn, has been described to transcriptionally upregulate HIF1α.[200] However, one concern with this model is whether Huh7 cells, or hepatocytes, express the CCR2 protein. Indeed, Clement et al, in their report on MCP-1 induced lipid accumulation *in vitro*, were unable to detect CCR2 mRNA in primary hepatocyte cultures, and also detected only a low level of CCR2 mRNA in Huh7 cells. Furthermore, they were not able to prevent lipid accumulation in Huh7 cells after treating them with a CCR2 antagonist. Two methodological concerns with regards to their findings are apparent. For one, they concluded that CCR2 expression was very low in Huh7 cells by comparing the CCR2 expression level to a positive control of peripheral blood mononuclear cells (PBMCs). Although Huh7 cells had no more than 1% of the CCR2 expression found in PBMCs, this may still be sufficient to induce a biologically-relevant response. In contrast, they were not able to detect expression of CCR2 mRNA in primary mouse hepatocytes. A concern is that primary hepatocytes in cell culture rapidly dedifferntiate and lose cell-specific functions, and mRNA may be one of the earlier markers of hepatocyte dedifferentiation in culture; hence, lack of expression of mRNA for CCR2 in culture may not accurately convey the situation in vivo. A better method might be western blotting for CCR2 within freshly isolated hepatocytes, or performing immunostaining on liver tissue sections.

However, assuming that the MCP1 receptor antagonist experiments accurately convey that the effect of MCP-1 treatment on lipid accumulation is independent of the CCR2 receptor,

this raises the intriguing possibility that the effect of MCP-1 treatment on lipid accumulation is via an effect on HIF1α protein levels, and is independent of CCR2. Clement and colleagues reported that inhibition of ERK was sufficient to block lipid accumulation. In other systems, ERK activation has been shown to be involved in HIF1α activation following stimulation with TNFα.[201] We speculate that an unidentified receptor for MCP-1 may be identified that can activate HIF1α via an ERK-dependent mechanism.

One strategy to determine the specificity of each of these isoforms could include stable transfections of HIF1α or HIF2α shRNA and subsequent transfection with HIF1dPA or HIF2dPA transgenes. Optimizing parameters for that strategy is one ongoing project in the lab.

CHAPTER 5

EFFECT OF PARTIAL CELL-SPECIFIC HIF1α KNOCKDOWN ON THE PROGRESSION OF ALCOHOLIC STEATOHEPATITIS

Summary

We sought to determine whether cell-specific suppression of HIF1α could ameliorate alcoholic liver disease in an *in vivo* model. We used a cre-lox strategy to express a transcriptionally-inactive mutant of HIF1α in hepatocytes or cells of the myeloid lineage. Wild-Type, HepHIF(-), or MyeHIF(-) mice were treated with chronic ethanol for five weeks. A subset was also challenged with LPS. We found that HepHIF(-) mice after chronic alcohol feeding had lower levels of hepatic triglyceride, decreased LW/BW ratios, and decreased lipid accumulation by quantified Oil-Red O staining versus control mice. QRT-PCR analysis demonstrated that HepHIF(-) mice, but not MyeHIF(-) mice, were protected from upregulation of PAI-1 and iNOS mRNA. HepHIF(-) mice, but not MyeHIF(-) mice, had lower levels of serum ALT after chronic alcohol/LPS challenge. HepHIF(-) mice, and to some degree MyeHIF(-) mice, were protected from an increase in several cytokines after ethanol/LPS challenge including TNFα, KC, IL-6 and IL-17. All mice had suppressed PPARa mRNA, suggesting that protection from lipid accumulation in this model is independent of PPARa mRNA levels. Finally, we observed that WT mice, but not HepHIF(-) mice, had upregulation in the downstream target ADRP, a lipid

droplet surface marker. We conclude that hepatocyte specific HIF1α has a role in the progression of alcoholic steatohepatitis.

Acknowledgements

The author is grateful to Ivan Levin, MD, for assistance with mouse feedings as well as with collection of data. Dr. Levin is directly responsible for generation of serum ALT data from the second cohort of mouse feedings, reported in figure 25B and 25C, real-time PCR data in figure 34, and the western blot image in figure 24A. Dr. Levin and the author collaborated in generation of the triglyceride data reported in figure 24C. The author is also grateful to Michal Ganz MD for assistance with serum ALT data collection in figure 22. The author is grateful to Timea Csak, MD and Jan Petrasek MD for assistance with mouse sample collection and measurements (TC) and collection and preparation of mouse sera (JP).

Finally, multiplex cytokine data was collected with the assistance of Christian Mueller, PhD, with the use of equipment generously made available through the lab of Terence Flotte MD.

Introduction

Our previous studies have correlated HIF1α expression to hepatic lipid accumulation in ethanol-fed mice and demonstrated that pretreatment of Huh7 hepatoma cells with a HIF1α siRNA was sufficient to prevent lipid accumulation. Given these findings, we sought to determine whether disrupting HIF1α signaling would be able to prevent alcoholic liver disease in an *in vivo* mouse model.

A recurring theme in the pathogenesis of alcoholic liver disease is the interplay between cell types in the progression of liver injury. All aspects of ALD, from steatotic change in the hepatocyte, to inflammation, to fibrotic change, to cirrhosis, appear to be modifiable by multiple factors in different cell types.[130] A basic pathogenic mechanism in the progression of alcoholic steatosis to alcoholic steatohepatitis is the hyper-responsiveness of Kupffer cells upon stimulation with gut-derived lipopolysaccharide within the hepatic portal circulation, and subsequent release of necroinflammatory mediators including TNFα and other pro-inflammatory cytokines.[130] The steatotic hepatocyte, in turn, may have a diminished ability to survive an inflammatory insult.

Cre-lox strains have been used successfully in previous studies to characterize the specific contribution of various liver cell types in mouse models of alcoholic liver disease.[36] For example, mice bearing a mutant transgene that is activated or inactivated upon co-expression of the Cre-recombinase gene, and crossed into strains expressing Cre under the control of the Alb- or the LyzM- promoter, results in hepatocyte-specific (Alb-Cre) or myeloid lineage-specific (LyzM-Cre) transgene expression or inactivation, respectively. Using this system, for example, Horiguchi and colleagues offered data to suggest that hepatocyte-specific

deletion of STAT3 resulted in greater steatosis and upregulation of liposynthetic pathways, but less hepatic inflammation, whereas myeloid-lineage-specific STAT3 deletion resulted in greater levels of pro-inflammatory cytokines and hepatic inflammation after 8 weeks of an ethanol-containing diet. [36]

Previous work in other laboratories has demonstrated that HIF1α inactivation in cells of the myeloid lineage was protective against sepsis induced by high doses of LPS.[143] Other investigators have presented data suggesting that HIF1α inactivation in hepatocytes and immune cells (via the Mx-Cre interferon-inducible promoter) prevents fibrosis in an experimental bile duct ligation model.[160] HIF1α activation in hepatocytes resulted in mild lipid accumulation, whereas activation of both HIF1α and HIF2α resulted in marked steatosis.[155] In another model, hepatocyte-specific HIF1α knockout in combination with pVHL knockout (a phenotype resembling constitutive HIF2 activation) resulted in marked lipid accumulation, whereas VHL knockout in combination with HIF2α knockout (a phenotype resembling HIF1 activation) did not result in lipid accumulation, suggesting that HIF2 is a primary mediator of hepatic lipid accumulation.[155] In that report, inhibition of the HIF degradation pathway in combination with HIF1α(-) resulted in upregulation of fatty acid synthetic pathways along with the lipid droplet surface-associated protein Adipocyte Differentiation Related Protein (ADRP). Indeed, although we have described a consistent upregulation of HIF2 in alcohol-fed mice, we have also reported that HIF1dPA mice fed ethanol accumulated higher amounts of lipid as determined by tissue microscopy and triglyceride content of whole-liver lysates.

Given the central role of HIF1α activation in response to LPS stimulation, we postulated that specific suppression of HIF1α in cells of the myeloid lineage (MyeHIF(-) mice) would result

in prevention of hepatic injury through attenuation of the inflammatory response of gut derived endotoxin, whereas partial suppression of HIF1α in hepatocytes (HepHIF(-) mice) might result in less hepatomegaly and hepatic lipid accumulation, but have a similar cytokine profile in response to pro-inflammatory stimulus. In order to obtain a robust model of alcoholic liver disease, we performed alcohol or pair feeding for five weeks, and further randomized mice into LPS or saline injected groups.

Consistent with our hypothesis, we found that HepHIF(-) mice exhibited less hepatomegaly, hepatic triglyceride, and steatosis than wild-type mice or MyeHIf(-) mice. To our surprise, both HepHIF(-) mice and MyeHIF(-) mice had decreased expression of several cytokines, including, importantly, TNFα. Correspondingly, HepHIF(-) mice were strongly protected from increased serum ALT in response to LPS challenge, whereas MyeHIF(-) only displayed a nonsignificant trend towards protection. We conclude that HIF1α activity in both hepatocytes and myeloid cells affects the progression of alcoholic steatohepatitis, and that modifying HIF1α activity may have therapeutic value in the treatment of alcoholic liver disease.

Methods

Animal Studies

All animals received care in compliance with protocols approved by the Institutional Animal Use and Care Committee of the University of Massachusetts Medical School. HIF1(flox/flox) mice, Alb-Cre mice, and LyzM-Cre mice were purchased from Jackson Laboratories (Bar Harbor, ME). The HIF1α floxed allele has been previously described.[143] All mice were supplied backcrossed onto a pure C57/Bl6 background, and C57/Bl6 mice

purchased from Jackson Laboratories were used as wild-type controls. Offpsring of HIF1(flox/flox) and Alb-Cre homozygous mice (HIF1(flox)/Alb-Cre mice, HepHIF(-) mice, henceforth) and offspring of HIF1(Flox/flox) and LyzM-Cre mice (HIF1(flox)/LyzMCre mice, MyeHIF(-) mice, henceforth) were generated, tagged by ear notching, and housed in separate cages. For initial studies to guide the timing of lipopolysaccharide (LPS) injections and serum ALT and hepatic triglyceride measurements, WT mice were given intraperitoneal injections of LPS and sacrificed at 2, 4, 6, 18, and 24 hours. For all other mouse studies, mice were gradually habituated to a Lieber-DeCarli liquid diet with 5% ethanol (volume/volume) or isocaloric pair-fed diet over a period of two weeks, then maintained on the 5% diet for five weeks. Consumption was recorded daily, and isocaloric amounts of a non-alcohol containing diet (in which dextran-maltose replaced calories from ethanol) were dispensed to pair-fed animals. Weights were recorded before the introduction of the diet and weekly thereafter. Prior to the conclusion of the study, the mice were randomly assigned to receive lipopolysaccharide (LPS, Sigma) injection (50ug/kg) or saline injection. Mice were sacrificed 18 hours after LPS injection; alternatively, a second cohort of mice had blood drawn from the cheek venous plexus at 2 hours after injection, and subsequently sacrificed at 18 hours after LPS injection. At the conclusion of the feeding, mice were weighed and euthanized. Livers were excised and weighed, and divided and portions were snap frozen in liquid nitrogen for protein and biochemical assays, preserved in 10% neutral-buffered formalin for histopathological analysis, preserved in OCT frozen section preparation solution, or soaked in RNALater (Qiagen GmbH, Hilden, Germany) for RNA extraction. Blood was collected and serum separated for biochemical analysis.

Biochemical Analysis

Serum alanine aminotransferase (ALT) was determined using a commercially available reagent (Advanced Diagnostics Inc, Plainfield, NJ). Briefly, 15ul of serum was mixed with 100ul of reagent diluted according to the instructions of the manufacturer, and UV absorbance at 37 degrees celsius was measured over three minutes. The average change in absorbance per minute interval is then multiplied by a conversion factor to yield ALT levels.

For liver triglyceride levels, liver whole-cell lysates were prepared as described below and lipids separated by isopropanol precipitation of non-lipid components. A commercially available kit (Wako Chemicals USA Inc., VA) was used to determine the triglyceride concentration.

Protein concentrations were determined by adding 1uL of whole-cell lysate to Bradford reagent (BioRad) and by measuring the difference between absorbance at 650nM and 595nM on a 96 well plate using a plate reader. Concentrations were determined using a standard curve of bovine serum albumin.

RNA analysis

RNA was purified using the RNeasy Mini kit (Qiagen Sciences, Maryland, USA) with on-column DNA digestion (ProMega). cDNA was prepared using random hexamer primers and the Reverse Transcription System kit (Promega Corp., Madison WI). Real-time quantitative polymerase chain reaction was performed using an iCycler (Bio-Rad laboratories Inc., Hercules,

CA), using specific primers. Primer sequences are shown in Table 1. Fold-change in gene expression was determined by normalizing to 18S mRNA. Primers are listed in Table 1.

Histopathological Analysis

Sections of formalin-fixed livers were stained with hematoxylin/eosin and analyzed by microscopy. Frozen sections were prepared from liver tissue frozen in OCT media, and stained with Oil-Red O. Photomicrographs were collected as TIFF files and subsequently analyzed with Metamorph software. Images were thresholded to isolate the Oil-Red O positive staining section, and the percentage of image area thresholded in this manner was calculated by the program and recorded for statistical analysis.

Whole Cell Lysate

60mg of liver tissue was washed and subsequently homogenized in lysis buffer (9.5ml RIPA buffer, 1mM NaF, 2mM Na3VO4, 1 protease inhibitor tablet, 500ul PMSF) using rotor-stator homogenization. After 10 minutes of incubation on ice, homogenates were centrifuged at 10,000RPM for 10 minutes at 4 degrees C. The supernatant was collected and stored in aliquots at -80 degrees C.

Nuclear Extraction

60mg of snap-frozen liver tissue was washed in 10-fold excess volume TKM-0.32 buffer (0.32 molal sucrose, 50mM Tris-HCl, 25mM KCl, 5mM MgCl, 5mM PMSF, with protease inhibitor tablets (1 per 10ml of buffer, Sigma) and homogenized using a rotor-stator homogenizer (Ika). Homogenates were transferred to microcentrifuge tubes and centrifuged (10mins/

1000rpm/4 degrees C.) Pelleted material was resuspended in TKM-2.0 buffer (2 molal sucrose, 50mM Tris-HCl, 25mM KCl, 5mM PMSF) and homogenized again by rotor-stator. Pellets were collected by centrifugation (60mins/14000rpm/4 degrees C) and resuspended in 400ul Buffer A (10mM Hepes/KOH, pH 7.9, 2mM MgCl, 1mM EDTA, 10mM KCl, 1mM DTT, 5mM PMSF, 1 protease inhibitor tablet/5ml buffer). Pellets were again collected by centrifugation (2mins/ 14000rpm/4 degrees C) and resuspended in 50ul Buffer B (10mM Hepes/KOH pH 7.9, 2mM MgCl, 1mM EDTA, 50mM KCl, 300mM NaCl, 2mM DTT, 5mM PMSF, 1 protease inhibitor tablet (Sigma) per 5mL buffer, 10% glycerol). Resuspended material was frozen at -80 degrees overnight, thawed with gentle agitation at 4 degrees C. Supernatant containing nuclear extract was collected after centrifugation (10mins/14000rpm/4 degrees C) and assayed for protein concentration.

Western Blotting

30-50ug of nuclear extract was resolved on 10% polyacrylamide gels and transferred overnight to nitrocellulose support. Membranes were blocked overnight with blocking buffer (5% bovine serum albumin in Tris-Borate-SDS with 0.01% Tween 20) with refrigeration, and subsequently probed overnight with anti-HIF1α (R&D Biosciences) or anti-HIF2α (Chemicon) mouse monoclonal antibodies. Detection was performed using an anti-mouse horseradish-peroxidase conjugated secondary antibody and chemiluminescent substrates. Band density was quantified using Labworks 4.0 image analysis.

Multiplex Cytokine Bead Array

Multiplex cytokine bead array was performed using the BioRad Precision Pro multiplex cytokine bead array kit (BioRad) according to the instructions of the manufacturer. Briefly, serum aliquots stored at -80 degrees were diluted at a 1:4 ratio using dilution buffer provided in the kit. Serum was allowed to mix with beads coated with antibodies to one of 8 different cytokines and subsequently incubated with a second antibody that detects conjugated bead-cytokine pairs.

Results

We first established the manner in which samples would be collected by conducting a pilot experiment with wild-type mice challenged with lipopolysaccharide injection. LPS was administered intraperitoneally to wild-type mice, and livers and blood were collected at varying time points. Serum ALT was analyzed using a biochemical assay, and found to peak at 18 hours after LPS injection (Figure 21A). Whole liver lysates were prepared and analyzed for triglyceride content. Of interest, liver triglycerides increases appreciably within 18 hours after LPS injection, returning to baseline levels by 24 hours. (Figure 21B). Finally, we performed Western Blotting for HIF1α on nuclear extracts prepared from whole liver. HIF1α protein accumulated in nuclear extracts from whole liver by 4 hours post LPS injection, and appeared to be upregulated through the 24 hour time point. (Figure 21C and 21D). We thus decided to collect samples from mice 18 hours after LPS injection in subsequent experiments.

Figure 21. Time course of liver injury in Wild Type Mice after LPS injection. Wild-type mice were administered lipopolysaccharide intraperitoneally at a dose of 50ug/kg and sacrificed at various time points. A. Serum ALT was found to reach a peak between 12 and 18 hours after LPS injection ($U<0.05$, Mann-Whitney U Test). B. Whole liver lysates were prepared and analyzed for triglyceride content using a biochemical assay. Results were normalized to protein concentrations. Liver triglycerides also reached a peak at 18 hours post LPS injection. C. Nuclear extracts were prepared and western blotting was performed for HIF1α. HIF1α protein was upregulated by 4 hours after LPS injection, and remained elevated through the remaining time points ($p<0.05$ versus control.)

Figure 21

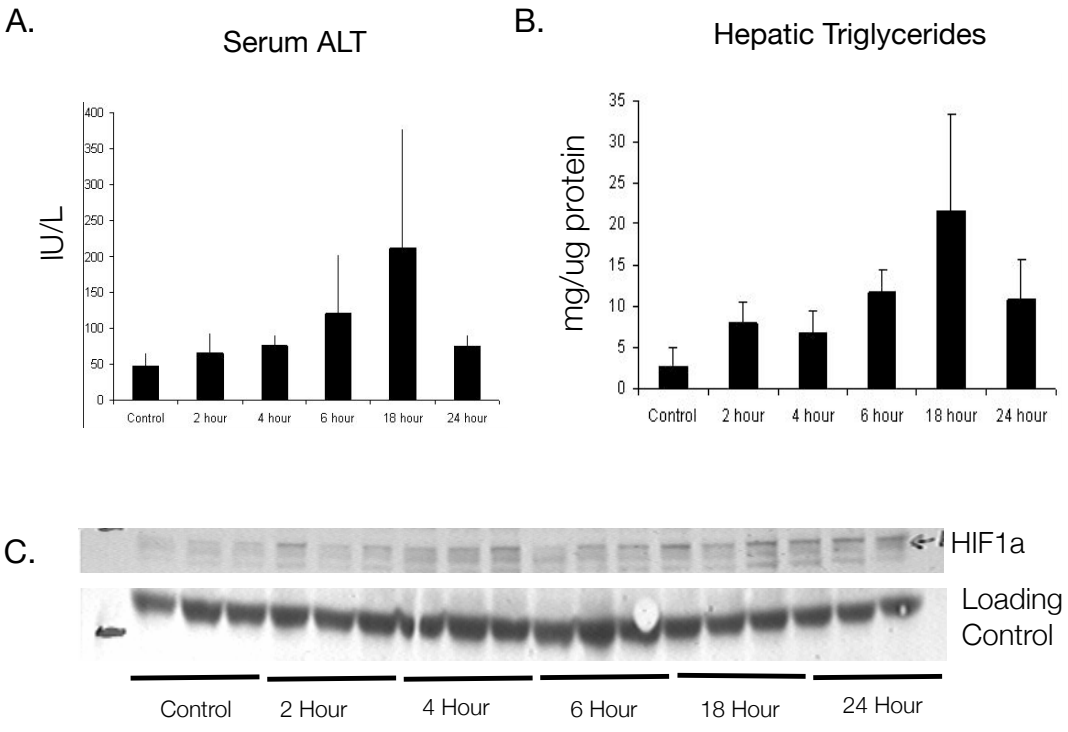
A.
Serum ALT
IU/L
400
350
300
250
200
150
100
50
0
Control
2 hour
4 hour
6 hour
18 hour
24 hour
B.
Hepatic Triglycerides
mg/ug protein
35
30
25
20
15
10
5
0
Control
2 hour
4 hour
6 hour
18 hour
24 hour
C.
HIF1a
Loading Control
Control
2 Hour
4 Hour
6 Hour
18 Hour
24 Hour
D.
* = p<0.05 vs cont.
Densitometry
60
50
40
30
20
10
0
*
*
*
Control
2 hour
4 hour
6 hour
18 hour
24 hour

Ethanol feeding and Parameters of Liver Injury in WT, HepHIF(-) and MyeHIF(-) mice

HepHIF(-), MyeHIF(-), or WT mice were acclimated to the 5% ethanol diet and maintained on the diet for five weeks. The experiment was repeated twice, with 6-8 mice per group. HepHIF(-), MyeHIF(-) and WT mice showed similar weight gains between pair-fed and ethanol-fed groups. (Figure 22A). Some mortality was observed in the WT group, with 3 of 12 mice (two males and one female) expiring before the end of the study in one cohort; in a second cohort, no mortality was noted in any of the groups. All deaths occurred in the final week of the five week feeding. No mortality was observed in the HepHIF(-) or the MyeHIF(-) groups. (Figure 22B.)

Analysis of liver-weight/body-weight ratios revealed increased liver weight/body weight in WT ethanol-fed mice versus control mice at 4 weeks. In contrast, HepHIF(-) mice showed little difference between pair-fed and ethanol fed groups, while a trend towards increased LW/BW ratio in MyeHIF(-) ethanol-fed mice was not significant. (Figure 22C.) We performed immunoblotting on nuclear extracts from wild-type and HepHIF(-) mice. Ethanol feeding resulted in a significant increase in HIF1α expression in nuclear extracts prepared from WT mice. In contrast, nuclear extracts from HepHIF(-) mice had very low levels of HIF1α expression, and no further upregulation with ethanol feeding was observed, confirming suppression of HIF1α signaling in our mouse model.(Figure 23A and B.) Consistent with the role of HIF1α in hepatocyte steatosis, HepHIF(-) mice were protected from the increase in triglyceride content observed in wild-type mice.(Figure 23C).

Figure 22. Weight gain, Mortality, and Liver-Weight/Body-Weight Ratio with ethanol feeding. WT, HepHIF(-), and MyeHIF(-) mice were maintained on the Lieber DeCarli ethanol diet for five weeks. **A.** Weight gain was similar between ethanol and pair-fed mice of each genotype. **B.** There was no mortality in the HepHIF(-) or the MyeHIF(-) mice; however, the alcohol-fed WT group had almost 10% mortality across the two feedings. All deaths occurred in the last week of the feeding. **C.** WT mice had significantly elevated LW/BW ratio with alcohol feeding (*=$p<0.05$). In contrast, HepHIF(-) mice were protected from an increase in LW/BW ratio (**=$P<0.05$ versus corresponding WT group). MyeHIF(-) mice trended towards an increase in LW/BW ratio, but the results were not significant ($p<0.08$, MyeHIF(-) PF vs MyeHIF(-) ET).

Figure 22

A.

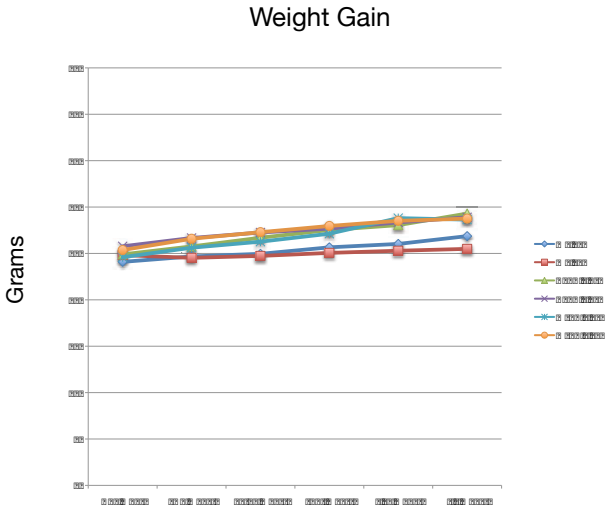

B.

		INITIAL NUMBERS	WEEK 4	WEEK 5	END OF EXP.
ETHANOL FED	WILD TYPE	12	12	11	9
	HEPHIF(-)	14	14	14	14
	MYEHIF(-)	12	12	12	12
PAIR FED	WILD TYPE	12	12	12	12
	HEPHIF(-)	15	15	15	15
	MYEHIF(-)	12	12	12	12

C.

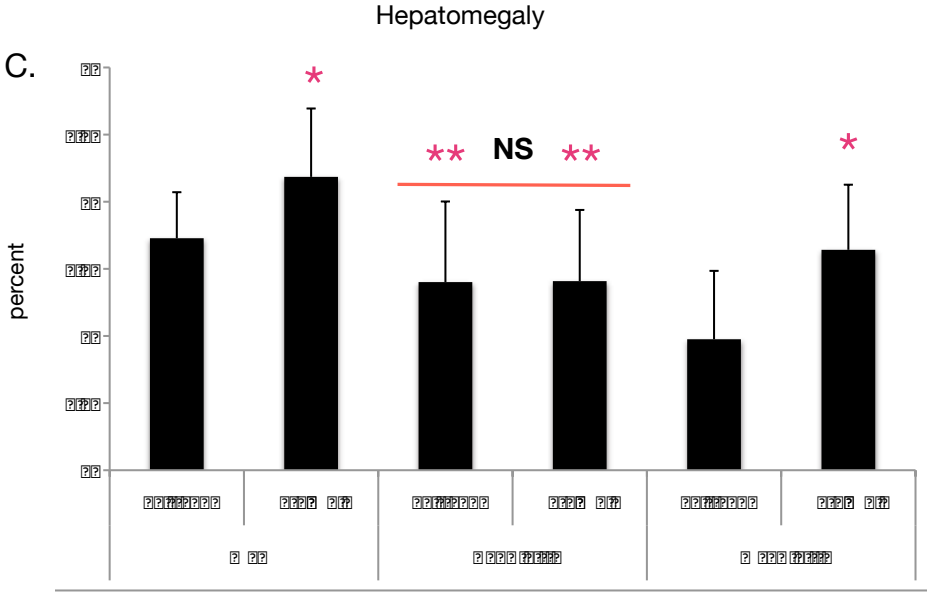

FIGURE 23. Western Blotting for HIF1α and hepatic triglycerides. A. Nuclear Extracts were prepared from the livers of WT and HepHIF(-) mice. 30ug total protein was loaded per lane. Ethanol resulted in an upregulation of HIF1α protein ($p<0.05$ versus WT PF group) in WT mice. In the HepHIF(-) mice, as expected, little HIF1α protein was detected, and no further upregulation was detected with chronic alcohol stimulation. Densitometry for immunoblot appears in **B. C.** Whole liver extracts were prepared, and triglyceride content was quantified using a biochemical assay. Data are the average from two cohorts (N=9-11 per group). HepHIF(-) ET-fed mice had significant protection against triglyceride increase (*=$P<0.05$ vs WT-ET group) versus WT ET-Fed mice. Due to high variability within the WT cohort, PF and ET-Fed WT mice did not differ significantly in the mean triglyceride content (#=$p<0.095$ versus WT Pair-Fed) although a similar trend as was observed repeatedly in earlier feedings was apparent.

Figure 23

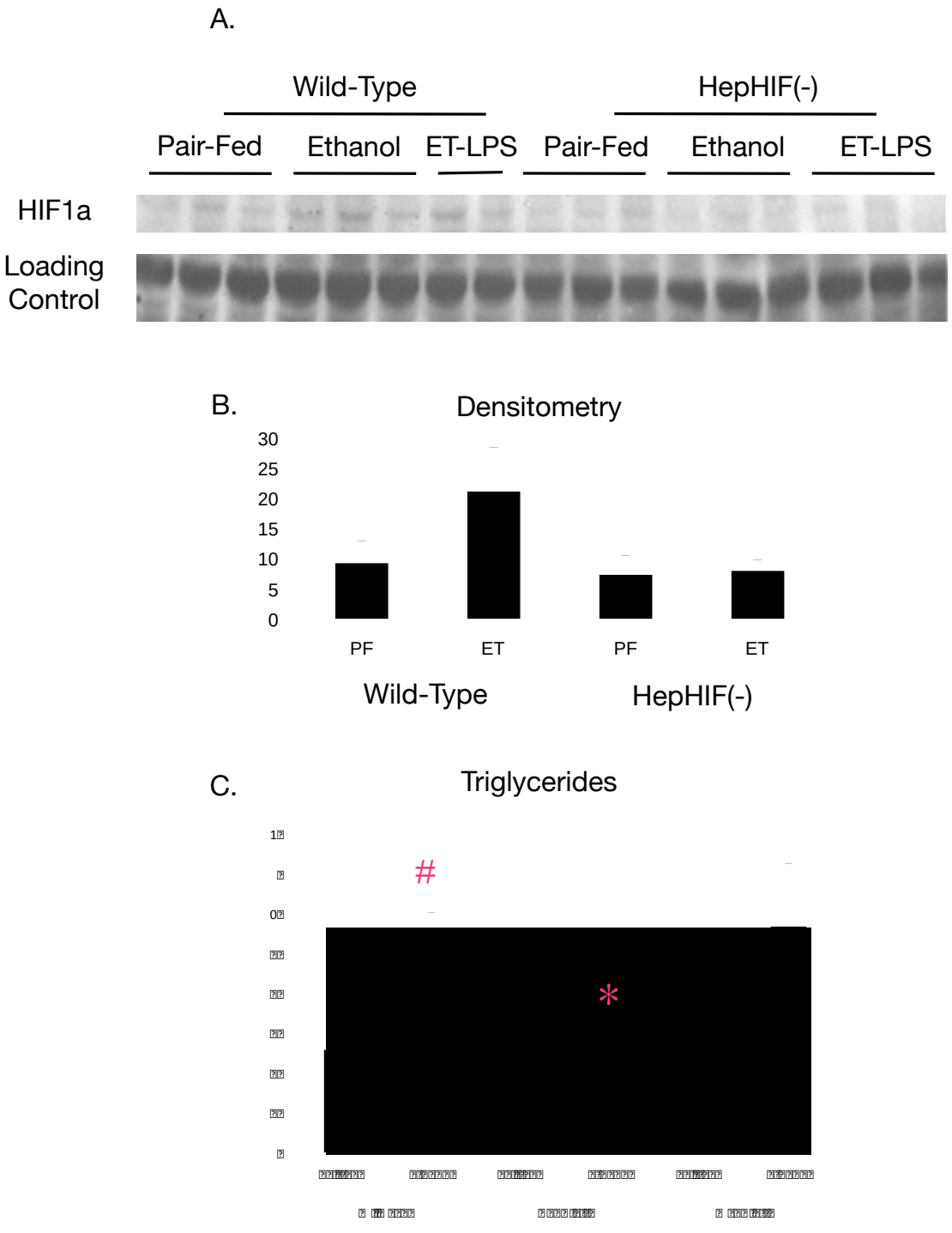
A.
Wild-Type
HepHIF(-)
Pair-Fed
Ethanol
ET-LPS
Pair-Fed
Ethanol
ET-LPS
HIF1a
Loading Control
B.
Densitometry
30
25
20
15
10
5
0
PF
ET
PF
ET
Wild-Type
HepHIF(-)
C.
Triglycerides
#
*

Serum ALT levels were not dramatically different among ethanol-fed and pair-fed mice in the absence of LPS stimulation. (Figure 24A) With LPS stimulation, however, a clear pattern emerged. Alcohol-fed WT mice had the greatest increase in serum ALT after LPS injection, significantly elevated over the ALT values obtained for WT pair-fed, LPS injected mice. In contrast, ethanol-fed HepHIF(-) mice were protected from serum ALT increase after LPS injection. Ethanol-fed, LPS injected MyeHIF(-) mice had the greatest average serum ALT among the MyeHIF(-) groups, however, this difference was not statistically significant in either cohort. (Figure 24).

HIF pathway suppression in hepatocytes also revealed some protection against lipid accumulation n HepHIF(-) mice after alcohol feeding(Fig 25). Tissue microscopy was somewhat ambiguous, with vacuolated spaces appearing in some ethanol fed animals from each cohort. Oil-Red O staining was performed on frozen section and quantified using MetaMorph image analysis software to discern differences between the groups (Figure 26A). Briefly, Oil Red O positive areas were thresholded, and the percent thresholded area was quantified by the software. We found that the average Oil-Red O positive area in HepHIF(-) ethanol-fed mice was similar to that in HepHIF(-) pair-fed mice. In contrast, WT ethanol-fed mice had greater Oil Red O positive areas than pair-fed mice, and a similar trend was observed in MyeHIF(-) mice (Figure 26B). In general, quantification of Oil Red O staining paralleled LW/BW ratio calculations, and supported a protective role for hepatocyte-specific HIF1α suppression in alcohol induced steatosis.

FIGURE 24. Serum ALT levels.

A. Serum ALT levels in the first cohort of mice. Blood was collected 18 hours after LPS injection. **B.** Serum ALT levels in the second cohort. Blood was drawn 2hrs post LPS injection from the cheek pouch venous plexus. **C**. Serum ALT levels in the second cohort. Blood was collected at sacrifice, 18 hours post LPS injection.

Figure 24

A. ALT, FIRST COHORT

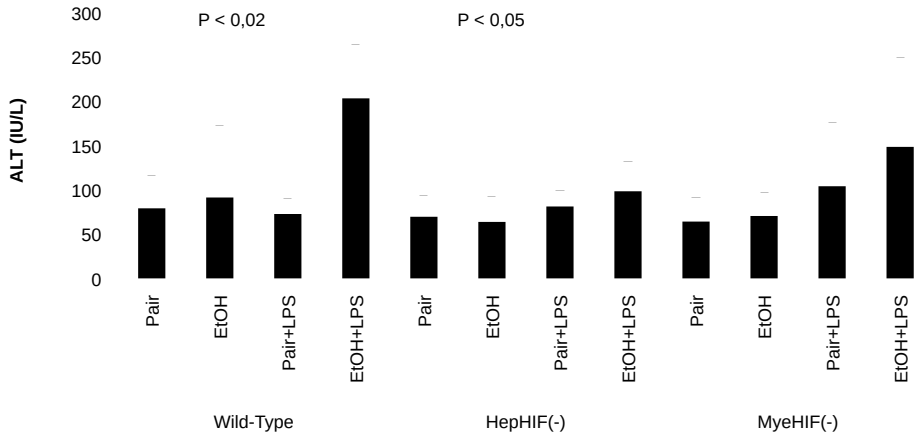

B. ALT, SECOND COHORT/2 HOURS POST LPS INJECTION

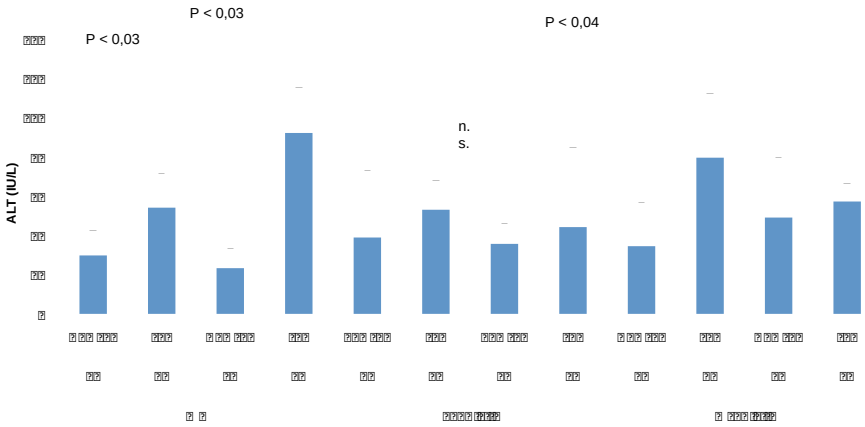

C. ALT, SECOND COHORT/18 HOURS POST LPS INJECTION

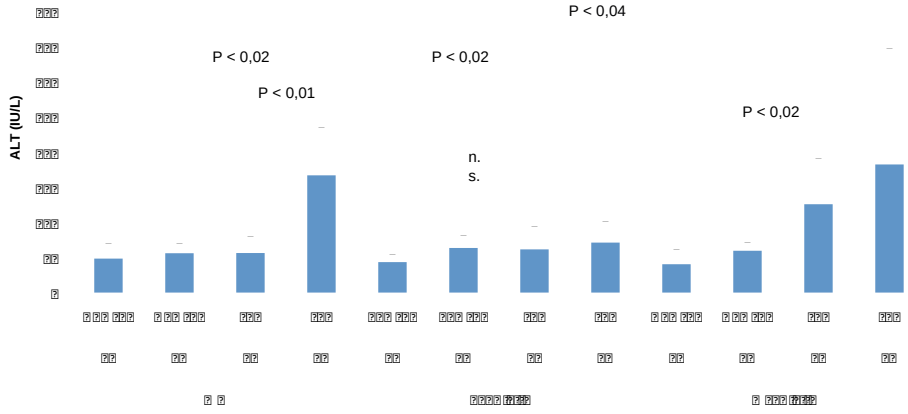

Figure 25. Histology, WT/HepHIF(-)/MyeHIF(-) mice with ethanol feeding.

Panels **A** and **B** show photomicrographs of H&E stained sections from ethanol and pair-fed wild-type mice, respectively. Ethanol-fed wild-type mice had prominent lipid vacuolization. Panels **C** and **D** show photomicrographs from ethanol-fed and pair-fed HepHIF(-) mice. Some lipid vacuolization was observable in both conditions, but was less, on average, than was observed for ethanol-fed WT mice. Panels **E** and **F** show photomicrographs from ethanol-fed and pair-fed MyHIF(-) mice. Similar lipid accumulation as was observed in WT mice was observed with chronic ethanol feeding.

Figure 25

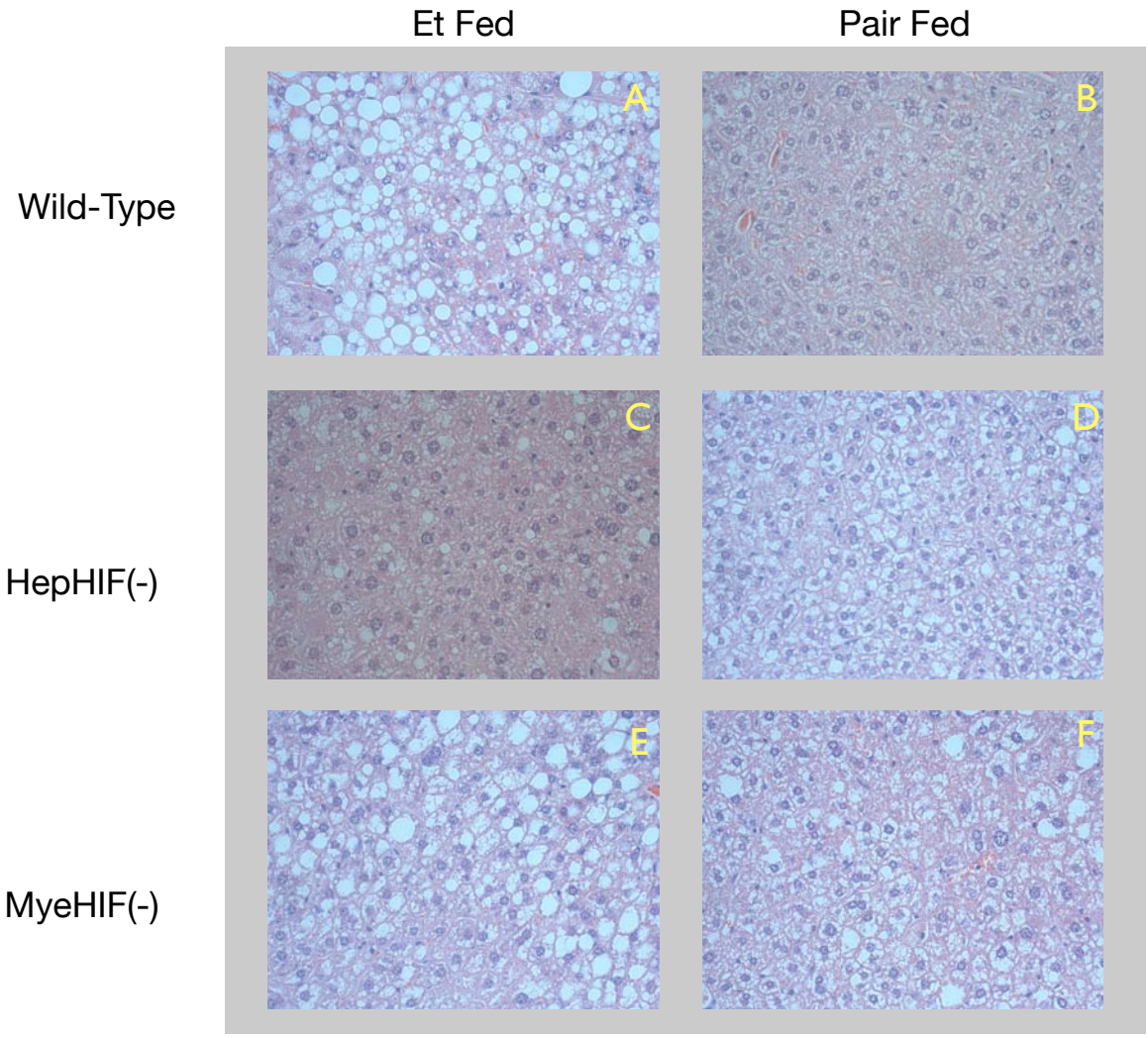

Figure 26. Quantification of Oil Red O positive areas. **A.** The column on the right shows representative micrographs from pair-fed animals from each genotype. The column in the middle shows representative micrographs from ethanol-fed animals from each genotype. The column on the left shows the binary image threshold mask created from the corresponding ethanol-fed micrograph appearing in the middle column. **B.** The average thresholded area as described in **A** was calculated. WT mice showed a significant increase in Oil-Red O positive area, whereas protection was observed in HepHIF(-) mice.

Figure 26

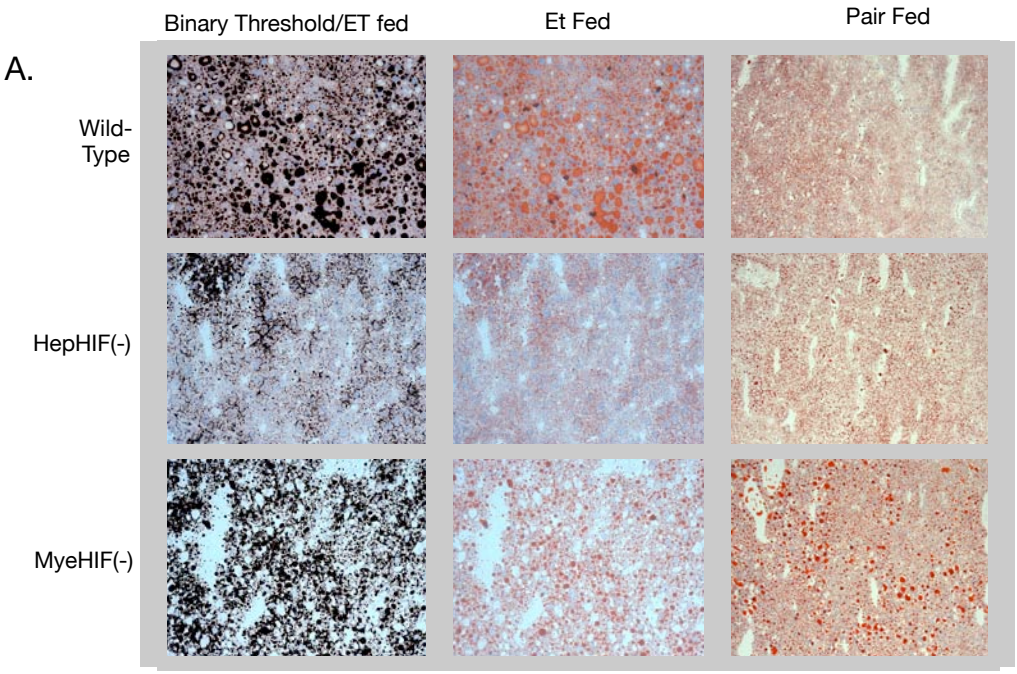
A.
Binary Threshold/ET fed
Et Fed
Pair Fed
Wild-Type
HepHIF(-)
MyeHIF(-)

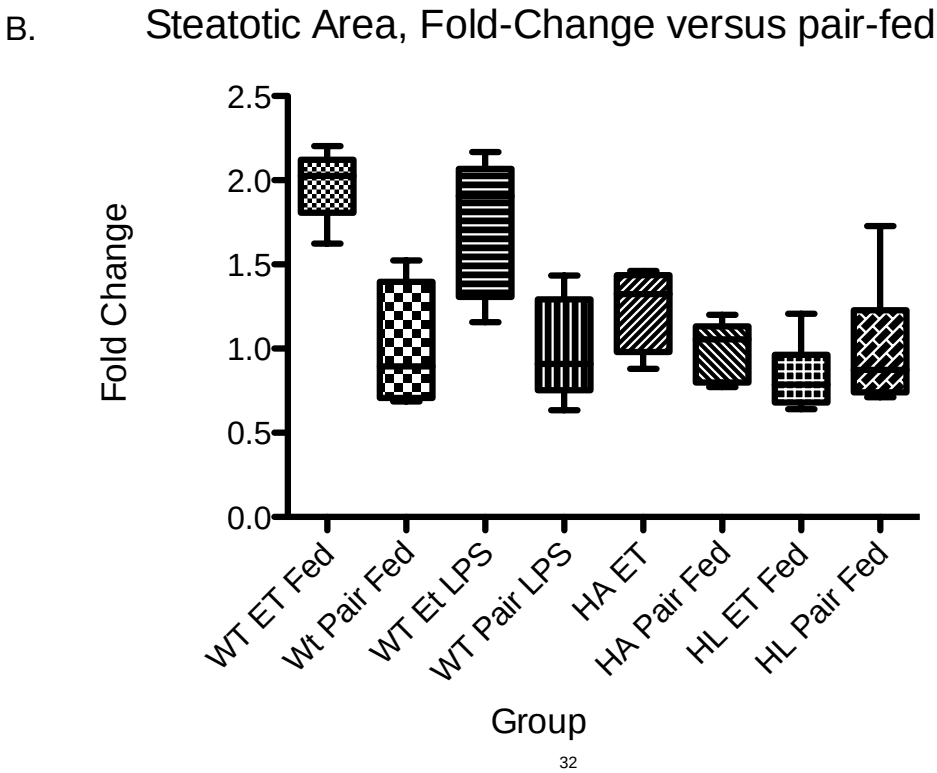
B.
Steatotic Area, Fold-Change versus pair-fed
Fold Change
2.5
2.0
1.5
1.0
0.5
0.0
WT ET Fed
Wt Pair Fed
WT Et LPS
WT Pair LPS
HA ET
HA Pair Fed
HL ET Fed
HL Pair Fed
Group

Secretion of Pro-inflammatory Cytokines is affected by hepatocyte-specific HIF1α

In addition to steatosis, alcohol liver disease is also associated with activation of the inflammatory cascade. The suppression of serum ALT increase after chronic alcohol and LPS injection in HepHIF(-) mice prompted us to look for changes in cytokine expression. Using a multiplex cytokine bead array, we analyzed serum levels of several cytokines. Most cytokines were observed at both 2 hours (from blood drawn from cheek venous plexuses) as well as at 18 hours after LPS injection, although some cytokines were only measured at 18 hours.

Serum TNFα increases dramatically after chronic alcohol feeding and LPS injection. At 2 hours, there was a profound upregulation of TNFα in WT ethanol-fed, LPS injected mice. At 18 hours, there was still a detectable elevation of TNFα in LPS versus non-LPS-injected WT mice. Surprisingly, in HepHIF(-) mice TNF-a was suppressed, and no synergistic upregulation with ethanol was observed. In MyeHIF(-) mice, TNFα was suppressed in ethanol/LPS treated mice versus WT mice, though still significantly elevated over HepHIF(-) mice. (Figure 27A)

The cytokine IL-6 has potent pro-inflammatory effects and has previously been implicated in the pathogenesis of alcoholic liver disease. We examined serum levels of IL-6 at 2 and 18 hours post LPS injection in our cohort of WT, HepHIF(-) and MyeHIF(-) mice. IL-6 was profoundly upregulated by LPS stimulation in WT mice within 2 hours of LPS injection. (Figure 27B) Alcohol increased the duration and amplitude of IL-6 secretion in response to LPS, as IL-6 was increased by 2 hours and remained elevated through the 18 hour time point (Figure 27C). In contrast, no synergism was observed in ethanol-fed, LPS injected HepHIF(-) or MyeHIF(-) mice, although LPS had potent stimulatory effects on IL-6 levels in both. By 18 hours, a cooperative

upregulation of IL-6 was observed in C57/BL6 ethanol-fed/LPS injected mice, whereas no such effect was observed in MyeHIF(-) or HepHIF(-) mice. (Figure 27D)

IFNγ showed a different pattern of regulation. IFNγ levels were quite low in comparison to the other cytokines observed. Ethanol had no effect on IFNγ levels in sera of ethanol-fed WT mice. IFNγ was upregulated by LPS to a statistically similar extend in sera of pair-fed and ethanol-fed LPS WT mice. Similar patterns were observed in HepHIF(-) mice, though an opposite pattern (of higher levels of IFNγ in PF mice) were observed in MyeHIF(-) mice. The biological relevance of these very low levels of IFNγ are unclear. (Figure 28A)

IL-13 is a chemokine that is thought to regulate allergic and anti-parasitic immune responses. Serum levels of IL-13 were consistently low and did not change significantly with any treatment in any group. (Figure 28B)

IL-10, an anti-inflammatory cytokine, is co-secreted with pro-inflammatory cytokines in alcoholic liver disease and was synergistically increased with LPS injection and ethanol in WT mice. In contrast, no synergistic upregulation is observed in HepHIF(-) mice, with serum levels of IL-10 remaining similar to that observed in pair-fed, LPS injected WT mice. This implies that the synergistic effect of ethanol and LPS is at least partially dependent upon high levels of hepatocyte-specific HIF activation. In MyeHIF(-) pair-fed/LPS injected mice, IL-10 levels were comparable to WT mice with ethanol/LPS injection, but were lower with ethanol feeding. This paradoxical suppression of IL-10 levels with ethanol/LPS injection in MyeHIF(-) mice suggests an unknown additional counter-regulatory mechanism in myeloid cells that is normally suppressed by HIF. (Figure 28C)

Figure 27. Serum Cytokines: TNFα and IL-6.

Serum cytokines were quantified using a multiplex bead array. **A.** A profound upregulation of TNFα was observed in WT-mice at 2 hours after LPS injection.(A) HepHIF(-) and MyeHIF(-) were completely protected from this upregulation with LPS injection. (*=P<0.01 versus WT PF/ LPS injected mice; **=P<0.01 versus WT ET/LPS mice.) **B.** Serum IL-6 showed a similar pattern, with synergistic upregulation with ethanol and LPS in WT mice after 2 hours. (*=p<0.01 versus WT PF/LPS mice). No synergistic effect of ethanol was observed in HepHIF(-) mice. MyeHIF(-) mice had high levels of IL-6, comparable to WT mice. **C.** By 18 hours, upregulation of IL-6 with ethanol/LPS challenge was still observable in WT mice, but not in HepHIF(-) or MyeHIF(-) mice. (*=P<0.05, WT ET-LPS versus Wt PF LPS mice; **=P<0.05 versus WT ET LPS mice).

Figure 27

A. Serum TNF-apha

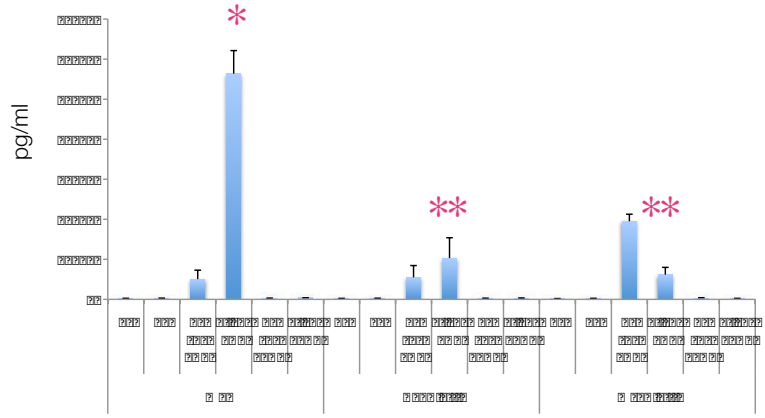

B. Serum IL6, 2 hours

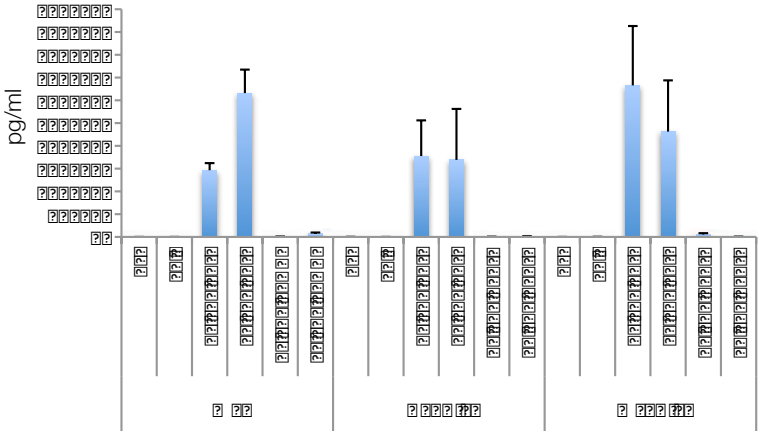

C. Serum IL6, 18 hours

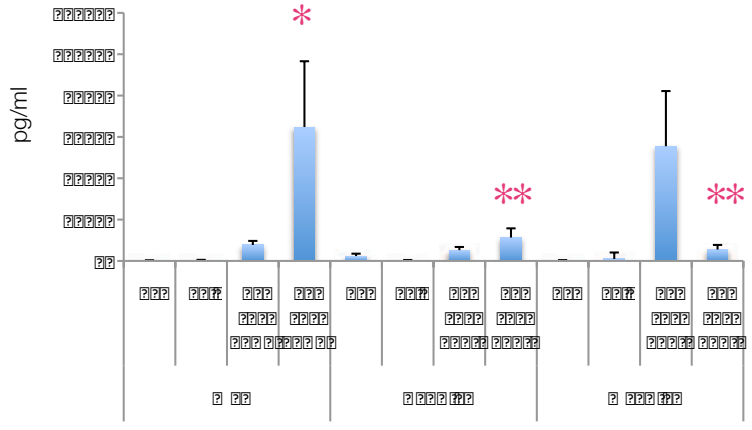

Figure 28. Serum Cytokines: IFNg, IL-13 and IL10.

Serum cytokines were quantified using a multiplex bead array. **A.** The cytokine IFNγ was significantly upregulated at 18 hours in WT ET LPS mice (*=P<0.05 versus WT PF LPS mice). HepHIF(-) ET LPS mice were not significantly different from WT ET-LPS mice, nor was the trend towards increased IFNγ in HepHIF(-) ET LPS mice significantly increased versus HepHIF(-) PF LPS mice. **B**. The cytokine IL-13 remained relatively unchanged among all the groups. **C.** Serum IL-10 was significantly upregulated by ethanol and LPS at 18 hours; a trend towards significance was also observed at 2 hours. Significant protection from IL-10 elevation was observed in HepHIF(-) and MyeHIF(-) mice.

Figure 28

A. Serum IFN-Gamma

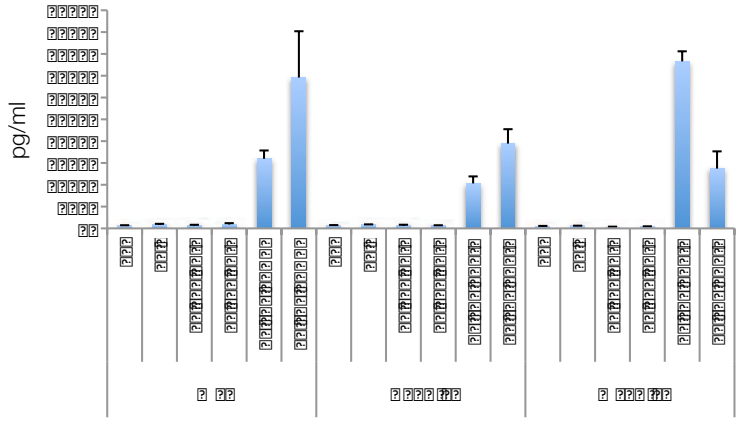

B. Serum IL-13

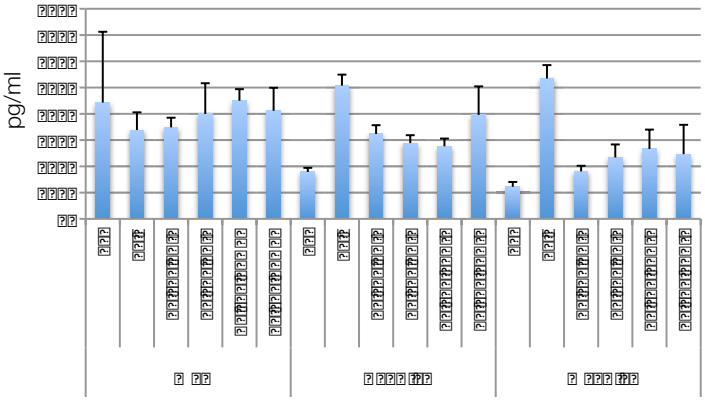

Serum IL-10

C.

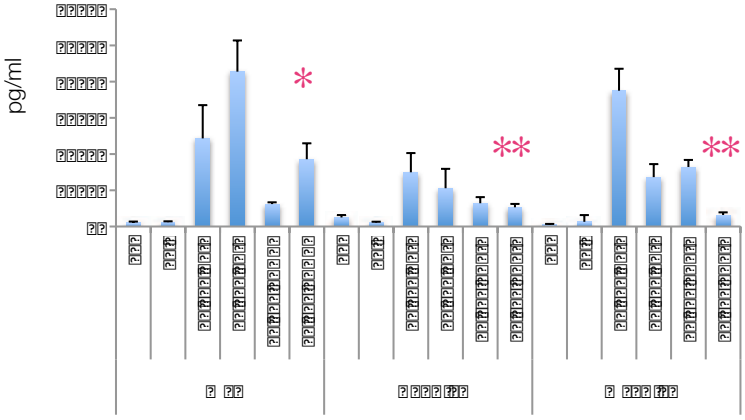

Differential secretion of chemoattractant cytokines in WT and HepHIF(-) mice

Inflammatory cell recruitment to the liver occurs in alcoholic liver disease, and is mediated by cytokines including the neutrophil chemoattractant IL8/KC, as well as the monocyte chemoattractant MCP-1. MCP-1 was synergistically upregulated by ethanol and LPS in WT mice. Again, no upregulation was observed with ethanol/LPS injection in HepHIF(-) mice at 2 hours. MyeHIF(-) groups also showed a significant protection against LPS/ethanol upregulation at 2 hours. By 18 hours, though significant differences were observed among the groups, all had levels that were under 4000pg/ml, whereas concentrations above 100,000pg/ml were achieved at 2 hours post LPS injection in WT mice. (Figure 29A and B)

The cytokine RANTES was upregulated with LPS challenge. No synergistic effect of alcohol was observed, and levels were similar in HepHIF(-) and MyeHIF(-) mice to those observed in WT mice. (Figure 30A)

KC, the murine homologue of IL-8, was modestly increased by ethanol and LPS at 2 hours in WT mice, although the significance did not pass the $p<0.05$ threshold. (Figure 30B) No synergistic upregulation with ethanol was observed in HepHIF(-) mice, although LPS did dramatically increase serum KC after two hours. At 18 hours, KC remained upregulated in WT ET-fed/LPS injected mice, but was suppressed in HepHIF(-) mice versus WT mice after ethanol/ LPS injection.(Figure 30C)

Real-Time PCR analysis

We first examined HIF1α mRNA expression. We found that after five weeks of chronic ethanol, HIF1α mRNA was significantly upregulated in hepatic tissue (Figure 33A). LPS

Figure 29. Serum MCP-1

A. Serum MCP-1 was significantly elevated with ethanol and LPS injection in WT mice (*=P<0.05 versus WT PF LPS). HepHIF(-) ET LPS mice were protected from this upregulation versus WT ET LPS mice. **B.** By 18 hours, significant MCP-1 elevation in WT ET LPS mice versus WT PF LPS mice was still observed; in contrast, the trend towards protection in HepHIF(-) ET LPS mice was not significant. (*=P<0.05 versus WT PF LPS; **=P<0.05 versus WT ET LPS).

Figure 29

A.

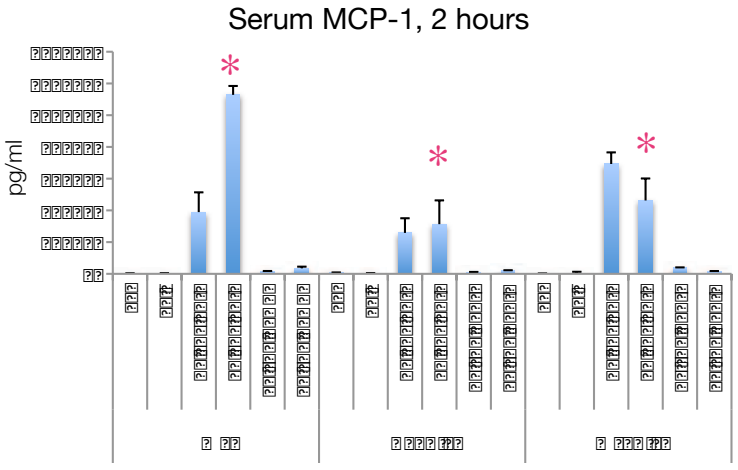

B.

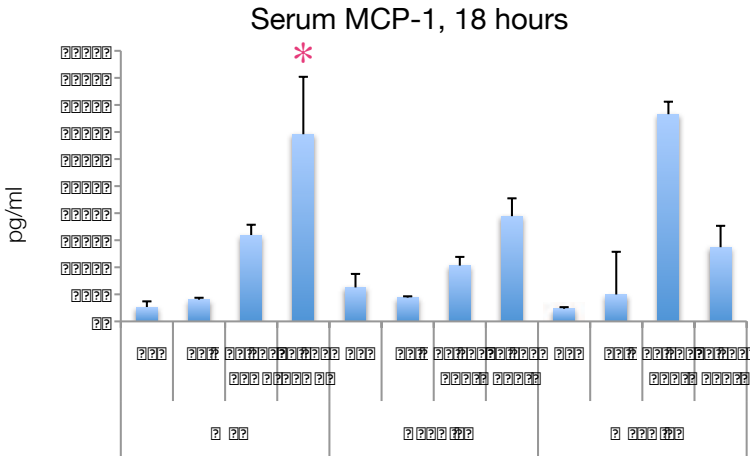

Figure 30. Serum Cytokines: RANTES and KC

Serum cytokines were quantified using a multiplex bead array. **A.** Serum RANTES was upregulated with LPS injection. No synergistic effect of ethanol was observed, and no significant differences between WT, HepHIF(-) and MyeHIF(-) groups was observed. **B.** Serum KC at 2 hours. High levels of KC were detected in all LPS samples at 2 hours. Although some protection was observed in HepHIF(-) mice, these data were compromised by the extremely high levels of cytokines that were at or extrapolated beyond the linear range of the assay. **C.** By 18 hours, a synergistic upregulation of KC was still measurable in sera from WT ET LPS mice, and prevented in HepHIF(-) mice. (*=$P<0.05$ versus WT PF LPS; **=$P<0.05$ versus WT ET LPS).

Figure 30

A.

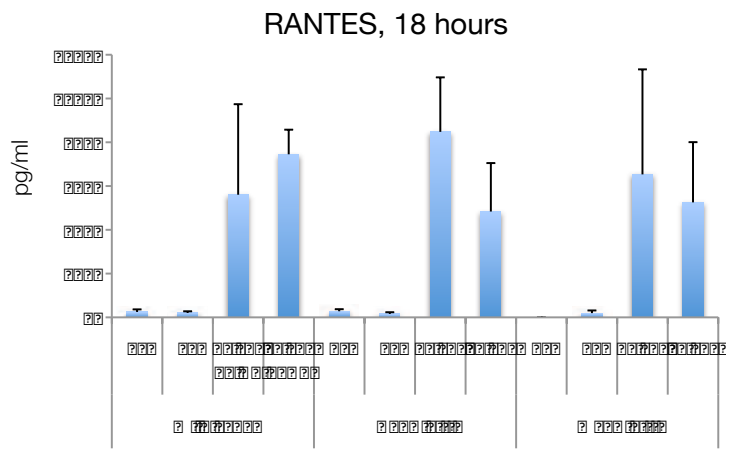

B.

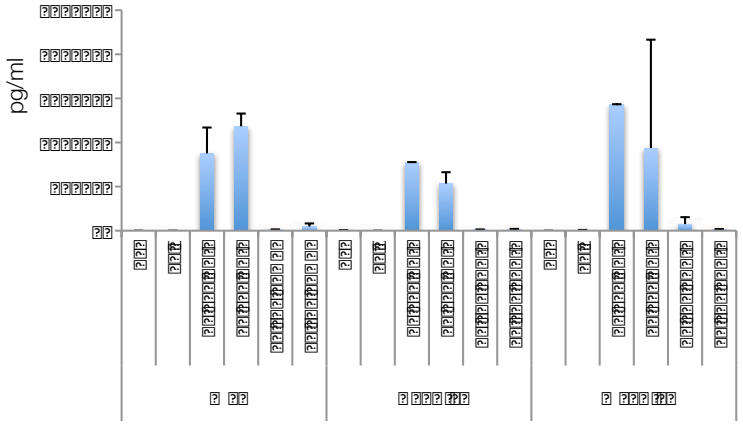

C.

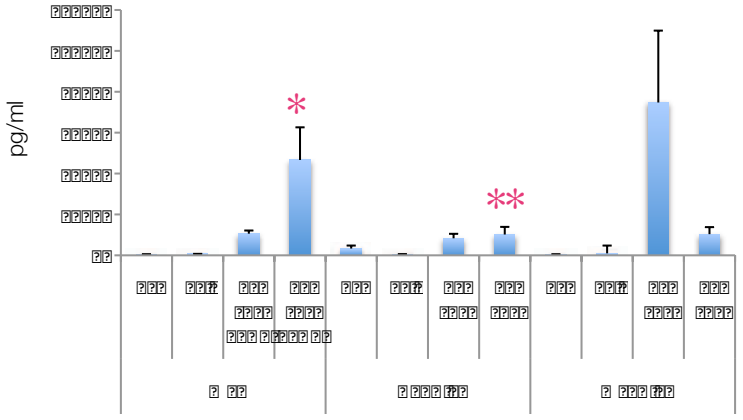

synergistically upregulated HIF1α mRNA to almost 6-fold over control (Figure 33A). In distinction, HIF1α mRNA remained low and unchanged by all conditions in HepHIF(-) mice as well as MyeHIF(-) mice, suggesting that transcriptionally active HIF1α mRNA involved in the pathogenesis of alcoholic liver disease is required in both hepatocytes as well as cells of the myeloid lineage. In the first feeding, HIF2α showed little regulation between the groups. however, in the second cohort, after including a blood draw at 2 hours after LPS injection, some upregulation of HIF2α was observed in WT mice after ethanol and LPS feeding, and a similar (though non-significant) trend was observed in HepHIF(-) mice. (Figure 31A and 31B)

Downstream targets of HIF implicated in the pathogenesis of alcoholic liver disease were upregulated by alcohol and LPS injection in WT mice. PAI-1 was synergistically upregulated by alcohol and LPS ($p<0.05$, PF-LPS versus ET-LPS groups) whereas iNOS showed a similar though nonsignificant trend. (Figure 31C) In HepHIF(-) mice, both PAI-1 and iNOS were upregulated with LPS injection, but no further upregulation was observed with chronic ethanol. (Figure 31C).

As differences in lipid accumulation were observed, we then turned our attention to PPARa, a master regulator of hepatic lipid metabolism. PPARa is reported to be decreased by chronic ethanol, and PPARa activation has been shown to ameliorate alcoholic liver disease. [130] Consistent with earlier reports, PPARa mRNA was suppressed by almost 50% in WT mice with chronic ethanol feeding. Surprisingly, this change was similar in HepHIF(-) mice, with suppression of PPARa to a similar extent observed in all conditions. (Figure 32A)

We then turned to examine other potential mediators of the effect on lipid accumulation. We identified the HIF-responsive gene Adipocyte Differentiation Related Protein (ADRP), which

Figure 31. QRT-PCR of HIF pathway genes with ethanol feeding and LPS injection A. We found significant upregulation of HIF1α mRNA with ethanol, and further upregulation with LPS injection in WT mice. (*=P<0.01 versus corresponding WT PF group) In contrast, HIF1α mRNA (normalized to same genotype mice) was unchanged in HepHIF(-) and MyeHIF(-) mice. **B.** HIF2α mRNA expression. **C.** Gene expression of PAI-1 and iNOS. Both PAI-1 and iNOS were upregulated with LPS injection. PAI-1 increased further with chronic ethanol in WT mice. However, no further upregulation was observed in HepHIF(-) mice. (*=P<0.05 versus PF-LPS group; #=P<0.05 versus Wt ET LPS group).

Figure 31

A.

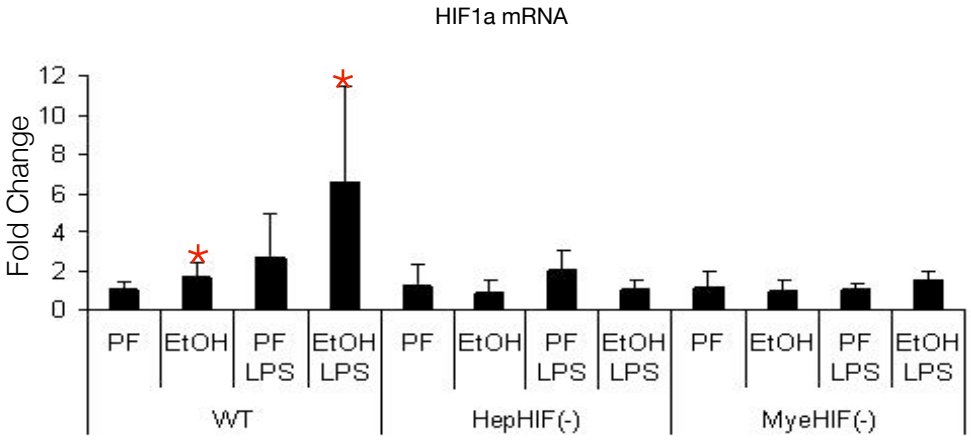

B.

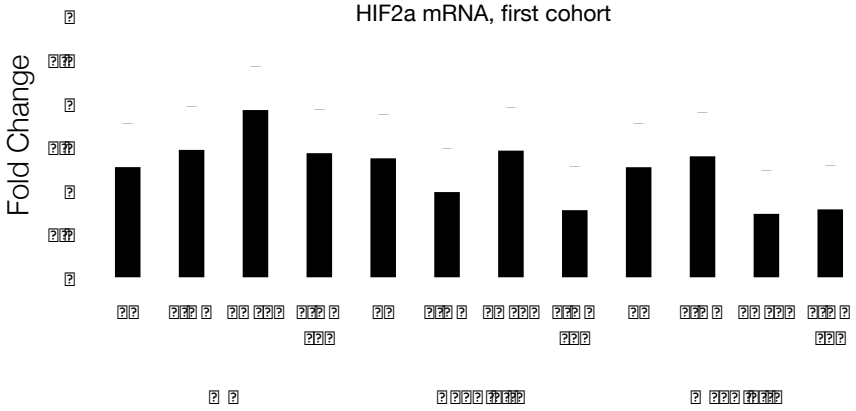

C.

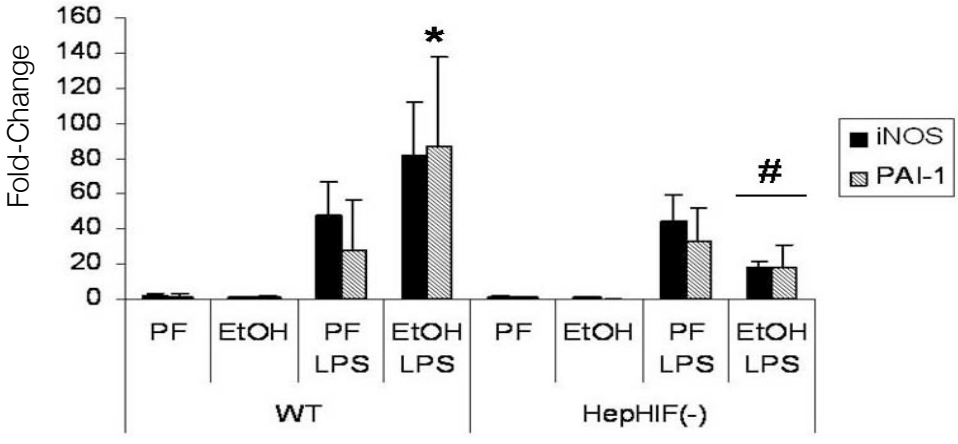

has recently been implicated elsewhere in hepatic lipid accumulation in a HIF-2 dependent manner. We found that hepatic expression of ADRP was significantly upregulated with ethanol and LPS injection in WT mice. There was no upregulation of ADRP observed in HepHIF(-) mice or MyeHIF(-) mice. (Figure 32B).

In a second cohort of mice that included a two hour blood draw after LPS stimulation prior to sacrifice at 18 hours, we found some elevation of HIF2a mRNA with ethanol alone, and more significant elevation of HIF2a with ethanol and LPS. HepHIF(-) mice did not differ significantly among the groups, and HepHIF(-) ET/LPS mice had significantly less HIF2a mRNA than WT ET/LPS mice. The altered patterns observed in HIF2a regulation may have been partially responsible for a somewhat different , though statistically similar, pattern observed in ADRP mRNA from this second cohort. (Figure 33).

Discussion

We found that disruption of HIF1α in hepatocytes was protective against numerous indices of alcoholic steatosis and steatohepatitis, including elevations in serum ALT, hepatomegaly and hepatic triglyceride accumulation, and increase in pro-inflammatory cytokine production. We were surprised to find an equally strong protection against TNFα induction in HepHIF(-) mice as we observed in MyeHIF(-) mice, strengthening other observations that the interaction between Kupffer cells and hepatocytes is crucial for the maximal development of injury in alcoholic steatohepatitis. Our results suggest dual protective roles for HIF1α inhibition in parenchymal cells and non-parenchymal cells of the liver in ALD. On the one hand, HIF1α appears to have a role in the development of steatosis, which may predispose hepatocytes to

Figure 32. PPARa and ADRP mRNA with ethanol and LPS injection.

(A) PPAR-alpha mRNA was suppressed by ethanol feeding in wild-type mice (#$p<0.05$ versus WT PF group) as well as in HepHIF(-) mice (*$p<0.05$ versus HepHIF(-) group.) (B) Adipocyte differentiation related protein (ADRP) was upregulated by ethanol/LPS injection in WT mice (*$p<0.05$ versus WT PF group) but was suppressed by ethanol and remain unchanged after ethanol/LPS injection in HepHIF(-) mice.

Figure 32

A.

PPARa mRNA

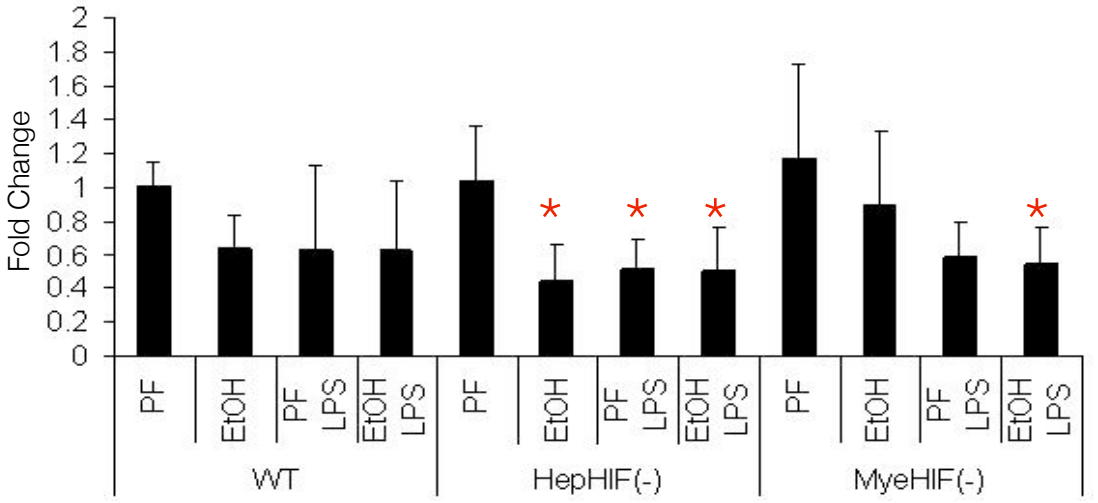

B.

ADRP mRNA

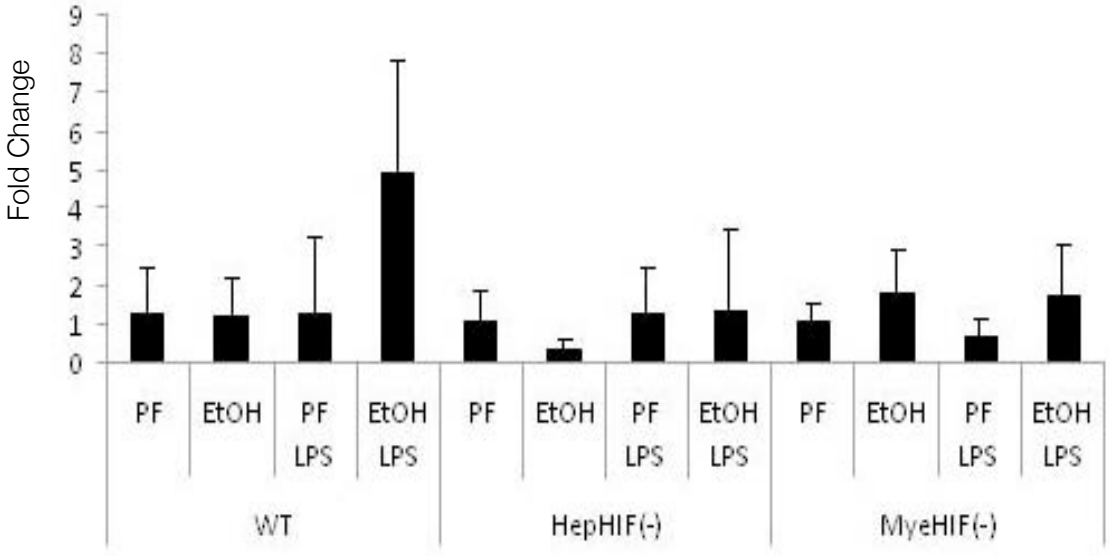

Figure 33. HIF2α and ADRP mRNA, second cohort. A. In the second cohort of ethanol feeding, we included a two-hour blood draw in all mice after LPS challenge and prior to sample collection at 18 hours. Some alteration in mRNA levels was apparent in whole liver RNA analysis by qRT-PCR at 18 hours. Notably, HIF2α levels were dramatically upregulated in WT mice with ethanol or ethanol and LPS challenge. Trends among HepHIF(-) groups were similar but non-significant, and significant suppression of HIF2α mRNA levels was observed in HepHIF(-) ET-LPS mice versus WT ET-LPS mice. (*=P<0.05, WT Ethanol versus WT Pair-fed groups; **=P<0.05, WT ET LPS versus all other WT groups; ***P<0.05 HepHIF(-) ET LPS versus WT ET LPS group). **B.** ADRP mRNA levels also showed a slightly different pattern, albeit with similar trends. WT ET-LPS mice continued to have the greatest amount of ADRP mRNA (#=p<0.06 versus all other WT groups. No significant changes were observed among HepHIF(-) or MyeHIF(-) mice.

Figure 33

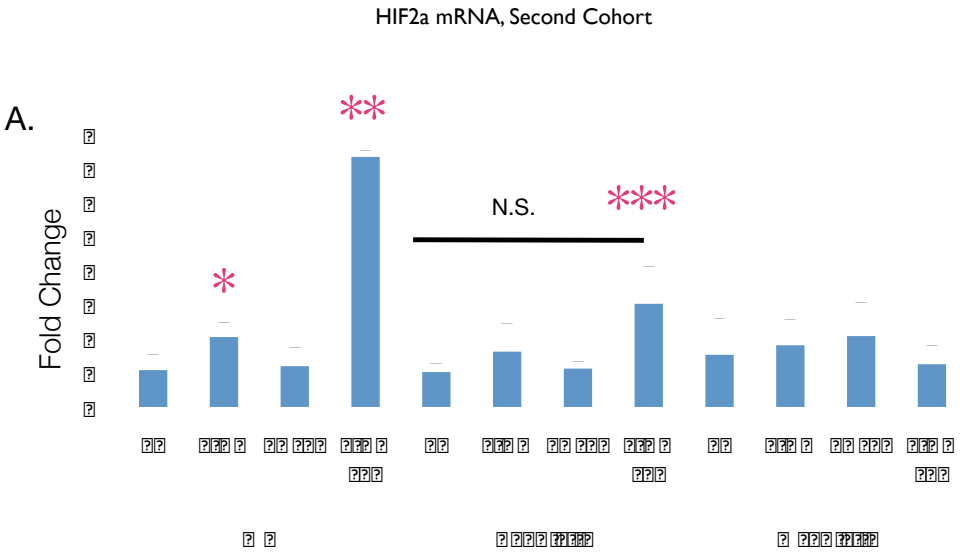
HIF2a mRNA, Second Cohort
A.
Fold Change
*
**
N.S.
***

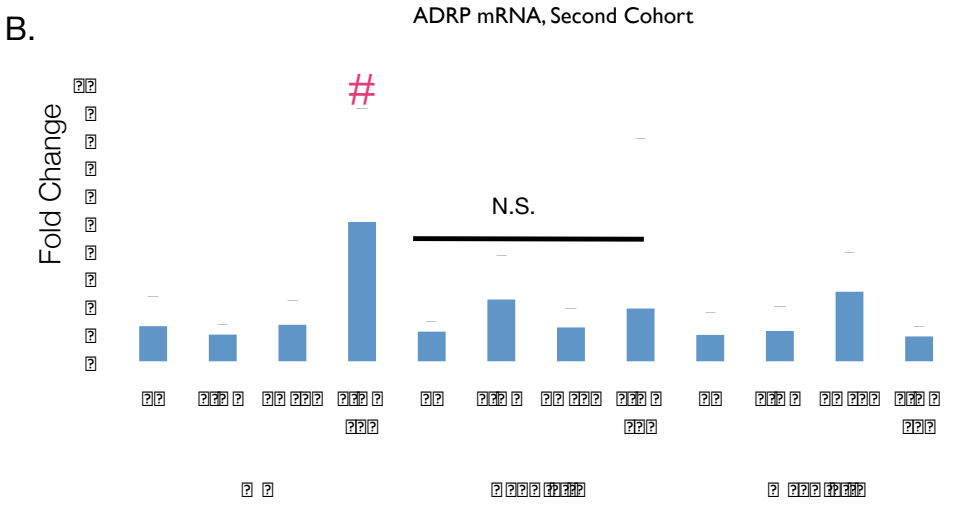
ADRP mRNA, Second Cohort
B.
Fold Change
#
N.S.

cellular damage after subsequent pro-inflammatory stimuli. On the other hand, HIF1α in both hepatocytes as well as myeloid cells appears to have protective effects against the secretion of those pro-inflammatory cytokines themselves. Additionally, although we did not directly measure inflammatory cell recruitment to the liver, we found differential regulation of the chemoattractant KC and MCP-1, but not RANTES, with alcohol and LPS injection.

Alcoholic Steatosis and HIF1α

Lipid homeostasis in the liver represents a complex balance of many factors, including metabolic load (for example, caloric load), catabolic pathways (e.g., b-oxidation), hormonal mediators, and regulation of lipid storage capacity. To this list, we can add inflammatory stimuli, as we demonstrated an upregulation of hepatic triglyceride in chow-fed mice within 18 hours after LPS challenge. The list of transcription factors associated with lipid accumulation now includes members of the hypoxia-inducible factor family. We offered data showing that HIF1α is upregulated after LPS challenge in chow-fed mice, and that the combination of chronic alcohol and LPS injection results in further upregulation of HIF1α mRNA. Others have also offered data suggesting that HIF1α is involved in lipid accumulation, as HIF1α activation has been reported to result in foam-cell formation from macrophages, result in lipid loading in cardiomyocytes, and cause hepatic lipid accumulation in other mouse models.[97, 148, 151, 155] Here we report the novel finding that partial disruption of HIF1α in hepatocytes results in a suppression of lipid accumulation in response to chronic ethanol. HepHIF(-) mice had less HIF1α protein in response to chronic alcohol as assayed by immunoblot. Hepatic lipid content was assayed by hepatomegaly, hepatic triglyceride, and quantitative analysis of lipid content in oil-red O stained

section; in each of those parameters, HepHIF(-) mice were protected in comparison with WT, ethanol-fed mice. These results correlate well with our findings in a mouse model that utilized the opposite condition, namely in which we saw increased triglyceride and gross appearance of steatosis in chronic ethanol-fed mice with constitutive hepatocyte-specific HIF1α expression. Notably, we did not detect an intermediate phenotype of HIFα mRNA expression in the MyeHIF(-) or the HepHIF(-) mice. This may be due to detection of the endogenous as well as the truncated HIF1α protein by the pCR strategy we utilized.

There are several possible explanations for the relationship between HIF1α and lipid accumulation, and in this study, we explored the contribution of Adipocyte Differentiation Related Protein (ADRP). ADRP is a lipid droplet-associated surface protein that has been reported to be regulated by hypoxia inducible factors in other models. [97, 155] ADRP has been shown to be upregulated in human steatosis as well as in mice developing steatosis after a high-fat diet.[202] Additionally administration of an ADRP antisense oligonucleotide ameliorated hepatic steatosis, while normal adipogenesis but diminished hepatic steatosis was observed in an ADRP knockout mouse.[203][204] While Rankin et al have reported that HIF2α has a more profound effect on the regulation of ADRP than HIF1α, data within their own reports suggests that HIF1α also regulates ADRP expression.[155] Importantly, we found upregulation of ADRP consistently in WT mice that had been chronically exposed to ethanol and challenged with LPS; indeed, little upregulation of ADRP was evident with chronic ethanol alone, while HepHIF(-) mice were protected from any upregulation of ADRP. We also found a consistent upregulation of HIF1α mRNA in chronic ethanol/LPS-challenged mice, but a less consistent effect on HIF2α mRNA. Taken together, these data suggest that while HIF2α may indeed be a stronger regulator

of hepatic ADRP expression, the use of profound mouse models of HIF activation (such as complete VHL protein loss, as in the model of Rankin et al) may not mimic the physiologically dominant modes of regulation of HIF expression.

If ADRP is a predominant regulator of hepatic lipid accumulation, the question remains why upregulation of ADRP mRNA was not observed in ethanol-fed, non-LPS injected WT mice. This likely represents the power of the chronic ethanol/LPS model to create a robust static picture of a dynamic process that occurs with chronic alcohol abuse. For example, chronic alcoholics are rarely, if ever, exposed to the level of lipopolysaccharide challenge as we utilize in the mouse model; however, the utility of the model lies in reproducing in a robust fashion a phenomenon that is occurring chronically at a lower level, e.g., with small increases in portal vein endotoxin resulting in chronic mild inflammation.

In support of the idea that ADRP is a dominant regulator of hepatic lipid accumulation, ADRP knockout was able to prevent hepatic steatosis in a high-fat diet model, and ADRP antisense oligonucleotides were able to reduce hepatic steatosis in leptin-pathway deficient mice. [204][203] However, the possibility that other genes affecting lipid metabolism are affected by HIF should not be discounted. If ADRP is a key regulator of hepatic steatosis in ALD downstream of HIF1α, however, the question remains about what the role of ADRP may be. One possibility is that increased ADRP limits lipid availability for efflux or oxidative/degradative pathways. Future work is needed to determine the functional dependence of lipid accumulation on the ADRP protein.

Hepatocyte-Specific HIF1α -dependent regulation of inflammation in ALD

Indeed, one emerging picture suggests that lipid accumulation is profoundly affected by pro-inflammatory stimuli. In this view, even the hepatic lipid accumulation owing to chronic ethanol exposure may be more a function of ethanol effects on immune hyper-responsiveness than solely an effect of ethanol. In support of this, the chemokine MCP-1 was recently demonstrated to cause increased triglyceride deposition in the human hepatoma cell line Huh7. We also found synergistic upregulation of serum MCP-1 in chronic ethanol/LPS treated mice. Our previous work demonstrated induction of HIF1α protein with MCP-1 treatment in Huh7 cells, as well prevention of lipid accumulation with HIF1α siRNA pretreatment in Huh7 cells, suggesting that hepatocytic HIF1α is intimately involved in the immune response. Indeed, we found a profound suppression of serum ALT levels after challenge with LPS in ethanol-fed HepHIF(-) mice. As expected, HepHIF(-) mice did not demonstrate an upregulation of HIF1α protein in hepatic nuclear extracts after chronic ethanol and/or chronic ethanol/LPS challenge, whereas, consistent with earlier studies, HIF1α was upregulated in chronic ethanol-fed mice, and also upregulated by LPS injection alone in WT mice. In order to characterize the changes in serum cytokines we utilized a multiplex cytokine bead array system. We found that chronic ethanol caused a dramatic increase in the secretion of several cytokines, including TNFα, IL-6, KC, MCP-1, IL-10, and IFNγ after LPS challenge in wild-type mice when compared to pair-fed, LPS-injected WT mice. Little synergistic upregulation of these cytokines was observed with chronic ethanol feeding in HepHIF(-) mice, underscoring the role of HIF1α as a master regulator of inflammation. Perhaps more surprising is the finding that these results were robust in HepHIF(-) mice as well as in MyeHIF(-) mice. Interestingly, the pattern of regulation of several cytokines, including TNFα, IL-6, IL-10, and MCP-1, suggested that MyeHIF(-) mice actually

had higher cytokine levels in pair-fed animals than in ethanol fed animals, whereas HepHIF(-) mice had comparable levels of cytokines between ethanol and pair-fed animals after LPS injection. This suggests a more complex pattern of HIF-dependent regulation.

In summary, we found that excision of a floxed HIF1α allele in hepatocytes by co-expression of the cre-recombinase transgene under the control of the albumin promoter resulted in decreased HIF1α expression after chronic alcohol feeding, and that this decreased expression correlated to decreased liver-weight body-weight ratios, decreased hepatic triglyceride, and decreased steatosis as determined through quantified Oil-red O staining. We further found that HepHIF(-) mice had vastly decreased secretion of pro-inflammatory cytokines in comparison with WT mice. In contrast, MyeHIF(-) mice had increases in LW/BW ratios and the triglyceride content of ethanol-fed MyeHIF(-) mice was similar to that in ethanol-fed wild-type mice. MyeHIF(-) mice also had diminished levels of several cytokines after ethanol/LPS challenge, including TNFα. Other cytokines, including KC, IL-6, and IL-10, were not diminished in MyeHIF(-) mice. The pattern of differential regulation of cytokines we report in myeHIF(-) mice is nearly identical to that reported by other investigators using myeloid-lineage-specific HIF1α KO mice in models of sepsis.[143] Either the increased steatosis or the lack of protection in other cytokines (such as KC) between MyeHIF(-) ethanol-fed/LPS challenged mice and WT ethanol-fed/LPS challenged mice, may be partially responsible for the lack of protection against elevations in serum ALT in ethanol-fed MyeHIF(-) mice. These results establish targeting of HIF1α as a potential therapeutic strategy in the treatment of alcoholic steatohepatitis.

CHAPTER 6

FINAL SUMMARY AND DISCUSSION

Our work has demonstrated a role for Hypoxia Inducible Factors in the pathogenesis of alcoholic liver disease. Broadly speaking, our results can be summarized in three areas. First, we provide evidence for a role for HIF1α in hepatic lipid accumulation; second, we provide evidence that HIF1α activation is a possible mechanism for the dysregulation of downstream signaling networks in alcoholic liver disease, particularly through regulation of PAI-1 and iNOS; and third, that HIF1α activation in hepatocytes alters immune activation as determined by measured levels of cytokines. A schematic illustrating some of these findings is included in Figure 34.

HIF1α and lipid accumulation

We have described that constitutive activation of HIF1α in hepatocytes accelerates lipid accumulation with chronic ethanol feeding, reporting in Chapter 3 that HIF1dPA mice had higher steatosis by microscopy and increased hepatic triglyceride versus control mice. Furthermore, using an in vitro system in Chapter 4, we offered data to suggests that inhibition of HIF1α prevents lipid accumulation. Finally, in Chapter 5, we described the finding that deficiency of HIF1α in hepatocytes results in prevention of increased liver-weight to body-weight ratio and diminished hepatic triglycerides.

Our findings differ from those of Rankin et al, in that they argue that HIF1α has little or no role in hepatic lipid accumulation. We have described that constitutive activation of HIF1α in

Figure 34. Pathways of HIF involvement in the Pathogenesis of Alcoholic Liver Disease

Chronic alcohol causes increased gut permeability, which results in increased LPS entering the portal circulation. This stimulates TLR4 receptors in the hepatic macrophage, which in turn cause TNFa secretion via an NFκB, HIF1α dependent mechanism. A remaining question is whether LPS may also stimulate hepatic TLR4 to result in HIF1α activation, which we did not address in this study. Chronic alcohol increases results in an increase in HIF1α in whole liver, possibly mediated through the known effects of ethanol on increased metabolic demand, alteration in cellular redox state, and the creation of reactive oxygen species, all of which can increase HIF1α. Suppression of HIF1α signaling i hepatocytes prevented upregulation of PAI-1 and iNOS in response to chronic alcohol and LPS challenge. HIF1α activation increases lipid accumulation. MCP-1 also increases lipid accumulation, and was shown to increase HIF1α in a hepatoma cell line *in vitro*. Finally, suppression of HIF1α in hepatocytes decreased TNFα and KC.

Figure 34

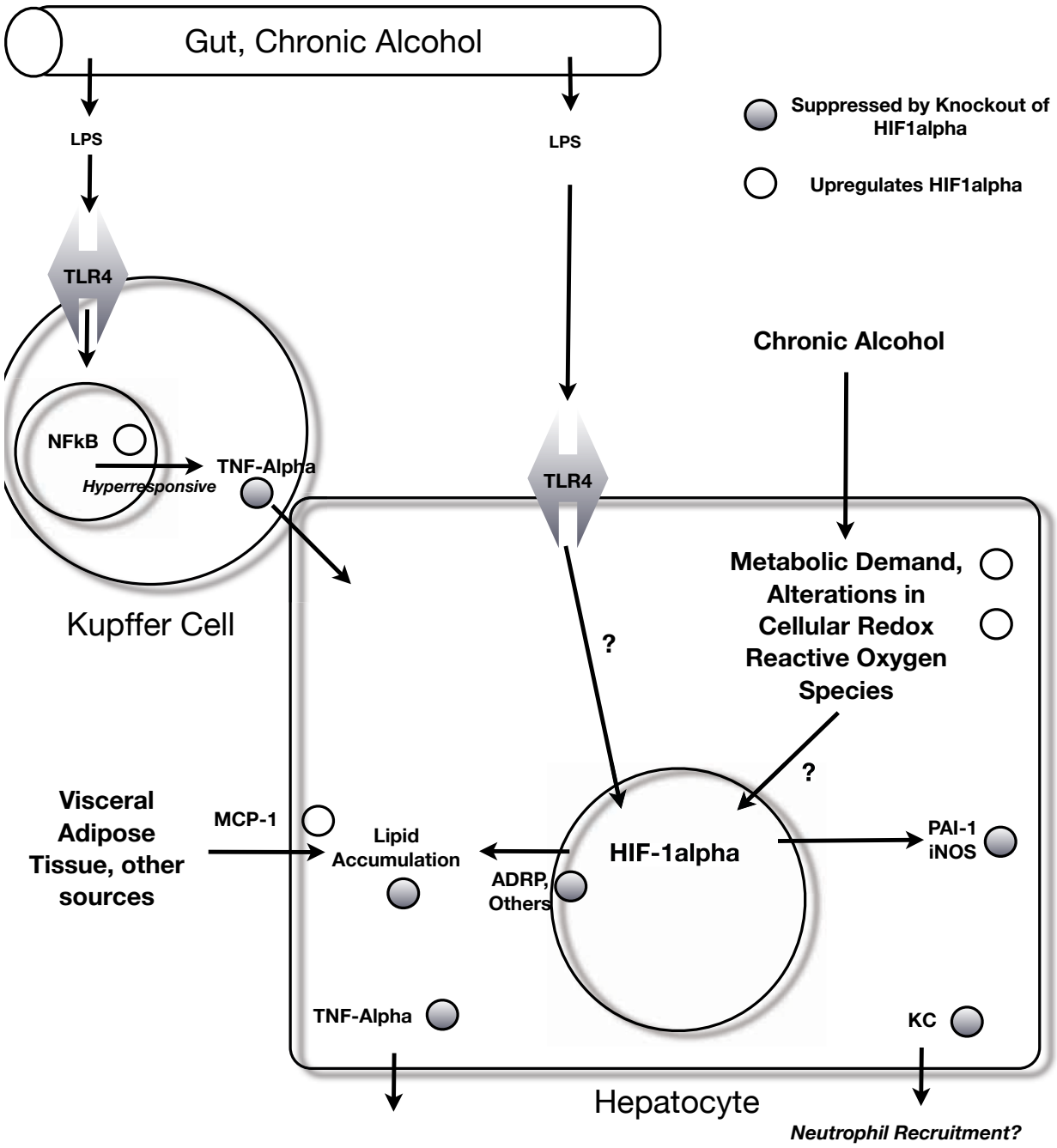
Gut, Chronic Alcohol
LPS
LPS
Suppressed by Knockout of HIF1alpha
Upregulates HIF1alpha
TLR4
Chronic Alcohol
NFkB
TNF-Alpha
Hyperresponsive
TLR4
Kupffer Cell
?
Metabolic Demand, Alterations in Cellular Redox Reactive Oxygen Species
?
Visceral Adipose Tissue, other sources
MCP-1
Lipid Accumulation
HIF-1alpha
ADRP, Others
PAI-1
iNOS
TNF-Alpha
KC
Hepatocyte
Neutrophil Recruitment?

hepatocytes accelerates lipid accumulation with chronic ethanol feeding, that inhibition of HIF1α prevents lipid accumulation *in vitro,* and that partial deficiency of HIF1α in hepatocytes results in prevention of increased liver-weight to body-weight ratio and diminished hepatic triglycerides.

Rankin et al demonstrated a role for HIF2-alpha in the regulation of hepatic lipid metabolism by utilizing compound cre-lox knockout mouse models. By knocking out pVHL in combination with HIF1α or HIF2α, they were able to create models of hepatocyte-specific constitutively active HIF1 or HIF2. Using this model, they suggested that constitutive activation of HIF2, but not HIF1, was a major regulator of lipid metabolism.[155] This is in sharp contrast to earlier work by Scortegagna et al, which demonstrated that in adult HIF2α KO mice, multiple organ pathologies including severe steatosis developed, suggesting that HIF2α is dispensable for the development of steatosis. Additionally, Scortegagna et al offered data to suggest that hepatic steatosis in HIF2α (-/-) mice could be reversed by treatment with a superoxide dismutase (SOD1) inhibitor. [153] In support of that mechanism, a more recent study has suggested that inhibition of HIF2α recruitment to the SOD1 promoter prevents SOD1 transcription.[205] Kim et al, on the other hand, found no significant contribution to hepatic lipid accumulation with a degradation-resistant mutant of HIF2, despite finding a robust effect on angiogenesis. On the other hand, they demonstrated a mild HIF1α dependent effect on lipid accumulation.[97] One important explanation of the discrepancies found in these studies derives from the varying strategies each employs. In the work of Rankin and colleagues, disruption of VHL creates a milieu where multiple protein-protein interactions may be compromised. Other proteins, including an RNA polymerase subunit and HIF3a, have been reported to be regulated by VHL-dependent ubiquitination.[206] Neither study considers a potential role for HIF3a, which has

been shown to have inhibitory effects on HIF transcription. HIF3a is transcriptionally upregulated by HIF1α; data demonstrating transcriptional upregulation of HIF3a by HIF2α is not currently available.[207] It is possible in the model of Rankin and colleagues that absence of HIF1α alters other counter-regulatory mechanisms, such as asparaginyl hydroxylation of HIF2α or induction of HIF3a, whereas in the model of Kim et al, native HIF1α and VHL functions are preserved, accounting for the difference observed in phenotype.

Others have described higher activity for asparaginyl hydroxylase-mediated inhibition of HIF1α transactivation than HIF2α transactivation; consequently, absence of degradation of HIF1α or HIF2α on the VHL scaffold may neglect effects of asparaginyl hydroxylation on transactivator recruitment, which would be anticipated to be greater for HIF1α than HIF2α.[208] Additionally, other alternative degradation pathways for HIF1α have been described that may be distinct from pVHL interactions.[209]

The distinctions between genetic models of constitutive activation of HIF subunits and diet-induced disease models are also quite significant. Some investigators have offered evidence to suggest cyclic regulation of HIF1α mRNA in chronic ethanol feeding models.[138] Those and other variations, including diurnal/circadian variations in gene expression, are lost in models of forced constitutive gene expression, and may have quite a large effect on resultant phenotype. For example, constitutive HIF1α expression or HIF1α expression mediated by chronic ethanol or intermittent activation of TLRs may in turn promote HIF2α activation. Thus, activation of HIF1α in a forced genetic model may only have effects when HIF2α signaling is also present; conversely, constitutively active HIF2α activity may not require HIF1α for effects on hepatic lipid accumulation. If that is the case, then the question arises: why was lipid accumulation not

observed in the constitutively active HIF2α model described by Kim et al? One explanation may be that in that model, native HIF1α activity or pVHL activity resulted in retained counter-regulatory mechanisms that limited some, but not all, effects of HIF2α-dependent transcription. For example, recent work has suggested that maximal activity of HIF2α is crucially dependent upon a protein-protein interaction (i.e., a non-histone related interaction) with the histone deacetylase Sirtuin 1[210]; it is possible that such protein protein interactions are also dependent upon regulation by other HIF pathway members.

Another significant difference between our work and the work of both Kim and colleagues and Rankin and colleagues is that while their models relied heavily on genetic knockout strategies alone, we added the additional stimulus of a pro-steatotic ethanol-containing diet. In fact, deeper analysis of the work of Rankin et al reveals that their VHL/HIF1α compound knockout (expected to have constitutive HIF2α activation) reveals that these mice expired at 4-8 weeks of age, and had severe total body weight loss, whereas VHL/HIF2α compound knockout mice were phenotypically normal; furthermore, they found a nearly two-fold increase in hepatic triglyceride content in VHL/HIF2α mice, a change that was statistically significant when compared to Alb-Cre control mice.[211] In fact, the changes they describe in mice with constitutive HIF1α activation are nearly identical to those described by Kim and colleagues. Since our studies involve the additional caloric stimulus of alcohol feeding, and our mice are sacrificed at a later age than Rankin and colleagues report, it follows that the accelerating effect on lipid accumulation we observed in HIF1dPA mice is not at odds with their findings. Furthermore, the profound effect on weight gain that Rankin and colleagues and Kim and colleagues both described in mice with constitutive HIF2α activation suggests that a

different mechanism may be at play. The phenotype that Rankin and colleagues describe in mice with constitutively active HIF2α is quite similar to that seen in a different diet induced model of fatty liver disease, the methionine-choline deficient model. This model restricts mice to a diet that is absolutely deficient in methionine and choline, with the resultant effect that mice display profound weight loss, and hepatic steatosis with significantly increased liver-weight/body-weight ratios, despite livers that are smaller (in absolute weight terms) than those in methionine-choline supplemented diet controls.[212] Our work is consonant with the work of Rankin and colleagues as well as Kim and colleagues in that their studies suggest that HIF1α promotes lipid accumulation, and our studies extend these findings by suggesting that alcohol promotes lipid accumulation via a HIF1α-dependent mechanism. While Rankin and colleagues find that the absence of HIF1α activation (in the constitutive HIF2α mouse) did not prevent lipid accumulation, the interpretation of the phenotype of that mouse is severely compromised by the severe weight loss, which suggests that the steatosis they observe may bear more similarity to that observed in human disease states such as fasting, rather than that induced by chronic alcohol.

Further work may clarify these findings. The use of mice with hepatocyte-specific HIF2α deletion, which only became available in the last six months of the work described here, in models of chronic alcohol feeding, may clarify whether HIF2α is truly required for alcohol-mediated hepatic steatosis.

HIF1α and cytokines in Alcoholic Liver Disease

We also found significant effects of HIF on the production of cytokines with chronic ethanol. In Chapter 3, we described the finding that constitutive activation of HIF in hepatocytes resulted in significantly higher levels of TNFα mRNA than in control mice. Conversely, in Chapter 5 we described the opposite scenario, namely, that ethanol-fed HepHIF(-) and MyeHIF(-) mice both had much lower levels of TNFα at two hours post LPS injection than did wild-type mice. While the extent of protection against TNFα elevation induced by LPS in MyeHIF(-) mice was in good agreement with published reports on the prevention of TNFα elevation induced by LPS, [155] the protection in HepHIF(-) mice was novel and surprising, and even more pronounced. The pattern observed in TNFα followed the trend observed in serum ALT, with HIF1dPA pair-fed mice having higher levels of TNFα mRNA and higher serum ALT values than pair-fed control mice, and conversely, HepHIF(-) mice having much lower levels of serum TNFα and decreased serum ALT after ethanol and LPS challenge. A regrettable absence in the HIF1dPA study was the lack of an LPS injection arm of the study, and ongoing efforts in the lab may include that experiment. Nevertheless, even in the absence of that experiment, the correlations we describe provide compelling evidence that hepatocyte-specific HIF1α dependent-modulation of TNFα levels is a potential mechanism of HIF involvement in the pathogenesis of alcoholic liver disease.

Other cytokines showed varying results. Notably, some protection in upregulation of KC was observed in HepHIF(-) at 2 hours, while by 18 hours both HepHIF(-) and MyeHIF(-) mice had low levels of KC after ET LPS challenge. Given this finding, a natural next step would be to assay neutrophil recruitment to the liver after ethanol and LPS challenge, and compare neutrophil recruitment in HepHIF(-) mice versus MyeHIF(-) mice; indeed, IL-8 is increased in alcoholic

hepatitis, (see [189] for review) and increased neutrophil recruitment and increased IL-8, among other CXC chemokines, is associated with a worse prognosis in human alcoholic hepatitis.[213] Although we were not able to complete such a study during the timeline of this project, the protection in HepHIF(-) mice against ethanol-induced upregulation of the chemoattractant cytokines KC and MCP-1 after LPS challenge offers a potential mechanism for the ability of HIF1α deficiency in hepatocytes to diminish the rise in serum ALT observed in WT mice. This potential mechanism would position hepatocyte HIF activation in response to chronic alcohol and LPS as part of an amplifying cascade that resulted in the recruitment of inflammatory cells, including neutrophils, monocytes and macrophages. This finding underscores the central premise that alcoholic liver injury proceeds via a multi-step process that depends on dysregulated signaling both within and without the hepatocyte.

Previous work in has identified HIF1α activation in other cell types as modifying the immune response; notably, two pivotal studies have identified different roles for HIF1α in the modulation of the immune response in cells of the myeloid lineage (such as hepatic Kupffer cells) and T cells.[143, 146] Whereas in the former, a suppression of cytokine levels in myeloid lineage-specific HIF1α knockout mice in response to LPS suggested that HIF activation is NFκB dependent and has a pro-inflammatory role in myeloid cells, in the latter study, knockout of HIF1α in T-cells was associated with increased cytokines, again via an NFκB dependent mechanism. In both studies, HIF1α suppression was associated with higher survival, however, as the first study used lethal doses of endotoxin as pro-inflammatory stimulus, and the latter used active bacterial infection, the mechanisms by which inflammation is related to survival in those two models is necessarily different. The emerging picture suggests that the role of HIF1α is

highly cell-specific, and our data suggests that in hepatocytes, HIF1α has a largely pro-inflammatory role.

A remaining question is the mechanism of HIF1α activation in hepatocytes and hepatic nonparenchymal cells. Numerous lines of evidence support a role for TLR4-NFκB-dependent signaling in the activation of HIF1α in macrophages.[142, 214] However, recent work has also suggested that alcoholic liver disease progresses via stimulation of the MyD88-independent-limb of the LPS-TLR4 signaling pathway.[58, 59] Further investigation may reveal the specific dependence of HIF1α signaling on LPS-TLR4 pathways in alcoholic liver disease. Some recent data from other laboratories suggests other possibilities for HIF regulation include novel protein-protein interactions, such as Sirt1 (in the case of HIF2α) or chaperone proteins such as those in the heat-shock proteins family.[210][215, 216]

HIF1α and dysregulation of downstream signaling networks

In both Chapter 3 and Chapter 5, we have also reported findings suggesting strong HIF1α-dependent effects on the expression of genes involved in the pathogenesis of alcoholic steatohepatitis. In chapter 3, HIF1dPA mice had much higher levels of PAI-1 and iNOS, both of which have been previously reported as upregulated in alcoholic liver disease. Furthermore, in Chapter 5, use of the hepatocyte-specific HIF1α mutant (HepHIF(-) mouse) prevented induction of HIF1α expression with chronic alcohol feeding,and resulted in decreased PAI-1 and iNOS expression after LPS challenge. As HIF1α is a master regulator of transcription, it is quite likely that further study will reveal multiple other gene targets that are both downstream of HIF1α activation and upregulated in alcoholic liver disease. With PAI-1, iNOS, and other HIF1α target

genes, an important question will be whether the upregulation of the gene is incidental to the pathogenesis of alcoholic liver disease, and merely correlated with the activation of broader transcriptional networks, or whether a gene product is truly implicated in the pathogenesis of the condition. For example, some protection was observed in PAI-1 KO mice maintained on a chronic ethanol diet.[217] Dissecting the relative contribution of PAI-1, or any other gene target, to phenotypes observed in constitutive activation or suppression of master regulator genes such as HIF1α will continue to be a formidable challenge. Several strategies, such as breeding cre-lox models onto genetic knockout strains, can be readily imagined and are promising ways to investigate these questions.

Future directions

The most proximal questions that arise from these studies include the role of ADRP in hepatic lipid accumulation, the path from MCP-1 treatment to HIF1α activation, and the role of hepatocyte-specific HIF1α in the cooperative induction of inflammatory cytokines, such as TNFα and others, by alcohol and lipopolysaccharide. With regards to the latter, the conventional wisdom is that the Kupffer cell is the source of TNFα. However, an intriguing possibility implied by our results is that whereas normoxic hepatocytes may remain unable to secrete TNFα, hypoxic hepatocytes may behave quite differently. If the combination of hypoxia and lipopolysaccharide treatment resulted in secretion of TNFα from hepatocytes, it also would explain the zonal necrosis observed in several forms of hepatitis, as reviewed in chapter 1B, above.

In final summary, we have offered compelling data to suggest that HIF1α is implicated in the pathogenesis of alcoholic liver disease. It is not at all surprising that human, as aerobic

organisms, are profoundly susceptible to hypoxic tissue injury; more surprising, however, is the fact that the regulatory networks activated in response to hypoxia result in such a broad set of responses that may be at turns adaptive, maladaptive, or somewhere in between. Given that alcoholic liver disease bears important similarities and differences to other forms of liver injury, and that many forms of liver injury are aggravated by hypoxia or implicate the hypoxia-inducible factors, the investigation of modification of hypoxia-inducible-factors activity in ALD and other hepatic diseases will likely have important roles in therapy.

Bibliography

1. Sozio, M. and D. Crabb, *Alcohol and lipid metabolism.* American journal of physiology. Endocrinology and metabolism, 2008. **295**(1).
2. Yin, H.Q., et al., Differential gene expression and lipid metabolism in fatty liver induced by acute ethanol treatment in mice. Toxicol Appl Pharmacol, 2007. **223**(3): p. 225-33.
3. Klassen, L.W., et al., An in vitro method of alcoholic liver injury using precision-cut liver slices from rats. Biochem Pharmacol, 2008. **76**(3): p. 426-36.
4. Bensinger, S.J. and P. Tontonoz, Integration of metabolism and inflammation by lipid-activated nuclear receptors. Nature, 2008. **454**(7203): p. 470-7.
5. Wan, Y.J., et al., Expression of the peroxisome proliferator-activated receptor gene is decreased in experimental alcoholic liver disease. Life Sci, 1995. **56**(5): p. 307-17.
6. Fischer, M., et al., Peroxisome proliferator-activated receptor alpha (PPARalpha) agonist treatment reverses PPARalpha dysfunction and abnormalities in hepatic lipid metabolism in ethanol-fed mice. J Biol Chem, 2003. **278**(30): p. 27997-8004.
7. Nanji, A., et al., Alcoholic liver injury in the rat is associated with reduced expression of peroxisome proliferator-alpha (PPARalpha)-regulated genes and is ameliorated by PPARalpha activation. The Journal of pharmacology and experimental therapeutics, 2004. **310**(1): p. 417.
8. Nakajima, T., et al., Peroxisome proliferator-activated receptor alpha protects against alcohol-induced liver damage. Hepatology (Baltimore, Md.), 2004. **40**(4): p. 972-80.
9. Gyamfi, M., et al., Hepatocyte retinoid X receptor alpha-dependent regulation of lipid homeostasis and inflammatory cytokine expression contributes to alcohol-induced liver injury. The Journal of pharmacology and experimental therapeutics, 2008. **324**(2): p. 443.
10. Nakamachi, T., et al., PPARalpha agonists suppress osteopontin expression in macrophages and decrease plasma levels in patients with type 2 diabetes. Diabetes, 2007. **56**(6): p. 1662-70.
11. Lee, J., et al., Potential relationship between hepatobiliary osteopontin and peroxisome proliferator-activated receptor {alpha} expression following ethanol-associated hepatic

injury in vivo and in vitro. Toxicological sciences : an official journal of the Society of Toxicology, 2008.

12. Chen, X., B.M. Sebastian, and L.E. Nagy, Chronic ethanol feeding to rats decreases adiponectin secretion by subcutaneous adipocytes. Am J Physiol Endocrinol Metab, 2007. **292**(2): p. E621-8.
13. You, M., et al., Role of adiponectin in the protective action of dietary saturated fat against alcoholic fatty liver in mice. Hepatology (Baltimore, Md.), 2005. **42**(3): p. 568-77.
14. Beraza, N., et al., Pharmacological IKK2 inhibition blocks liver steatosis and initiation of non-alcoholic steatohepatitis. Gut, 2008. **57**(5): p. 655.
15. Rogers, C., J. Ajmo, and M. You, Adiponectin and alcoholic fatty liver disease. IUBMB life, 2008.
16. Tomita, K., et al., AICAR, an AMPK activator, has protective effects on alcohol-induced fatty liver in rats. Alcoholism, clinical and experimental research, 2005. **29**(12 Suppl): p. 240.
17. Bergheim, I., et al., Metformin prevents alcohol-induced liver injury in the mouse: Critical role of plasminogen activator inhibitor-1. Gastroenterology, 2006. **130**(7): p. 2099.
18. Ye, P., et al., The alteration of plasminogen activator inhibitor-1 expression by linoleic acid and fenofibrate in HepG2 cells. Blood Coagul Fibrinolysis, 2007. **18**(1): p. 15-9.
19. Kono, H., et al., NADPH oxidase-derived free radicals are key oxidants in alcohol-induced liver disease. The Journal of clinical investigation, 2000. **106**(7): p. 867.
20. Lu, Y. and A.I. Cederbaum, CYP2E1 and oxidative liver injury by alcohol. Free Radic Biol Med, 2008. **44**(5): p. 723-38.
21. Koop, D.R. and D.J. Tierney, Multiple mechanisms in the regulation of ethanol-inducible cytochrome P450IIE1. Bioessays, 1990. **12**(9): p. 429-35.
22. Lu, Y., et al., Cytochrome P450 2E1 contributes to ethanol-induced fatty liver in mice. Hepatology (Baltimore, Md.), 2008. **47**(5): p. 1483.
23. Kono, H., et al., CYP2E1 is not involved in early alcohol-induced liver injury. The American journal of physiology, 1999. **277**(6 Pt 1).

24. Wan, Y.Y., et al., Regulation of peroxisome proliferator activated receptor alpha-mediated pathways in alcohol fed cytochrome P450 2E1 deficient mice. Hepatol Res, 2001. **19**(2): p. 117-130.
25. Ohata, M., et al., Pioglitazone prevents acute liver injury induced by ethanol and lipopolysaccharide through the suppression of tumor necrosis factor-alpha. Alcohol Clin Exp Res, 2004. **28**(8 Suppl Proceedings): p. 139S-144S.
26. Enomoto, N., et al., Prevention of ethanol-induced liver injury in rats by an agonist of peroxisome proliferator-activated receptor-gamma, pioglitazone. The Journal of pharmacology and experimental therapeutics, 2003. **306**(3): p. 846.
27. Tomita, K., et al., Pioglitazone prevents alcohol-induced fatty liver in rats through up-regulation of c-Met. Gastroenterology, 2004. **126**(3): p. 873-85.
28. Mitra, S.K., et al., Liv.52 regulates ethanol induced PPARgamma and TNF alpha expression in HepG2 cells. Mol Cell Biochem, 2008. **315**(1-2): p. 9-15.
29. Lieber, C.S., et al., Effect of chronic alcohol consumption on Hepatic SIRT1 and PGC-1alpha in rats. Biochem Biophys Res Commun, 2008. **370**(1): p. 44-8.
30. Qin, X., et al., Peroxisome proliferator-activated receptor-delta induces insulin-induced gene-1 and suppresses hepatic lipogenesis in obese diabetic mice. Hepatology (Baltimore, Md.), 2008.
31. You, M., et al., Involvement of mammalian sirtuin 1 in the action of ethanol in the liver. Am J Physiol Gastrointest Liver Physiol, 2008. **294**(4): p. G892-8.
32. Ajmo, J.M., et al., Resveratrol alleviates alcoholic fatty liver in mice. Am J Physiol Gastrointest Liver Physiol, 2008. **295**(4): p. G833-42.
33. Oliva, J., et al., Sirt1 is involved in energy metabolism: The role of chronic ethanol feeding and resveratrol. Experimental and molecular pathology, 2008.
34. You, M., et al., Ethanol induces fatty acid synthesis pathways by activation of sterol regulatory element-binding protein (SREBP). J Biol Chem, 2002. **277**(32): p. 29342-7.
35. Ji, C., C. Chan, and N. Kaplowitz, Predominant role of sterol response element binding proteins (SREBP) lipogenic pathways in hepatic steatosis in the murine intragastric ethanol feeding model. J Hepatol, 2006. **45**(5): p. 717-24.

36. Horiguchi, N., et al., Cell type-dependent pro- and anti-inflammatory role of signal transducer and activator of transcription 3 in alcoholic liver injury. Gastroenterology, 2008. **134**(4): p. 1148-58.
37. Hebbachi, A.M., et al., Peroxisome proliferator-activated receptor alpha deficiency abolishes the response of lipogenic gene expression to re-feeding: restoration of the normal response by activation of liver X receptor alpha. J Biol Chem, 2008. **283**(8): p. 4866-76.
38. Yoshikawa, T., et al., Cross-talk between peroxisome proliferator-activated receptor (PPAR) alpha and liver X receptor (LXR) in nutritional regulation of fatty acid metabolism. I. PPARs suppress sterol regulatory element binding protein-1c promoter through inhibition of LXR signaling. Mol Endocrinol, 2003. **17**(7): p. 1240-54.
39. Thakur, V., et al., Regulation of macrophage activation in alcoholic liver disease. J Gastroenterol Hepatol, 2007. **22 Suppl 1**: p. S53-6.
40. Seki, E. and D. Brenner, Toll-like receptors and adaptor molecules in liver disease: Update. Hepatology (Baltimore, Md.), 2008. **48**(1): p. 322.
41. Yin, M., et al., Essential role of tumor necrosis factor alpha in alcohol-induced liver injury in mice. Gastroenterology, 1999. **117**(4): p. 942-52.
42. Iimuro, Y., et al., Antibodies to tumor necrosis factor alfa attenuate hepatic necrosis and inflammation caused by chronic exposure to ethanol in the rat. Hepatology, 1997. **26**(6): p. 1530-7.
43. Bjarnason, I., T.J. Peters, and R.J. Wise, The leaky gut of alcoholism: possible route of entry for toxic compounds. Lancet, 1984. **1**(8370): p. 179-82.
44. Nanji, A.A., et al., Severity of liver injury in experimental alcoholic liver disease. Correlation with plasma endotoxin, prostaglandin E2, leukotriene B4, and thromboxane B2. Am J Pathol, 1993. **142**(2): p. 367-73.
45. Tang, Y., et al., Effect of alcohol on miR-212 expression in intestinal epithelial cells and its potential role in alcoholic liver disease. Alcohol Clin Exp Res, 2008. **32**(2): p. 355-64.
46. Lencer, W.I., Patching a leaky intestine. N Engl J Med, 2008. **359**(5): p. 526-8.

47. Jin, W., et al., Increased intestinal inflammatory response and gut barrier dysfunction in Nrf2-deficient mice after traumatic brain injury. Cytokine, 2008.
48. Lu, Y.C., W.C. Yeh, and P.S. Ohashi, *LPS/TLR4 signal transduction pathway.* Cytokine, 2008. **42**(2): p. 145-51.
49. Lukkari, T.A., et al., Short-term ethanol exposure increases the expression of Kupffer cell CD14 receptor and lipopolysaccharide binding protein in rat liver. Alcohol Alcohol, 1999. **34**(3): p. 311-9.
50. Romics, L., et al., Increased lipopolysaccharide sensitivity in alcoholic fatty livers is independent of leptin deficiency and toll-like receptor 4 (TLR4) or TLR2 mRNA expression. Alcoholism, clinical and experimental research, 2005. **29**(6): p. 1018.
51. Gustot, T., et al., Differential liver sensitization to toll-like receptor pathways in mice with alcoholic fatty liver. Hepatology (Baltimore, Md.), 2006. **43**(5): p. 989.
52. Yin, M., et al., Reduced early alcohol-induced liver injury in CD14-deficient mice. J Immunol, 2001. **166**(7): p. 4737-42.
53. Uesugi, T., et al., Role of lipopolysaccharide-binding protein in early alcohol-induced liver injury in mice. J Immunol, 2002. **168**(6): p. 2963-9.
54. Takeda, K. and S. Akira, *TLR signaling pathways.* Semin Immunol, 2004. **16**(1): p. 3-9.
55. Vogel, S.N., K.A. Fitzgerald, and M.J. Fenton, TLRs: differential adapter utilization by toll-like receptors mediates TLR-specific patterns of gene expression. Mol Interv, 2003. **3**(8): p. 466-77.
56. Uematsu, S. and S. Akira, Toll-like receptors and Type I interferons. J Biol Chem, 2007. **282**(21): p. 15319-23.
57. Severa, M. and K.A. Fitzgerald, TLR-mediated activation of type I IFN during antiviral immune responses: fighting the battle to win the war. Curr Top Microbiol Immunol, 2007. **316**: p. 167-92.
58. Hritz, I., et al., The critical role of toll-like receptor (TLR) 4 in alcoholic liver disease is independent of the common TLR adapter MyD88. Hepatology (Baltimore, Md.), 2008.

59. Zhao, X.J., et al., TRIF and IRF-3 binding to the TNF promoter results in macrophage TNF dysregulation and steatosis induced by chronic ethanol. J Immunol, 2008. **181**(5): p. 3049-56.
60. Geisler, F., et al., Genetic inactivation of RelA/p65 sensitizes adult mouse hepatocytes to TNF-induced apoptosis in vivo and in vitro. Gastroenterology, 2007. **132**(7): p. 2489.
61. Beraza, N., et al., Hepatocyte-specific IKK gamma/NEMO expression determines the degree of liver injury. Gastroenterology, 2007. **132**(7): p. 2504.
62. Mandrekar, P., et al., Acute alcohol exposure exerts anti-inflammatory effects by inhibiting IkappaB kinase activity and p65 phosphorylation in human monocytes. J Immunol, 2007. **178**(12): p. 7686-93.
63. Foster, S.L., D.C. Hargreaves, and R. Medzhitov, Gene-specific control of inflammation by TLR-induced chromatin modifications. Nature, 2007. **447**(7147): p. 972-8.
64. Park, P.H., et al., Suppression of lipopolysaccharide-stimulated tumor necrosis factor-alpha production by adiponectin is mediated by transcriptional and post-transcriptional mechanisms. J Biol Chem, 2008. **283**(40): p. 26850-8.
65. Gobejishvili, L., et al., Enhanced PDE4B expression augments LPS inducible TNF expression in ethanol primed monocytes: relevance to alcoholic liver disease. American journal of physiology. Gastrointestinal and liver physiology, 2008.
66. McMullen, M.R., et al., Early growth response-1 transcription factor is essential for ethanol-induced fatty liver injury in mice. Gastroenterology, 2005. **128**(7): p. 2066-76.
67. Thakur, V., et al., Chronic ethanol feeding increases activation of NADPH oxidase by lipopolysaccharide in rat Kupffer cells: role of increased reactive oxygen in LPS-stimulated ERK1/2 activation and TNF-alpha production. J Leukoc Biol, 2006. **79**(6): p. 1348-56.
68. Kohgo, Y., et al., Dysregulation of systemic iron metabolism in alcoholic liver diseases. J Gastroenterol Hepatol, 2008. **23 Suppl 1**: p. S78-81.
69. Suzuki, M., et al., Induction of transferrin receptor by ethanol in rat primary hepatocyte culture. Alcohol Clin Exp Res, 2004. **28**(8 Suppl Proceedings): p. 98S-105S.

70. Ohtake, T., et al., Hepcidin is down-regulated in alcohol loading. Alcohol Clin Exp Res, 2007. **31**(1 Suppl): p. S2-8.
71. Harrison-Findik, D.D., et al., Iron-mediated regulation of liver hepcidin expression in rats and mice is abolished by alcohol. Hepatology, 2007. **46**(6): p. 1979-85.
72. Tsukamoto, H., et al., Iron primes hepatic macrophages for NF-kappaB activation in alcoholic liver injury. Am J Physiol, 1999. **277**(6 Pt 1): p. G1240-50.
73. Xiong, S., et al., Hepatic macrophage iron aggravates experimental alcoholic steatohepatitis. Am J Physiol Gastrointest Liver Physiol, 2008. **295**(3): p. G512-21.
74. Duvigneau, J.C., et al., A novel endotoxin-induced pathway: upregulation of heme oxygenase 1, accumulation of free iron, and free iron-mediated mitochondrial dysfunction. Lab Invest, 2008. **88**(1): p. 70-7.
75. Szabo, G. and P. Mandrekar, A recent perspective on alcohol, immunity, and host defense. Alcohol Clin Exp Res, 2009. **33**(2): p. 220-32.
76. Muhanna, N., et al., Lymphocyte-hepatic stellate cell proximity suggests a direct interaction. Clin Exp Immunol, 2007. **148**(2): p. 338-47.
77. Winau, F., et al., Ito cells are liver-resident antigen-presenting cells for activating T cell responses. Immunity, 2007. **26**(1): p. 117-29.
78. Brown, L.A., et al., Acute and chronic alcohol abuse modulate immunity. Alcohol Clin Exp Res, 2006. **30**(9): p. 1624-31.
79. Gamble, L., C.M. Mason, and S. Nelson, The effects of alcohol on immunity and bacterial infection in the lung. Med Mal Infect, 2006. **36**(2): p. 72-7.
80. Lau, A.H., M. Abe, and A.W. Thomson, Ethanol affects the generation, cosignaling molecule expression, and function of plasmacytoid and myeloid dendritic cell subsets in vitro and in vivo. J Leukoc Biol, 2006. **79**(5): p. 941-53.
81. Bedogni, G., et al., Natural course of chronic HCV and HBV infection and role of alcohol in the general population: the Dionysos Study. Am J Gastroenterol, 2008. **103**(9): p. 2248-53.

82. Ohnishi, K., et al., Interferon therapy for chronic hepatitis C in habitual drinkers: comparison with chronic hepatitis C in infrequent drinkers. Am J Gastroenterol, 1996. **91**(7): p. 1374-9.
83. Zhang, T., et al., Alcohol potentiates hepatitis C virus replicon expression. Hepatology, 2003. **38**(1): p. 57-65.
84. Plumlee, C.R., et al., Effect of ethanol on innate antiviral pathways and HCV replication in human liver cells. Virol J, 2005. **2**: p. 89.
85. Otani, K., et al., Hepatitis C virus core protein, cytochrome P450 2E1, and alcohol produce combined mitochondrial injury and cytotoxicity in hepatoma cells. Gastroenterology, 2005. **128**(1): p. 96-107.
86. Willis, M.S., et al., Adduction of soluble proteins with malondialdehyde-acetaldehyde (MAA) induces antibody production and enhances T-cell proliferation. Alcohol Clin Exp Res, 2002. **26**(1): p. 94-106.
87. Vay, D., et al., Anti-phospholipid antibodies associated with alcoholic liver disease target oxidized phosphatidylserine on apoptotic cell plasma membranes. Journal of hepatology, 2006. **44**(1): p. 183.
88. Vidali, M., et al., Immune responses against oxidative stress-derived antigens are associated with increased circulating tumor necrosis factor-alpha in heavy drinkers. Free Radic Biol Med, 2008. **45**(3): p. 306-11.
89. Viitala, K., et al., Autoimmune responses against oxidant stress and acetaldehyde-derived epitopes in human alcohol consumers. Alcohol Clin Exp Res, 2000. **24**(7): p. 1103-9.
90. Latvala, J., et al., Immune Responses to Ethanol Metabolites and Cytokine Profiles Differentiate Alcoholics with or without Liver Disease. Am J Gastroenterol, 2005. **100**(6): p. 1303-10.
91. Clot, P., et al., Cytochrome P4502E1 hydroxyethyl radical adducts as the major antigen in autoantibody formation among alcoholics. Gastroenterology, 1996. **111**(1): p. 206.
92. Mangia, A., et al., Anticardiolipin antibodies in patients with liver disease. The American journal of gastroenterology, 1999. **94**(10): p. 2983.

93. Cook, R.T., et al., Thymocytes, pre-B cells, and organ changes in a mouse model of chronic ethanol ingestion--absence of subset-specific glucocorticoid-induced immune cell loss. Alcohol Clin Exp Res, 2007. **31**(10): p. 1746-58.
94. Jungermann, K. and T. Kietzmann, Oxygen: modulator of metabolic zonation and disease of the liver. Hepatology (Baltimore, Md.), 2000. **31**(2): p. 255-60.
95. Kietzmann, T., et al., Perivenous expression of the mRNA of the three hypoxia-inducible factor alpha-subunits, HIF1alpha, HIF2alpha and HIF3alpha, in rat liver. The Biochemical journal, 2001. **354**(Pt 3): p. 531-7.
96. Jaakkola, P., et al., Targeting of HIF-alpha to the von Hippel-Lindau ubiquitylation complex by O2-regulated prolyl hydroxylation. Science, 2001. **292**(5516): p. 468-72.
97. Kim, W., et al., Failure to prolyl hydroxylate hypoxia-inducible factor alpha phenocopies VHL inactivation in vivo. The EMBO journal, 2006. **25**(19): p. 4650.
98. Krones, A., T. Kietzmann, and K. Jungermann, Periportal localization of glucagon receptor mRNA in rat liver and regulation of its expression by glucose and oxygen in hepatocyte cultures. FEBS letters, 1998. **421**(2): p. 136-40.
99. Krones, A., T. Kietzmann, and K. Jungermann, Perivenous localization of insulin receptor protein in rat liver, and regulation of its expression by glucose and oxygen in hepatocyte cultures. The Biochemical journal, 2000. **348 Pt 2**: p. 433-8.
100. Krones, A., K. Jungermann, and T. Kietzmann, Cross-talk between the signals hypoxia and glucose at the glucose response element of the L-type pyruvate kinase gene. Endocrinology, 2001. **142**(6): p. 2707-18.
101. Broughan, T.A., et al., Effects of hepatic zonal oxygen levels on hepatocyte stress responses. J Surg Res, 2008. **145**(1): p. 150-60.
102. Chen, C., et al., Early inhibition of HIF-1alpha with small interfering RNA reduces ischemic-reperfused brain injury in rats. Neurobiol Dis, 2009. **33**(3): p. 509-17.
103. Zhao, H.X., et al., Attenuation of myocardial injury by postconditioning: role of hypoxia inducible factor-1alpha. Basic Res Cardiol, 2009.
104. Cai, Z., et al., Complete loss of ischaemic preconditioning-induced cardioprotection in mice with partial deficiency of HIF-1 alpha. Cardiovasc Res, 2008. **77**(3): p. 463-70.

105. Ma, D., et al., Xenon preconditioning protects against renal ischemic-reperfusion injury via HIF-1alpha activation. J Am Soc Nephrol, 2009. **20**(4): p. 713-20.
106. Iguchi, M., et al., Acute inactivation of the VHL gene contributes to protective effects of ischemic preconditioning in the mouse kidney. Nephron Exp Nephrol, 2008. **110**(3): p. e82-90.
107. Hill, P., et al., Inhibition of hypoxia inducible factor hydroxylases protects against renal ischemia-reperfusion injury. J Am Soc Nephrol, 2008. **19**(1): p. 39-46.
108. Cursio, R., et al., Liver HIF-1 Alpha Induction Precedes Apoptosis Following Normothermic Ischemia-Reperfusion in Rats. Transplantation proceedings, 2008. **40**(6): p. 2042.
109. Alchera, E., et al., Adenosine-dependent activation of hypoxia-inducible factor-1 induces late preconditioning in liver cells. Hepatology (Baltimore, Md.), 2008. **48**(1): p. 230.
110. Tacchini, L., et al., Transferrin receptor gene expression and transferrin-bound iron uptake are increased during postischemic rat liver reperfusion. Hepatology, 2002. **36**(1): p. 103-11.
111. Tacchini, L., L. Radice, and A. Bernelli-Zazzera, Differential activation of some transcription factors during rat liver ischemia, reperfusion, and heat shock. J Cell Physiol, 1999. **180**(2): p. 255-62.
112. Tsuchihashi, S., et al., Vascular endothelial growth factor antagonist modulates leukocyte trafficking and protects mouse livers against ischemia/reperfusion injury. Am J Pathol, 2006. **168**(2): p. 695-705.
113. Seeto, R.K., B. Fenn, and D.C. Rockey, Ischemic hepatitis: clinical presentation and pathogenesis. Am J Med, 2000. **109**(2): p. 109-13.
114. Raurich, J.M., et al., Incidence and outcome of ischemic hepatitis complicating septic shock. Hepatol Res, 2009. **39**(7): p. 700-5.
115. Henrion, J., et al., Hypoxic hepatitis: clinical and hemodynamic study in 142 consecutive cases. Medicine (Baltimore), 2003. **82**(6): p. 392-406.

116. Metukuri, M.R., et al., Expression and subcellular localization of BNIP3 in hypoxic hepatocytes and liver stress. Am J Physiol Gastrointest Liver Physiol, 2009. **296**(3): p. G499-509.
117. Hoppin, A.G., et al., Case records of the Massachusetts General Hospital. Case 31-2006. A 15-year-old girl with severe obesity. N Engl J Med, 2006. **355**(15): p. 1593-602.
118. Mishra, P., et al., Apnoeic-hypopnoeic episodes during obstructive sleep apnoea are associated with histological nonalcoholic steatohepatitis. Liver Int, 2008. **28**(8): p. 1080-6.
119. Jouet, P., et al., Relationship between obstructive sleep apnea and liver abnormalities in morbidly obese patients: a prospective study. Obes Surg, 2007. **17**(4): p. 478-85.
120. Polotsky, V.Y., et al., Obstructive sleep apnea, insulin resistance, and steatohepatitis in severe obesity. Am J Respir Crit Care Med, 2009. **179**(3): p. 228-34.
121. Tatsumi, K. and T. Saibara, Effects of obstructive sleep apnea syndrome on hepatic steatosis and nonalcoholic steatohepatitis. Hepatol Res, 2005. **33**(2): p. 100-4.
122. Tanne, F., et al., Chronic liver injury during obstructive sleep apnea. Hepatology, 2005. **41**(6): p. 1290-6.
123. Savransky, V., et al., Chronic intermittent hypoxia predisposes to liver injury. Hepatology, 2007. **45**(4): p. 1007-13.
124. Li, J., et al., Chronic intermittent hypoxia upregulates genes of lipid biosynthesis in obese mice. J Appl Physiol, 2005. **99**(5): p. 1643-8.
125. Savransky, V., et al., Chronic intermittent hypoxia causes hepatitis in a mouse model of diet-induced fatty liver. Am J Physiol Gastrointest Liver Physiol, 2007. **293**(4): p. G871-7.
126. Savransky, V., et al., Chronic intermittent hypoxia and acetaminophen induce synergistic liver injury in mice. Exp Physiol, 2009. **94**(2): p. 228-39.
127. James, L.P., et al., Induction of the nuclear factor HIF-1alpha in acetaminophen toxicity: evidence for oxidative stress. Biochem Biophys Res Commun, 2006. **343**(1): p. 171-6.
128. Wu, Y.L., et al., Protective effects of salidroside against acetaminophen-induced toxicity in mice. Biol Pharm Bull, 2008. **31**(8): p. 1523-9.

129. Salhanick, S., et al., *Hyperbaric oxygen reduces acetaminophen toxicity and increases HIF-1alpha expression.* Academic emergency medicine : official journal of the Society for Academic Emergency Medicine, 2006. **13**(7): p. 707-14.

130. Nath, B. and G. Szabo, Alcohol-induced modulation of signaling pathways in liver parenchymal and nonparenchymal cells: implications for immunity. Semin Liver Dis, 2009. **29**(2): p. 166-77.

131. Zakhari, S., Overview: how is alcohol metabolized by the body? Alcohol Res Health, 2006. **29**(4): p. 245-54.

132. Videla, L., J. Bernstein, and Y. Israel, Metabolic alterations produced in the liver by chronic ethanol administration. Increased oxidative capacity. Biochem J, 1973. **134**(2): p. 507-514.

133. Yuki, T. and R.G. Thurman, The swift increase in alcohol metabolism. Time course for the increase in hepatic oxygen uptake and the involvement of glycolysis. Biochem J, 1980. **186**(1): p. 119-26.

134. Arteel, G.E., et al., Acute alcohol produces hypoxia directly in rat liver tissue in vivo: role of Kupffer cells. Am J Physiol, 1996. **271**(3 Pt 1): p. G494-500.

135. Arteel and et al., Chronic Enteral Ethanol Treatment Causes Hypoxia in Rat Liver Tissue In Vivo.

136. Yin, H., et al., Analysis of hepatic gene expression during fatty liver change due to chronic ethanol administration in mice. Toxicology and applied pharmacology, 2009. **235**(3): p. 312-20.

137. Li, L., et al., Is the hypoxia-inducible factor-1 alpha mRNA expression activated by ethanol-induced injury, the mechanism underlying alcoholic liver disease? Hepatobiliary & pancreatic diseases international : HBPD INT, 2006. **5**(4): p. 560-3.

138. Li, J., et al., Liver hypoxia and lack of recovery after reperfusion at high blood alcohol levels in the intragastric feeding model of alcohol liver disease. Experimental and molecular pathology, 2004. **77**(3): p. 184-92.

139. Bailey, S., et al., Ethanol and tobacco smoke increase hepatic steatosis and hypoxia in the hypercholesterolemic apoE(-/-) mouse: implications for a "multihit" hypothesis of fatty liver disease. Free radical biology & medicine, 2009. **46**(7): p. 928-38.
140. Uesugi, T., et al., Toll-like receptor 4 is involved in the mechanism of early alcohol-induced liver injury in mice. Hepatology, 2001. **34**(1): p. 101-8.
141. Scharte, M., et al., LPS increases hepatic HIF-1alpha protein and expression of the HIF-1-dependent gene aldolase A in rats. The Journal of surgical research, 2006. **135**(2): p. 262-7.
142. Blouin, C.C., et al., Hypoxic gene activation by lipopolysaccharide in macrophages: implication of hypoxia-inducible factor 1alpha. Blood, 2004. **103**(3): p. 1124-30.
143. Peyssonnaux, C., et al., Cutting edge: Essential role of hypoxia inducible factor-1alpha in development of lipopolysaccharide-induced sepsis. J Immunol, 2007. **178**(12): p. 7516-9.
144. van Uden P, N. Kenneth, and S. Rocha, Regulation of hypoxia-inducible factor-1alpha by NF-kappaB. The Biochemical journal, 2008. **412**(3): p. 477-84.
145. Rius, J., et al., NF-kappaB links innate immunity to the hypoxic response through transcriptional regulation of HIF-1alpha. Nature, 2008.
146. Thiel, M., et al., Targeted deletion of HIF-1alpha gene in T cells prevents their inhibition in hypoxic inflamed tissues and improves septic mice survival. PLoS ONE, 2007. **2**(9): p. e853.
147. Wolman, M., et al., Pathological changes in organs of rats chronically exposed to hypoxia. Development of pulmonary lipidosis. Histol Histopathol, 1993. **8**(2): p. 247-55.
148. Bostrom, P., et al., Hypoxia converts human macrophages into triglyceride-loaded foam cells. Arterioscler Thromb Vasc Biol, 2006. **26**(8): p. 1871-6.
149. Jiang, G., et al., RNA interference for HIF-1alpha inhibits foam cells formation in vitro. Eur J Pharmacol, 2007. **562**(3): p. 183-90.
150. Wada, T., S. Shimba, and M. Tezuka, Transcriptional regulation of the hypoxia inducible factor-2alpha (HIF-2alpha) gene during adipose differentiation in 3T3-L1 cells. Biological & pharmaceutical bulletin, 2006. **29**(1): p. 49-54.

151. Belanger, A., et al., Hypoxia-inducible factor 1 mediates hypoxia-induced cardiomyocyte lipid accumulation by reducing the DNA binding activity of peroxisome proliferator-activated receptor alpha/retinoid X receptor. Biochemical and biophysical research communications, 2007. **364**(3): p. 567-72.

152. Furuta, E., et al., Fatty acid synthase gene is up-regulated by hypoxia via activation of Akt and sterol regulatory element binding protein-1. Cancer Res, 2008. **68**(4): p. 1003-11.

153. Scortegagna, M., et al., Multiple organ pathology, metabolic abnormalities and impaired homeostasis of reactive oxygen species in Epas1-/- mice. Nature genetics, 2003. **35**(4): p. 331-40.

154. Park, S., V. Haase, and R. Johnson, von Hippel Lindau tumor suppressor regulates hepatic glucose metabolism by controlling expression of glucose transporter 2 and glucose 6-phosphatase. International journal of oncology, 2007. **30**(2): p. 341-8.

155. Rankin, E.B., et al., HIF-2 regulates hepatic lipid metabolism. Mol Cell Biol, 2009.

156. Peyssonnaux, C., et al., Regulation of iron homeostasis by the hypoxia-inducible transcription factors (HIFs). J Clin Invest, 2007. **117**(7): p. 1926-32.

157. Yim, S.H., et al., Disruption of the Arnt gene in endothelial cells causes hepatic vascular defects and partial embryonic lethality in mice. Hepatology, 2006. **44**(3): p. 550-60.

158. Mastrogiannaki, M., et al., HIF-2alpha, but not HIF-1alpha, promotes iron absorption in mice. The Journal of clinical investigation, 2009. **119**(5): p. 1159-66.

159. Li, Z., et al., Correlation between the expression of divalent metal transporter 1 and the content of hypoxia-inducible factor-1 in hypoxic HepG2 cells. J Cell Mol Med, 2008. **12**(2): p. 569-79.

160. Moon, J., et al., *Reduced liver fibrosis in hypoxia-inducible factor-1{alpha}-deficient mice.* American journal of physiology. Gastrointestinal and liver physiology, 2009. **296**(3): p. G582-92.

161. Copple, B., et al., *Hypoxia-inducible factor-dependent production of profibrotic mediators by hypoxic hepatocytes.* Liver international : official journal of the International Association for the Study of the Liver, 2009.

162. Corpechot, C., et al., Hypoxia-induced VEGF and collagen I expressions are associated with angiogenesis and fibrogenesis in experimental cirrhosis. Hepatology (Baltimore, Md.), 2002. **35**(5): p. 1010-21.

163. Novo, E., et al., Proangiogenic cytokines as hypoxia-dependent factors stimulating migration of human hepatic stellate cells. The American journal of pathology, 2007. **170**(6): p. 1942-53.

164. Shi, Y.F., et al., Hypoxia induces the activation of human hepatic stellate cells LX-2 through TGF-beta signaling pathway. FEBS Lett, 2007. **581**(2): p. 203-10.

165. Xie, H., et al., The expression of hypoxia-inducible factor-1alpha in hepatitis B virus-related hepatocellular carcinoma: correlation with patients' prognosis and hepatitis B virus X protein. Dig Dis Sci, 2008. **53**(12): p. 3225-33.

166. Han, H.K., et al., Role of hypoxia-inducible factor-alpha in hepatitis-B-virus X protein-mediated MDR1 activation. Biochem Biophys Res Commun, 2007. **357**(2): p. 567-73.

167. Yoo, Y., et al., Hepatitis B virus X protein induces the expression of MTA1 and HDAC1, which enhances hypoxia signaling in hepatocellular carcinoma cells. Oncogene, 2008. **27**(24): p. 3405-13.

168. Moin, S.M., et al., The hepatitis E virus ORF3 protein stabilizes HIF-1alpha and enhances HIF-1-mediated transcriptional activity through p300/CBP. Cell Microbiol, 2009.

169. Nasimuzzaman, M., et al., Hepatitis C virus stabilizes hypoxia-inducible factor 1alpha and stimulates the synthesis of vascular endothelial growth factor. Journal of virology, 2007. **81**(19): p. 10249-57.

170. Maeno, H., et al., Expression of hypoxia inducible factor-1alpha during liver regeneration induced by partial hepatectomy in rats. Liver international : official journal of the International Association for the Study of the Liver, 2005. **25**(5): p. 1002-9.

171. Olazabal, I., et al., Prolactin's role in the early stages of liver regeneration in rats. Journal of cellular physiology, 2009. **219**(3): p. 626-33.

172. Ren, P., et al., Hyperbaric oxygen preconditioning promotes angiogenesis in rat liver after partial hepatectomy. Life Sci, 2008. **83**(7-8): p. 236-41.

173. Vollmer, S., et al., Hypoxia-inducible factor 1alpha is up-regulated by oncostatin M and participates in oncostatin M signaling. Hepatology, 2009. **50**(1): p. 253-60.
174. Nakamura, K., et al., Vascular endothelial growth factor, its receptor Flk-1, and hypoxia inducible factor-1alpha are involved in malignant transformation in dysplastic nodules of the liver. Human pathology, 2007. **38**(10): p. 1532-46.
175. Tanaka, H., et al., Hypoxia-independent overexpression of hypoxia-inducible factor 1alpha as an early change in mouse hepatocarcinogenesis. Cancer research, 2006. **66**(23): p. 11263-70.
176. Sun, X., et al., Antisense hypoxia-inducible factor-1alpha augments transcatheter arterial embolization in the treatment of hepatocellular carcinomas in rats. Human gene therapy, 2009. **20**(4): p. 314-24.
177. Ryu, S.H., et al., Metastatic tumor antigen 1 is closely associated with frequent postoperative recurrence and poor survival in patients with hepatocellular carcinoma. Hepatology, 2008. **47**(3): p. 929-36.
178. Bangoura, G., et al., Expression of HIF-2alpha/EPAS1 in hepatocellular carcinoma. World journal of gastroenterology : WJG, 2004. **10**(4): p. 525-30.
179. Bangoura, G., et al., Prognostic significance of HIF-2alpha/EPAS1 expression in hepatocellular carcinoma. World journal of gastroenterology : WJG, 2007. **13**(23): p. 3176-82.
180. Greenberger, L., et al., A RNA antagonist of hypoxia-inducible factor-1{alpha}, EZN-2968, inhibits tumor cell growth. Molecular cancer therapeutics, 2008.
181. Liu, F., et al., Antisense hypoxia-inducible factor 1alpha gene therapy enhances the therapeutic efficacy of doxorubicin to combat hepatocellular carcinoma. Cancer science, 2008. **99**(10): p. 2055-61.
182. Wang, W., et al., Antitumoral Activity of Rapamycin Mediated Through Inhibition of HIF-1alpha and VEGF in Hepatocellular Carcinoma. Digestive diseases and sciences, 2008.

183. GarcÌa-Maceira, P. and J. Mateo, Silibinin inhibits hypoxia-inducible factor-1alpha and mTOR/p70S6K/4E-BP1 signalling pathway in human cervical and hepatoma cancer cells: implications for anticancer therapy. Oncogene, 2008.
184. Tsukamoto, H., et al., Cyclical pattern of blood alcohol levels during continuous intragastric ethanol infusion in rats. Alcohol Clin Exp Res, 1985. **9**(1): p. 31-7.
185. Fromenty, B., et al., Chronic ethanol consumption lessens the gain of body weight, liver triglycerides and diabetes in obese ob/ob mice. J Pharmacol Exp Ther, 2009.
186. Stern, Z., et al., Effects of arachidonic acid on hepatic lipids in ethanol-fed rats. Alcohol Clin Exp Res, 1990. **14**(1): p. 127-9.
187. Scortegagna, M., et al., Multiple organ pathology, metabolic abnormalities and impaired homeostasis of reactive oxygen species in Epas1-/- mice. Nat Genet, 2003. **35**(4): p. 331-40.
188. Arteel, G.E., New role of plasminogen activator inhibitor-1 in alcohol-induced liver injury. J Gastroenterol Hepatol, 2008. **23 Suppl 1**: p. S54-9.
189. Bautista, A.P., Neutrophilic infiltration in alcoholic hepatitis. Alcohol, 2002. **27**(1): p. 17-21.
190. Bergheim, I., et al., Metformin prevents alcohol-induced liver injury in the mouse: Critical role of plasminogen activator inhibitor-1. Gastroenterology, 2006. **130**(7): p. 2099-112.
191. Melgarejo, E., et al., Monocyte chemoattractant protein-1: a key mediator in inflammatory processes. Int J Biochem Cell Biol, 2009. **41**(5): p. 998-1001.
192. Kolios, G., et al., Nitric oxide and MCP-1 regulation in LPS activated rat Kupffer cells. Mol Cell Biochem, 2008. **319**(1-2): p. 91-8.
193. Woo, C.W., Y.L. Siow, and K. O, Homocysteine induces monocyte chemoattractant protein-1 expression in hepatocytes mediated via activator protein-1 activation. J Biol Chem, 2008. **283**(3): p. 1282-92.
194. Desai, M.S., et al., Atherogenic diet-induced hepatitis is partially dependent on murine TLR4. J Leukoc Biol, 2008. **83**(6): p. 1336-44.

195. Gabele, E., et al., Role of TLR9 in hepatic stellate cells and experimental liver fibrosis. Biochem Biophys Res Commun, 2008. **376**(2): p. 271-6.

196. Tsuruta, S., et al., Anti-monocyte chemoattractant protein-1 gene therapy prevents dimethylnitrosamine-induced hepatic fibrosis in rats. Int J Mol Med, 2004. **14**(5): p. 837-42.

197. Clement, S., et al., Monocyte chemoattractant protein-1 secreted by adipose tissue induces direct lipid accumulation in hepatocytes. Hepatology, 2008. **48**(3): p. 799-807.

198. Hong, K.H., J. Ryu, and K.H. Han, Monocyte chemoattractant protein-1-induced angiogenesis is mediated by vascular endothelial growth factor-A. Blood, 2005. **105**(4): p. 1405-7.

199. Niu, J., et al., Monocyte chemotactic protein (MCP)-1 promotes angiogenesis via a novel transcription factor, MCP-1-induced protein (MCPIP). J Biol Chem, 2008. **283**(21): p. 14542-51.

200. Rius, J., et al., NF-kappaB links innate immunity to the hypoxic response through transcriptional regulation of HIF-1alpha. Nature, 2008. **453**(7196): p. 807-11.

201. Westra, J., et al., Regulation of cytokine-induced HIF-1alpha expression in rheumatoid synovial fibroblasts. Ann N Y Acad Sci, 2007. **1108**: p. 340-8.

202. Motomura, W., et al., Up-regulation of ADRP in fatty liver in human and liver steatosis in mice fed with high fat diet. Biochem Biophys Res Commun, 2006. **340**(4): p. 1111-8.

203. Imai, Y., et al., Reduction of hepatosteatosis and lipid levels by an adipose differentiation-related protein antisense oligonucleotide. Gastroenterology, 2007. **132**(5): p. 1947-54.

204. Chang, B.H., et al., Protection against fatty liver but normal adipogenesis in mice lacking adipose differentiation-related protein. Mol Cell Biol, 2006. **26**(3): p. 1063-76.

205. Tuller, E.R., et al., Docosahexaenoic acid inhibits superoxide dismutase 1 gene transcription in human cancer cells: the involvement of PPAR{alpha} and HIF-2{alpha} signaling. Mol Pharmacol, 2009.

206. Kuznetsova, A.V., et al., von Hippel-Lindau protein binds hyperphosphorylated large subunit of RNA polymerase II through a proline hydroxylation motif and targets it for ubiquitination. Proc Natl Acad Sci U S A, 2003. **100**(5): p. 2706-11.

207. Makino, Y., et al., Transcriptional up-regulation of inhibitory PAS domain protein gene expression by hypoxia-inducible factor 1 (HIF-1): a negative feedback regulatory circuit in HIF-1-mediated signaling in hypoxic cells. J Biol Chem, 2007. **282**(19): p. 14073-82.
208. Bracken, C.P., et al., Cell-specific regulation of hypoxia-inducible factor (HIF)-1alpha and HIF-2alpha stabilization and transactivation in a graded oxygen environment. J Biol Chem, 2006. **281**(32): p. 22575-85.
209. Olmos, G., et al., 15-Deoxy-Delta(12,14)-prostaglandin-J(2) reveals a new pVHL-independent, lysosomal-dependent mechanism of HIF-1alpha degradation. Cell Mol Life Sci, 2009. **66**(13): p. 2167-80.
210. Dioum, E., et al., Regulation of hypoxia-inducible factor 2alpha signaling by the stress-responsive deacetylase sirtuin 1. Science (New York, N.Y.), 2009. **324**(5932): p. 1289-93.
211. Rankin and et al., HIF-2 Regulates hepatic lipid metabolism.
212. Rinella, M.E., et al., Mechanisms of hepatic steatosis in mice fed a lipogenic methionine choline-deficient diet. J Lipid Res, 2008. **49**(5): p. 1068-76.
213. Dominguez, M., et al., Hepatic expression of CXC chemokines predicts portal hypertension and survival in patients with alcoholic hepatitis. Gastroenterology, 2009. **136**(5): p. 1639-50.
214. Liu, F., et al., Hypoxia modulates lipopolysaccharide induced TNF-alpha expression in murine macrophages. Experimental cell research, 2008. **314**(6): p. 1327-36.
215. Huang, W.J., et al., Transcriptional upregulation of HSP70-2 by HIF-1 in cancer cells in response to hypoxia. Int J Cancer, 2009. **124**(2): p. 298-305.
216. Kang, M.J., et al., DNA-dependent protein kinase is involved in heat shock protein-mediated accumulation of hypoxia-inducible factor-1alpha in hypoxic preconditioned HepG2 cells. FEBS J, 2008. **275**(23): p. 5969-81.